Real options-based models of economic decisions toward sustainability: The cases of blockchain-based supply chain enhancements, asphalt roads resurfacing, and conversion from conventional to cool roofs

by

Zhuoyi Zhao

A dissertation submitted to the graduate faculty

in partial fulfillment of the requirements for the degree of

DOCTOR OF PHILOSOPHY

Major: Industrial Engineering

Program of Study Committee:
Kyung Jo Min, Major Professor
John Jackman
Cameron MacKenzie
Sarah Ryan
Somak Dutta

Iowa State University

Ames, Iowa

2023

DEDICATION

This dissertation is dedicated to my parents and my grandparents.

TABLE OF CONTENTS

LIST OF FIGURES

Page

LIST OF TABLES

ACKNOWLEDGMENTS

First, I would like to thank my major professor, Dr. Kyung Jo Min, for his professional guidance, continuous inspiration, and constructive feedback throughout my Ph.D. journey. Without his support, I would not have completed my Ph.D. degree. He has been a role model to me because of his rigorous attitude toward research, diligence at work, and wisdom in life.

My sincere gratitude also goes to my committee members, Dr. Cameron MacKenzie, Dr. Sarah Ryan, Dr. John Jackman, and Dr. Somak Dutta, for their insightful and developmental advice and help in my research and this dissertation.

In addition, I would also like to express my gratitude to Dr. Gary Mirka, Dr. Michael Dorneich, Dr. Stephen Gilbert, Jess Severe, Devna Popejoy-Sheriff, Michael Renze, Krista Briley and other faculty and staff in the IMSE department, course instructors, and my friends for making my time at Iowa State University a fruitful and wonderful experience.

Moreover, I would like to thank Jack Wang, Luciano Morra, Jeff Bladon, Curt Kole, and Fred G Volk III from PeriShip for the learning experience, professional skills, career advice and continuous support during and after my internship.

Finally, I would like to extend my sincere thanks to my parents (Meihua Gao and Yunhong Zhao), my grandparents (Jinglan Zhao and Jincheng Tan), my boyfriend (Pak Hon Cheung), Jack Wang and Marie Wang. It was their love, belief, encouragement, and support that helped me through the most difficult times.

ABSTRACT

Economic transition endeavors are ubiquitous in businesses and industries every day, which are costly, irreversible, and uncertain in key aspects such as cost or demand. In this dissertation, we view these transition endeavors as options (cf. obligations), explore the optimal decisions, and analyze the economic consequences in the context of blockchain technology, asphalt roads, and cool roofs - all toward a higher level of environmental sustainability. For each case, we construct and analyze stochastic optimal control (i.e., real options) models to determine the optimal transition action and time. We also derive managerial insights and economic implications from analytical and numerical analyses and numerical examples.

This dissertation mainly consists of three papers. In the first paper, we consider a perishable agricultural product supply chain, where the retailer decides when to switch from a conventional supply chain information management system (SCIMS) to a blockchain-based SCIMS. Blockchain technology reduces waste and disposal as a precaution during recalls by shortening the time to trace the contamination origination. We model the uncertain customers' demand as a geometric Brownian motion (GBM) process and show how to obtain the optimal demand threshold above which the switch occurs and the corresponding expected time. Next, the model is extended by incorporating two types of government subsidies (i.e., a fixed subsidy on the switching cost and a variable subsidy per unit demand).

In the second paper, we consider an asphalt road where resurfacing (i.e., placing a new layer over the existing pavement) is implemented upon which the pavement condition will be like new, and the maintenance cost is reduced to the new pavement level. Under the assumption that the maintenance cost of a road follows a GBM process, we construct and analyze a stochastic optimal control (a real options approach) model for a profit-maximizing decision-

maker where the threshold in the maintenance cost to resurface the road is the decision variable. Given this framework, we also mathematically derive the expected resurfacing interval, i.e., the average time between two consecutive resurfacing activities.

In the third paper, we consider a commercial building that consumes electricity for cooling and natural gas for heating, where converting the current conventional roof to a cool roof will lead to lower electricity consumption but higher natural gas consumption. Under the assumption that the building's electricity consumption sufficiently exceeds its natural gas consumption, we aim to provide decision support for the roof conversion for profit-maximizing decision-makers (e.g., commercial building owners). Specifically, in the basic model, the electricity price follows a GBM process, and the natural gas price is characterized as a constant multiplied by the electricity price. We analytically solve for the optimal electricity price threshold to implement roof conversion and the corresponding expected time. In the extended model, where the electricity and natural gas prices follow correlated GBM processes, we value the roof conversion option using the Least Squares Monte Carlo simulation (i.e., using Least Squares to estimate the expected payoff from continuation with current energy prices and obtain the option value by Monte Carlo simulation).

Finally, we conclude with an overall summary of research findings and discussions for future research.

CHAPTER 1. GENERAL INTRODUCTION

Economic transition endeavors are ubiquitous in businesses and industries every day. Examples are the internal combustion engine vehicles to electric vehicles (Hoeft, 2021) or the community of Newtok relocating due to melting permafrost (State of Alaska - Department of Commerce, Community and Economic Development, 2019). Many of these transition endeavors share the common attributes of being costly, irreversible, and uncertain in key aspects such as cost or demand. In this dissertation, we view these transition endeavors as options (cf. obligations), explore the optimal decisions and analyze the economic consequences under such circumstances.

Specifically, in the context of blockchain technology, asphalt roads, and cool roofs - all toward a higher level of environmental sustainability, we construct and analyze stochastic optimal control (i.e., real options) models to determine the optimal transition action and time. For each case, managerial insights and economic implications derived from analytical and numerical analyses and numerical examples are discussed.

This document follows a journal article format consisting of three journal articles/manuscripts. Specifically, in Chapter 2, we consider the supply chain enhancements, from a conventional supply chain information management system (SCIMS) to a blockchain-based SCIMS under the uncertainty of the demand for a perishable agricultural product. In a conventional SCIMS, many stakeholders in the perishable record traceability data on paper, while the rest record it digitally (Yiannas, 2018). Such inconsistency makes it challenging for stakeholders to communicate and trace the origins of the perishable agricultural product within a short time. As a result, during recalls, products that are potentially not contaminated are wasted and disposed of as a precaution. Such circumstance incentivizes the retailer to switch to a blockchain-based SCIMS, where all the information throughout every step (e.g., product identification, batch codes, purchase orders, and time codes of harvesting, processing, shipping, and receiving) is collected and shared by all stakeholders (e.g., farms, distribution centers, stores; Walmart Food Safety & Health, 2018). Blockchain technology enables the stakeholders to pinpoint the contamination origination, reduce unnecessarily broad recalls (Guo et al., 2018) and reduce waste and disposal as a precaution during recalls (Marin et al., 2019). Moreover, motivated by the examples such as the government subsidizing supermarkets in high-need areas to improve the food environment in underserved neighborhoods (Elbel et al., 2015) and the U.S. Department of Health and Human Services (HHS) awarding 49 Health Center Controlled Networks nearly 42 million dollars to expand health information technology in health centers nationwide (HHS, 2019), we extend the model by incorporating the subsidies provided by the government to the retailer in the SCIMS switch decision as the blockchain technology improves the public’s welfare by enhancing the supply chain traceability.

Under the above background, in Chapter 2, we consider a supply chain of perishable agricultural products that consists of a wholesaler, a retailer, and customers, where the retailer has an option to switch from a conventional supply chain information management system (SCIMS) to a blockchain-based SCIMS. Assuming that the customers’ demand follows a geometric Brownian motion (GBM) process, we (1) valuate the traceability in the supply chain to determine the optimal threshold of demand and the expected time of switching using a real options approach in the basic model, (2) extend the basic model by incorporating two types of government subsidies, namely, a fixed subsidy on the switching cost and a variable subsidy per unit demand, and determine the new optimal threshold of demand and the expected time of switching, (3) derive managerial insights and economic implications for the retailer’s switch decision from analytical/numerical analyses, and (4) provide policy implications on motivating retailers to switch to a blockchain-based SCIMS from the government's perspective. This chapter is published in the *International Journal of Operations Research and Information Systems (IJORIS)*.

In Chapter 3, we consider the resurfacing endeavor for asphalt roads under maintenance cost uncertainty. Resurfacing a road means placing a new layer over the existing pavement to extend the pavement life rather than replacing the entire roadway (Wisconsin Department of Transportation, n.d.; Thames Street Works, n.d.), upon which the pavement condition is like new (Alqadhi et al., 2018). The resurfacing decision requires a careful study a priori because it is costly, irreversible, and made under maintenance cost uncertainty. The maintenance cost of an asphalt road has been substantially increasing (Tornquist, 2007; PCA, 2012), where fluctuations are often observed. The escalation of the maintenance cost can be attributed to pavement aging (Ohio Auditor of State, 2012), a complicated and uncertain process (Solatifar, 2021).

In Chapter 3, we assume that the maintenance cost of the road follows a GBM process and is reset to its initial value upon each resurfacing and model the resurfacing decision for a profit-maximizing decision-maker (e.g., a private-sector company under a Public-Private Partnership over a road where its objective is to maximize profit). Specifically, we (1) construct and analyze a real options approach model where the threshold in the maintenance cost to resurface the road is the decision variable; (2) mathematically derive how much time, on average, is between two resurfacing activities; (3) analytically and numerically illustrate key features of our model via analytical derivation and an extensive numerical example for managerial insights and economic implications. This chapter is under the review of the *European Journal of Industrial Engineering (EJIE)*.

In Chapter 4, we focus on the conversion from a conventional roof to a cool roof under energy price uncertainties. Compared with a conventional roof, a cool roof has high solar reflection (ability to reflect sunlight) and high thermal emittance (ability to emit thermal radiation), which improves building energy efficiency (Gao et al., 2014). We consider a commercial building that consumes electricity for cooling and natural gas for heating (U.S. EIA, 2021d, p. 28), where its electricity consumption sufficiently exceeds its natural gas consumption. The roof conversion will reduce electricity consumption but increase natural gas consumption (Akbari et al., 1999). This endeavor is costly yet irreversible and made under the uncertainties of electricity and natural gas prices. The electricity and natural gas prices increase on average and fluctuate over time (U.S. EIA, 2021c; U.S. EIA, 2022b), and a correlation relationship can be observed (Lukes, 2021; U.S. EIA, 2021a; Pressler, 2022) considering that natural gas is used for power generation (Maribu et al., 2007).

In Chapter 4, we provide the decision support for the conversion from a conventional roof to a cool roof through two models. In the basic model, we assume the electricity price follows a GBM process, and the natural gas price is equal to a constant multiplied by the electricity price. We (1) construct and analyze the roof conversion decision using a real options approach; (2) derive the optimal electricity price threshold and the corresponding expected time on average to implement the roof conversion; (3) examine how the parameter values impact the roof conversion decision through a numerical example; (4) derive managerial insights and economic implications. In the extended model, a more general and complicated case, we assume that the electricity and natural gas prices follow correlated GBM processes. We obtain the value of the roof conversion option using the Least Squares Monte Carlo simulation, i.e., using Least Squares to estimate the expected payoff from continuation with current energy prices and obtain the option value by Monte Carlo simulation. We also investigate how the option value is impacted when the parameter values change. This chapter is under the review of *The Engineering Economist (TEE)*.

Commonalities and Differences

There are three main commonalities across Chapters 2, 3, and 4 (see Table 1.1 for details).

(1) The economic decisions enhance sustainability.

(2) Uncertainties are incorporated into the decision-making processes.

(3) A real options approach is applied.

Table 1.1 Commonalities across Chapters 2, 3, and 4

Commonalities	**Chapter**	**Details**
Sustainability	2	The switch from a conventional SCIMS to a blockchain-based SCIMS enhances the sustainability of the supply chain of perishable agricultural products.
	3	Resurfacing the asphalt road renews the pavement condition, improving the road's sustainability.
	4	The conversion from a conventional roof to a cool roof improves the sustainability of the commercial building.
Uncertainties	2	The uncertainty of the demand for a perishable agricultural product
	3	The uncertainty of the maintenance cost of an asphalt road
	4	The uncertainties of electricity and natural gas prices

Table 1.1 continued

Commonalities	Chapter	Details
Real options approach	2	We analytically derive the closed-form solutions for the optimal demand threshold to switch from a conventional SCIMS to a blockchain-based SCIMS with/without government subsidies.
	3	Although the closed-form solution cannot be derived, we arrive at an equation with which the optimal threshold of the maintenance cost to resurface an asphalt road can be numerically solved.
	4	Basic model: We analytically derive the closed-form solution to the optimal electricity price threshold for the roof conversion. Extended model: We apply the Least Squares Monte Carlo simulation to obtain the value of the roof conversion option.

The main differences in Chapters 2, 3, and 4 are as follows (see Table 1.2 for details).

(1) The numbers of GBM processes considered are different.

(2) The changes after the conversion are different.

Table 1.2 Differences in Chapters 2, 3, and 4

Chapter	Number of GBM processes	Change after conversion
2	One GBM process (demand for a perishable agricultural product)	Amount of wastage and disposal of perishable agricultural products as a precaution during recalls is reduced.
3	One GBM process (maintenance cost of an asphalt road)	Maintenance cost is reset to its initial value.

Table 1.2 continued

Chapter	Number of GBM processes	Change after conversion
4	Two correlated GBM processes (electricity and natural gas prices)	Annual electricity consumption decreases while annual natural gas consumption increases.

This dissertation consists of five chapters. Chapter 1 is the general introduction of this dissertation. In Chapter 2, we show how to obtain the optimal demand threshold above which a retailer should switch from a conventional SCIMS to a blockchain-based SCIMS under the uncertainty of the demand for a perishable agricultural product. In Chapter 3, we construct and analyze a model for the road resurfacing decision under the maintenance cost uncertainty, where the threshold in the maintenance cost to resurface the road is the decision variable. In Chapter 4, under the energy price uncertainties, in the basic model, where the natural gas is equal to a constant multiplied by the electricity price, we analytically derive the closed-form solution to the optimal electricity price threshold, above which the conventional roof should be converted to a cool roof. In the extended model, where the electricity and natural gas prices are correlated, we apply the Least Squares Monte Carlo simulation to obtain the value of the roof conversion option. Chapter 5 is the general conclusions of this dissertation.

References

Akbari, H., Konopacki, S., & Pomerantz, M. (1999). Cooling energy savings potential of reflective roofs for residential and commercial buildings in the United States. *Energy*, *24*(5), 391-407.

Alqadhi, S., Ghahari, S. A., Chen, S., Volovski, M., & Woldemariam, W. (2018). Costs and benefits of highway resurfacing: a case study of Interstate 465 in Indiana, USA. *Infrastructure Asset Management*, *5*(2), 45–55. https://doi.org/10.1680/jinam.17.00036

Elbel, B., Moran, A., Dixon, L. B., Kiszko, K., Cantor, J., Abrams, C., & Mijanovich, T. (2015). Assessment of a government-subsidized supermarket in a high-need area on household food availability and children's dietary intakes. *Public health nutrition*, *18*(15), 2881-2890.

Gao, Y., Xu, J., Yang, S., Tang, X., Zhou, Q., Ge, J., ... & Levinson, R. (2014). Cool roofs in China: Policy review, building simulations, and proof-of-concept experiments. *Energy Policy*, *74*, 190-214.

Guo, M., Liu, X. J., & Zhang, W. (2018). Using Blockchain Technology in Human Food Chain Provenance. *WIT Transactions on The Built Environment*, *179*, 391-396.

Hoeft, F. (2021). Internal combustion engine to electric vehicle retrofitting: Potential customer's needs, public perception and business model implications. *Transportation Research Interdisciplinary Perspectives*, *9*, 100330.

HHS (Health and Human Services). (2019, July 25). HHS Awards Nearly $42 Million to Expand Health Information Technology In Health Centers Nationwide. Retrieved from https://www.hhs.gov/about/news/2019/07/25/hhs-awards-nearly-42-million-to-expand-health-information-technology.html

Lukes, T. (2021). Electricity vs. Natural Gas Generation - Utility Costs, Price Correlation, and How to Save Your Facility Money. Retrieved from https://unisonenergy.com/insight/electric-and-gas-price-correlation-means-your-cogeneration-savings-will-stay-stable/ (report: https://www.unisonenergy.com/wp-content/uploads/2021/06/UNI-Why-Electric-and-Gas-Prices-Are-Correlated-for-Cogeneration-Systems-1.pdf)

Maribu, K. M., Galli, A., & Armstrong, M. (2007). Valuation of Spark-spread Options with Mean Reversion and Stochastic Volatility. *Int. J. Electron. Bus. Manag.*, *5*(3), 173-181.

Marin, M. P., Marin, I., & Vidu, L. (2019). Learning about the Reduction of Food Waste Using Blockchain Technology. In *INTED 2019 Proceedings* (pp. 3274-3277).

Ohio Auditor of State. (2012). *Are Your Road Dollars Struggling to Keep Up With Deterioration?* https://ohioauditor.gov/trainings/lgoc/2012/Are%20Your%20Road%20Dollars%20Struggling%20to%20Keep%20Up%20with%20Deterioration.pdf

Portland Cement Association (PCA). (2012, February). *The New Paving Realities: The Impact of Asphalt Cost Escalator Clauses on State Finances*. Portland Cement Association (PCA) Market Intelligence. http://www2.cement.org/econ/pdf/escalator_report_2-27-12.pdf

Pressler, M. (2022, February 18). Average US Electricity Costs & The Effect of Energy Deregulation. Retrieved from https://quickelectricity.com/average-electricity-prices-and-deregulation/

Solatifar, N. (2021). Analysis of Uncertainties in Deterioration Process of Asphalt Pavements based on Roughness Index Using LTPP Data. *Amirkabir Journal of Civil Engineering*, *53*(4), 1-1. https://doi.org/10.22060/CEEJ.2019.16072.6116

State of Alaska - Department of Commerce, Community, and Economic Development. (2019, October). Newtok Planning Group - Newtok Relocation News. Retrieved from https://www.commerce.alaska.gov/web/dcra/PlanningLandManagement/NewtokPlanningGroup/RelocationNews.aspx

Thames Street Works. (n.d.). *What is Road Resurfacing?* Retrieved November 21, 2021, from https://www.thbuk.co.uk/what-is-road-resurfacing/

Tornquist, D. (2007, September). *Growth in Highway Construction and Maintenance Costs* (CR-2007-079). Federal Highway Administration. https://www.oig.dot.gov/sites/default/files/Growth_in_Highway_Construction_and_Maintenance_Costs_Final.pdf

U.S. Energy Information Administration (EIA). (2021a, April 12). Electricity explained - Factors affecting electricity prices. Retrieved from https://www.eia.gov/energyexplained/electricity/prices-and-factors-affecting-prices.php

U.S. Energy Information Administration (EIA). (2021c, September 15). Electricity Detailed State Data - Average Price by State by Provider (EIA-861). Retrieved from https://www.eia.gov/electricity/data/state/

U.S. Energy Information Administration (EIA). (2021d, September). 2018 Commercial Buildings Energy Consumption Survey. Retrieved from https://www.eia.gov/consumption/commercial/

U.S. Energy Information Administration (EIA). (2022b, January 31). Illinois Price of Natural Gas Sold to Commercial Consumers. Retrieved from https://www.eia.gov/dnav/ng/hist/n3020il3a.htm

Walmart Food Safety & Health. (2018). *Fresh Leafy Greens New Walmart Food Traceability Initiative Questions and Answers.* Retrieved from https://corporate.walmart.com/media-library/document/leafy-greens-food-safety-traceability-requirements-faq/_proxyDocument?id=00000166-0c8e-dc77-a7ff-4dff95cb0001

Wisconsin Department of Transportation. (n.d.). *Highway Improvement Type Definitions*. Retrieved November 21, 2021, from https://wisconsindot.gov/Documents/doing-bus/local-gov/astnce-pgms/highway/tools/definitions.pdf

Yiannas, F. (2018). A New Era of Food Transparency Powered by Blockchain. *Innovations: Technology, Governance, Globalization*, *12*(1-2), 46-56.

CHAPTER 2. BLOCKCHAIN TRACEABILITY VALUATION FOR PERISHABLE AGRICULTURAL PRODUCTS UNDER DEMAND UNCERTAINTY

Zhuoyi Zhao, Kyung Jo Min

Department of Industrial and Manufacturing Systems Engineering

Iowa State University

Modified from a manuscript published in the *International Journal of Operations Research and Information Systems (IJORIS)*

Abstract

Nowadays, various perishable agricultural products are recalled due to harmful health risks. Blockchain has been used to reduce the amount of such products wasted and disposed. Specifically, a supply chain with a wholesaler, a retailer, and customers is considered where the retailer decides when to switch from a conventional supply chain information management system (SCIMS) to a blockchain-based SCIMS. This article models the uncertain customers' demand as a geometric Brownian motion process and shows how to obtain the optimal demand threshold above which the switch occurs and the corresponding expected time. Next, the model is extended by incorporating two types of government subsidies (i.e., a fixed subsidy on the switching cost and a variable subsidy per unit demand). Through sensitivity analysis and numerical studies, the impacts of key parameters on the optimal demand threshold and expected switching time are presented. Finally, managerial insights and policy implications are derived.

Keywords: Real Options, Demand Uncertainty, Blockchain, Government Subsidy, Traceability Valuation, Supply Chains, Perishable Agricultural Products, Geometric Brownian Motion (GBM)

Introduction

It has been frequently reported that various perishable agricultural products, such as romaine lettuce, are recalled and disposed due to harmful health risks. In such a case, in a conventional supply chain information management system (SCIMS), the traceability of the source of the harmful health risks is low and time-consuming (Blissett & Harreld, 2008). The reason is that data is simply recorded on paper for traceability purposes by numerous stakeholders in the supply chain of perishable agricultural products, while the rest use digital methods (Yiannas, 2018). This leads to the inconsistency in the use of SCIMS, and stakeholders cannot communicate with each other or effectively trace the origins of products on short notice. As a result, many perishable agricultural products that are potentially not contaminated are wasted and disposed of as a precaution during perishable agricultural product recalls. This situation calls for a solution for enhanced traceability in the supply chain of perishable agricultural products.

To address this problem, the perishable food industry has been implementing blockchain, "… a shared, immutable ledger that facilitates the process of recording transactions and tracking assets in a business network" (Gupta, 2018). In a blockchain network, timestamped transaction data is stored in blocks linked in a chain by hashes. This mechanism prevents the alternation or insertion of any block. In a blockchain-based SCIMS, all the information throughout every step, such as product identification, batch codes, purchase orders, and time codes of harvesting, processing, shipping, and receiving, is collected and shared by all stakeholders (e.g., farms, distribution centers, stores; Walmart Food Safety & Health, 2018). With Hyperledger Fabric (a blockchain framework), blockchain offers a more efficient way to pinpoint where the contamination originated and reduce the unnecessarily broad recalls (Guo, Liu, & Zhang, 2018).

For example, in a pilot study of mango products, blockchain substantially reduced the time to identify the originating farm from nearly seven days to 2.2 seconds (Yiannas, 2018).

Also, typically, large retailers (e.g., Walmart, Sam’s Club) perform like pioneers in adopting new technology. In 2018, Walmart and Sam’s Club required all the leafy green vegetable suppliers to utilize blockchain for traceability purposes by September 2019 to reduce the loss of retailers and suppliers during recalls (Walmart, 2018).

Meanwhile, the government grants subsidies for the public's welfare, especially when it is related to information technology. For instance, the government subsidizes supermarkets in high-need areas to improve the food environment in underserved neighborhoods (Elbel, Moran, Dixon, Kiszko, Cantor, Abrams & Mijanovich, 2015). In 2019, through the Health Resources and Services Administration (HRSA), the U.S. Department of Health and Human Services (HHS) subsidized 49 Health Center Controlled Networks (HCCNs) with almost $42 million to expand the use of health information technology (HHS, 2019). Considering that the blockchain enhances the traceability in the supply chain and reduces the harmful health risks, it is reasonable to assume that government provides the retailers in a perishable product supply chain with subsidies to facilitate their switching to a blockchain-based SCIMS.

Considering the lump sum switching cost and a series of transition actions that occur at the time of switching, the retailer’s decision on switching from the conventional SCIMS to the blockchain-based SCIMS is large and highly irreversible. Moreover, such a switch is often made under uncertainties such as the demand uncertainty of retail customers. Specifically, when the retail customers’ demand is low, for the retailer, the profit saved by the blockchain-based SCIMS may not offset the costs associated with the switching. Method-wise, the real options approach is used in this paper as it captures the uncertainty in the decision-making process instead of the traditional Net Present Value (NPV) approach. A real option refers to the right but not the obligation to take ownership of a real asset or project at a specific time in the future (Tallon, Kauffman, Lucas, Whinston, & Zhu, 2002; Wu, Wu, & Wen, 2010). The real options approach originated from the finance area and has been extended to the decision-making in the engineering discipline.

Under these circumstances, it is highly desirable to understand how a retailer can make economically rational decisions on switching from a conventional SCIMS to a blockchain-based SCIMS and how the government subsidies influence the retailer's decision on such a switch. Towards these goals, in this paper, under the assumption that the retail customers' demand for a single perishable agricultural product follows a Geometric Brownian Motion (GBM) process, the authors (1) valuate the traceability in the supply chain to determine the optimal time for a retailer to switch from a real options perspective in the basic model, (2) extend the basic model by incorporating two types of government subsidies, namely, a fixed subsidy on the switching cost and a variable subsidy per unit demand, and determine the new optimal time for the retailer to switch, (3) derive managerial insights and economic implications for the retailer's switch decision from analytical/numerical sensitivity analyses, and (4) provide policy implications from the government's perspective.

The critical contributions of this research include (1) closed-form solutions for the optimal threshold of retail customers' demand above which the SCIMS switch occurs and the corresponding expected time without/with the presentence of government subsidies, (2) an insight that, as the retail customers' demand becomes more volatile, the retailer should defer the switch of SCIMS, (3) from a government's perspective, a small amount of variable subsidy is more efficient for a rapid switch among retailers, while a fixed subsidy anticipates for a more even pace of switch. Also, the fixed subsidy is more efficient at a higher level than the variable subsidy, which is more efficient at a lower level.

The remainder of this article is organized as follows. A review of the literature on the blockchain and real options is presented in the next section. Then the authors present the model formulation and analysis for a basic model and an extended model with two government subsidies. After that, a numerical example of romaine lettuce is conducted to demonstrate how the key parameters change impacts the optimal demand threshold and the expected switching time. Finally, conclusions, limitations, and future research are presented, respectively.

Literature Review

Blockchain

The development of blockchain has boosted a series of discussions and attempts at its application in perishable agricultural supply chains. For instance, Tian (2016) developed a conceptual framework for an agricultural product supply chain traceability system combining blockchain with RFID technology. Moreover, it is estimated that every year, around 1/3 of food is lost or wasted in the world (FAO, 2020). Among such loss and waste, 8% is caused by improper packaging and storage, especially for perishable products such as fresh produce, meat, and dairy products, since they require strict temperature and packaging conditions (Blockchain Guru, 2019). One promising solution is to use RFID tags and sensors to track the transportation and storage conditions along the shipping journey and use Smart Contracts (a special feature of blockchain) to notify all stakeholders in the network whenever abnormal conditions occur. Also, according to IBM Research (2020), 45% of fruits and vegetables are spoiled and wasted because of a chaotic distribution system. This is because the imprecise nature of supply chains based on such systems forces farmers to make planting and harvesting decisions based on guesswork and sellers to predict customer demand and behavior based on incomplete information. The solution to this problem is implementing a blockchain-enabled food supply chain enhanced by Internet of Things (IoT) devices and Artificial Intelligence (AI) computing. IoT sensors track fruits, vegetables, or any other food items along the journey from field to grocery store, and AI-enhanced, real-time data enables retailers to better understand consumers' eating patterns. In this way, farmers and suppliers know the amount of perishable produce they should grow or order to meet the demand, and thus the perishable produce is fresher, and less amount is thrown away.

Regarding the reduction of wastage and disposal in the perishable agricultural supply chain in this paper, the advantages and disadvantages of using the blockchain-based SCIMS are summarized in Table 2.1.

Table 2.1. Advantages and Disadvantages of Using the Blockchain-Based SCIMS to Reduce the Wastage and Disposal in the Supply Chain of Perishable Agricultural Products

Advantage	**Disadvantages**
- Blockchain provides end-to-end traceability, which allows the stakeholders in the supply chain to access the remaining shelf life of perishable food by tracking its journey and freshness (IBM, 2018). - Blockchain invites stakeholders to trade in a trusting relationship (Zhang, Lee, & van de Ligt, 2016). - Blockchain efficiently improves food traceability regarding its safety and transparency in agriculture and food supply chains (Kamilaris, Fonts, & Prenafeta-Boldѵ́, 2019).	- When the demand is low, the profit saved from the reduction of wastage and disposal may not offset the costs associated with the retailer’s switch to the blockchain-based SCIMS.

Real Options

Derived from financial options, the real options approach has been broadly applied in solving decision-making problems as it incorporates the flexibility the decision-makers confront in operating decisions (Trigeorgis & Tsekrekos, 2017). In the existing literature, there are mainly three option valuation approaches, i.e., partial differential equations (Black and Scholes, 1973), trees and lattices (Cox, Ross, & Rubinstein, 1979), and simulations (Boyle, 1977). Examples of using the real options approach in investments under uncertainties are as follows. Schwartz and Zozaya-Gorostiza (2003) evaluated IT investment projects by simultaneously modeling the uncertainties in project costs and cash flows. Tauer (2006) established entry and exit decision models for dairy farmers under the milk price uncertainty. Takashima and Yagi (2009) modeled a single investment and a sequential investment using the real options approach and showed the influence of a catastrophic event on the flexibility of the sequential one by comparing the option values of both investments under the cash flow uncertainty. They also determined the optimal investment timing and location of the power plant, given construction costs and the catastrophic event depend on the location. Wu and Liou (2011) evaluated enterprise resource planning (ERP) investment incorporating revenue and cost uncertainties and determined the optimal threshold of the ratio of revenue to cost.

In most cases, deterministic models are used in technology transition problems. However, they are not able to incorporate uncertainties. For instance, in 2010, Cook and Ali used the NPV approach to evaluate quality improvement projects. Woo, Kim, Sung, Lee, Shin, and Lee (2019) evaluated biopharmaceutical technology regarding new drug development using an improved risk-adjusted NPV valuation model.

To the authors' knowledge, no stochastic models can be found that emphasize demand volatility where the blockchain-based SCIMS reduces wastage and disposal, and the retailer in the perishable agricultural product supply chain faces the SCIMS switch decision. Although the real options approach has many advantages, such that it captures the uncertainties as opposed to deterministic models, there are circumstances where it is not worth it (see Table 2.2).

Table 2.2 Advantages and Disadvantages of Using Real Options Approach to Solve the Switching Problem

Advantage	Disadvantages
- Real options approach captures uncertainties and provides straightforward closed-form solutions (Miller & Park, 2002). - Real options approach is not critically dependent on an accurate prediction of the retail customers' demand. Instead, economic thresholds are provided that are typically not regrettable.	- When the demand has little volatility, using the real options approach to solving the problem is not well worth it.

Model Formulation and Analysis

Basic Model

In a single perishable agricultural product supply chain consisting of a wholesaler, a retailer, and retail customers (see Figure 2.1), the authors consider a switching problem of the retailer's perspective from a conventional SCIMS to a blockchain-based SCIMS. The reason for this switch is that the blockchain-based SCIMS facilitates the traceability of the perishable product, which will reduce wastage and disposal because, for example, in the case of a virus or bacteria outbreak, the contaminated products can be pinpointed rapidly.

Figure 2.1 Supply Chain of a Single Perishable Agricultural Products

To facilitate the modeling and analysis, the following assumptions are proposed.

Assumption 2.1: The retail customers' demand for a single perishable agricultural product at time point t, D_t (lb at a day), follows a GBM process where the time granularity is a day.

$$dD_t = \alpha D_t dt + \sigma D_t dz_t \tag{2.1}$$

where α (% per day; > 0) and σ (% per square root of day; >0) are the instantaneous growth rate and volatility of the demand, respectively. dz_t is the increment of a Wiener process, and $dz_t = \epsilon\sqrt{dt}$, $\epsilon \sim N(0, 1)$.

Proposition 2.1: Suppose the retail customers' demand at time point 0 is D_0, the expected value of D_t is $E(D_t) = D_0 e^{\alpha t}$ (Dixit & Pindyck, 1994, p. 71-72). See Appendix 2A for proof.

Assumption 2.1 is based on the observation that the retail customers' demand for a perishable agricultural product increases on average and fluctuates over time. Empirical data support can be found in Table 2.3, where the authors estimate the consumption of fresh lettuce (romaine and leaf) at a day in Houston, TX from 2000 to 2017. As is shown in Figure 2.2, the consumption of fresh lettuce at a day has a positive growth rate with fluctuations over time.

Table 2.3 Estimated Consumption of Fresh Lettuce at a Day in Houston, TX, from 2000 to 2017

Year	**Annual per capita (lb) (Shahbandeh, 2019)**	**Population (million) (U.S. Census Bureau, 2019)**	**Daily consumption (lb) (Estimated)**
2000	8.4	1.9774	45,507
2001	8.0	1.9943	43,711
2002	9.6	2.0156	53,013
2003	10.8	2.0197	59,761
2004	12.0	2.0174	66,325
2005	9.7	2.0219	53,733
2006	12.0	2.0587	67,683
2007	11.5	2.0651	65,065
2008	10.4	2.0844	59,391

Table 2.3 continued

Year	**Annual per capita (lb)** **(Shahbandeh, 2019)**	**Population (million)** **(U.S. Census Bureau, 2019)**	**Daily consumption (lb)** **(Estimated)**
2009	10.0	2.1186	58,044
2010	12.0	2.0993	69,018
2011	11.7	2.1255	68,132
2012	11.9	2.1598	70,415
2013	11.4	2.1982	68,656
2014	10.8	2.2388	66,244
2015	11.9	2.2822	74,406
2016	14.5	2.3045	91,549
2017	15.0	2.3127	95,042

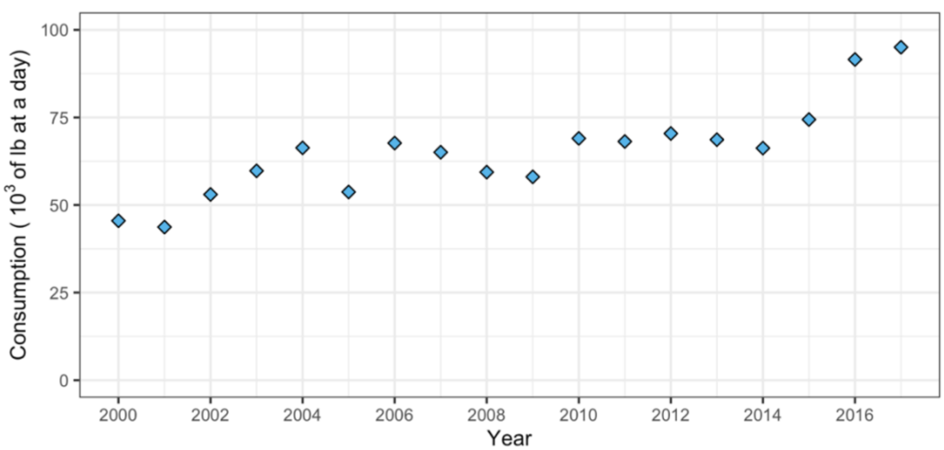

Figure 2.2 Estimated Consumption of Fresh Lettuce over Time (Houston, TX, from 2000 to 2017)

For ease of reference, the rest notations used in this paper are summarized in Table 2.4.

Table 2.4 Notations and Descriptions

Notation	**Description**
P	Unit selling price that retail customers pay to the retailer ($/lb)
C	Unit purchase price that the retailer pays to the wholesaler ($/lb)
w	The ratio of the amount of the wastage and disposal as a precaution during recalls over the demand at time point t
I	Switching cost incurred to the retailer at the time of switching ($)
r	The ratio of the amount of wastage and disposal as a precaution during recalls using the blockchain-based SCIMS over that amount using the conventional SCIMS
C_b	Payment for using the blockchain-based SCIMS that the retailer pays to IBM ($/day)
ρ	Discount rate for money (% per day)
V_1	Project value function in phase 1 ($)
V_2	Project value function in phase 2 ($)
D^*	Optimal demand threshold above which the SCIMS switch occurs ($/lb)
T^*	Expected switching time (day)

The unit selling price P and the unit purchase price C are assumed to remain unchanged over time. Meanwhile, the costs associated with processing activities (e.g., shipping, storage, disposal) and the corresponding labor costs are not considered.

For the conventional SCIMS, the authors make the following assumptions.

Assumption 2.2: At time point t, w fraction of the demand D_t is wasted and disposed as a precaution during recalls. Hence, the total amount of the perishable product that the retailer purchases from the wholesaler is $(1 + w)D_t$ (lb at a day).

w is a constant that can be estimated from historical data by dividing the total amount of the perishable product wasted and disposed as a precaution during recalls over the retail customers' demand within the last year. This assumption yields the following proposition.

Proposition 2.2: The total amount of the perishable product that the retailer purchases from the wholesaler at time point t before switching, $(1 + w)D_t$ (lb at a day) also follows a GBM process with the same growth rate and volatility as D_t. See Appendix 2B for proof.

Assumption 2.3: The payment for using the conventional SCIMS (i.e., costs associated with phone calls, emails, and paper copies) are ignored.

Assumption 2.4: At a certain time point, the retailer switches from the conventional SCIMS to the blockchain-based SCIMS at a switching cost of I($).

Referring to the definition of adoption costs of information technology upgrades in Mukherji, Rajagopalan, & Tanniru's work (2006), in this paper, the switching cost I is defined as the cost associated with purchasing or upgrading necessary equipment, as well as training and transitioning employees completely to the blockchain-based SCIMS.

For the blockchain-based SCIMS, the authors make the following assumptions.

Assumption 2.5: At time point t, the amount of wastage and disposal as a precaution during recalls is reduced to r $(0 < r < 1)$ fraction of that amount before switching. That is, the total amount of product the retailer purchases from the wholesaler is $(1 + rw)D_t$ (lb at a day).

By collecting the product information and storing it on the network, blockchain creates a more transparent supply chain where the source of contamination can be rapidly identified, and thus, unnecessarily broad recalls are reduced (Guo et al., 2018). For instance, in the case of dairy products contamination, Marin, Marin, and Vidu (2019) claimed that blockchain could trace the originating farm within seconds, and only a batch of dairy products needs to be removed from distribution. With the above qualitative data support, the authors assume that the blockchain-based SCIMS reduces the amount of wastage and disposal of perishable agricultural products as a precaution during recalls and use a coefficient r to denote the reduction efficiency. Notably, a smaller r indicates more amount of perishable product is saved from being wasted and disposed. This assumption yields the following proposition.

Proposition 2.3: The total amount of the perishable product that the retailer purchases from the wholesaler at time point t after switching, $(1 + rw)D_t$ (lb at a day) also follows a GBM process with the same growth rate and volatility as D_t. See Appendix 2C for proof.

Assumption 2.6: Once the retailer switches to the blockchain-based SCIMS, the retailer will use it forever.

The timeline with respect to the switching of SCIMS is divided into two phases by T^*, namely, phase 1 and phase 2 (see Figure 2.3).

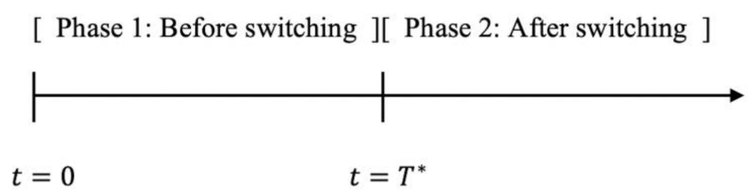

Figure 2.3 The Timeline with Respect to the Switching of SCIMS

The problem can be described as maximizing the total expected discounted value by choosing T^* as follows:

$$maxE\left[\int_0^{T^*} e^{-\rho t}[PD_t - C(1+w)D_t]dt - Ie^{-\rho T^*} + \int_{T^*}^{\infty} e^{-\rho t}[PD_t - C(1+rw)D_t - C_b]\,dt\right] \tag{2.2}$$

where $T^* = inf\,\{t \ \geq \ 0 \mid D_t \geq D^*\}$.

Phase 2: After Switching

At time point t in phase 2, when operating, the retailer has a cash flow of max $[PD_t - C(1+rw)D_t - C_b, 0]$. This implies that when $P > (1+rw)C$ and $D_t > D_{min} = \frac{C_b}{P-C(1+rw)}$, the retailer profits from the selling of the perishable agricultural product. Under a technical condition of $\rho - \alpha > 0$, the project value at time point t, $V_2(D_t)$, is equal to the expected value of discounted future cash flows as follows (Murto, 2007). The proof is given in Appendix 2D.

$$V_2(D_t) = E\left\{\int_t^{\infty} e^{-\rho(x-t)}[PD_x - C(1+rw)D_x - C_b]\,dx\right\} = \frac{[P-C(1+rw)]D_t}{\rho-\alpha} - \frac{C_b}{\rho} \qquad (2.3)$$

Phase 1: Before Switching

In phase 1, when operating, the cash flow function at time point t is given by max$[PD_t - C(1+w)D_t, 0]$. Similarly, for the retailer to make a profit, P is supposed to be greater than $(1+w)C$, and there is no requirement for D_t. The project value at time point t, $V_1(D_t)$, must satisfy the following Bellman optimality principle equation:

$$\rho V_1(D_t)dt = [PD_t - C(1+w)D_t]dt + E[dV_1(D_t)|D_t] \qquad (2.4)$$

Equation (2.4) means that at time point t, the return for holding the switching option should equal the immediate profit when holding the switching option plus the expected appreciation of the project value conditioning on the demand level.

By applying Ito's Lemma on dV_1, the following differential equation can be derived:

$$\frac{1}{2}\sigma^2 {D_t}^2 \frac{\partial^2 V_1}{\partial {D_t}^2} + \alpha D_t \frac{\partial V_1}{\partial D_t} - \rho V_1 + (P-C)D_t - CwD_t = 0 \qquad (2.5)$$

Equation (2.5) is subject to the following two boundary conditions (Siddiqui & Takashima, 2012).

$$V_1(D^*) = V_2(D^*) - I \qquad (2.6)$$

$$V_1'(D^*) = V_2'(D^*) \qquad (2.7)$$

Equation (2.6) and Equation (2.7) are the value matching and smooth pasting conditions, respectively. The value matching condition ensures that at the time of exercising the switching option, the project value before switching is equal to the project value after switching minus the switching cost. The smooth pasting condition guarantees that the slopes of the left-hand side and the right-hand side of the value matching condition are equal at the optimal demand threshold.

Under technical conditions of $\rho - \alpha > 0$ and $\alpha - \frac{\sigma^2}{2} > 0$ (Dixit & Pindyck, 1994), the general solution to Equation (2.5) is given by (see Appendix 2E for proof):

$$V_1(D_t) = A_1 {D_t}^{\beta_1} + \frac{[P-C(1+w)]D_t}{\rho-\alpha} \tag{2.8}$$

where $\beta_1 = \frac{1}{\sigma^2}\left[\frac{\sigma^2}{2} - \alpha + \sqrt{\left(\frac{\sigma^2}{2} - \alpha\right)^2 + 2\rho\sigma^2}\right]$, $\beta_1 > 1$.

Using the two boundary conditions, the coefficient A_1 and the optimal demand threshold D^* can be solved. That is, $A_1 = \frac{Cw(1-r)}{(\rho-\alpha)\beta_1 {D^*}^{\beta_1-1}}$, and D^* is given by:

$$D^* = \frac{\left(\frac{C_b}{\rho}+I\right)(\rho-\alpha)\beta_1}{Cw(1-r)(\beta_1-1)} \tag{2.9}$$

It can be verified that the expected time for the retailer to optimally switch is (Appendix 2F for proof):

$$T^* = \frac{\ln\frac{\left(\frac{C_b}{\rho}+I\right)(\rho-\alpha)\beta_1}{Cw(1-r)(\beta_1-1)} - \ln D_0}{\alpha-\frac{1}{2}\sigma^2} \tag{2.10}$$

Extended Model with Subsidies

Next, the basic model is extended by incorporating two types of government subsidies. That is, the government provides the retailer with a one-time fixed subsidy of U($) on the switching cost to initiate the switch of SCIMS and a variable subsidy S ($/lb) per unit demand for using the blockchain-based SCIMS in the supply chain of the perishable agricultural product.

Phase 2: After Switching

In phase 2, when operating, the retailer's cash flow at time point t is max $[PD_t - C(1 + rw)D_t - C_b + SD_t, 0]$, and it is required that $P > (1 + rw)C$ and $D_t > D_{min} = \frac{C_b}{P-C(1+rw)+S}$. Given $\rho - \alpha > 0$, the project value, $V_2(D_t)$, is equal to the expected value of discounted cash flows as follows (Murto, 2007). The proof is given in Appendix 2G.

$$V_2(D_t) = E\left\{\int_t^{\infty} e^{-\rho(x-t)}[PD_x - C(1 + rw)D_x + SD_x - C_b]\, dx\right\} = \frac{[P-C(1+rw)+S]D_t}{\rho-\alpha} - \frac{C_b}{\rho} \quad (2.11)$$

Phase 1: Before Switching

When operating, the project value at time point t, $V_1(D_t)$, remains the same as Equation (2.8) in the basic model, i.e., $V_1(D_t) = A_1 {D_t}^{\beta_1} + \frac{[P-C(1+w)]D_t}{\rho-\alpha}$, but now $V_1(D_t)$ is subjective to the following two boundary conditions:

$$V_1(D^*) = V_2(D^*) - (I - U) \quad (2.12)$$

$$V_1{}'(D^*) = V_2{}'(D^*) \quad (2.13)$$

Equation (2.12) is the value matching condition, which suggests that at the time of exercising the switching option, the project value before switching should be equal to the project value after switching minus the switching cost net of the fixed subsidy. Equation (2.13) is the smooth pasting condition, and it ensures the slopes of both sides of Equation (2.12) are equal at the switching time.

Sequentially, it can be verified that $A_1 = \frac{Cw(1-r)+S}{(\rho-\alpha)\beta_1 {D_1^*}^{\beta_1-1}}$, and the optimal demand threshold D^* is:

$$D^* = \frac{(\frac{C_b}{\rho}+I-U)(\rho-\alpha)\beta_1}{[Cw(1-r)+S](\beta_1-1)} \quad (2.14)$$

Similarly, with the two types of government subsidies, the expected switching time becomes:

$$T^* = \frac{\ln\frac{\left(\frac{C_b}{\rho}+I-U\right)(\rho-\alpha)\beta_1}{[Cw(1-r)+S](\beta_1-1)} - \ln D_0}{\alpha-\frac{1}{2}\sigma^2} \tag{2.15}$$

Analytical Sensitivity Analysis

Among the ten parameters that determine the optimal demand threshold D^*, the authors conduct analytical sensitivity analysis on seven of them (C, w, r, I, C_b, U, S), and numerically examine the impact of the rest three (σ, α and ρ) on D^* as the partial derivatives with respect to them cannot be explicitly obtained. Also, in the stochastic optimal control theory, the optimal project value corresponds to timing, so sensitivity analysis on T^* is included as well.

Corollary 2.1: Given $\rho > \alpha$ and $\alpha - \frac{\sigma^2}{2} > 0$, $\frac{\partial D^*}{\partial C} < 0$, $\frac{\partial T^*}{\partial C} < 0$, $\frac{\partial D^*}{\partial w} < 0$, and $\frac{\partial T^*}{\partial w} < 0$.

The proof is given in Appendix 2H. This corollary indicates that when the unit purchase price of the perishable product increases or a larger proportion of the perishable product is wasted and disposed as a precaution during recalls, the optimal demand threshold and the expected switching time decrease. In such cases, the retailer loses more money due to wastage and disposal. Consequently, the retailer will switch to the blockchain-based SCIMS earlier from an economic perspective.

Corollary 2.2: Given $\rho > \alpha$ and $\alpha - \frac{\sigma^2}{2} > 0$, $\frac{\partial D^*}{\partial r} > 0$, $\frac{\partial T^*}{\partial r} > 0$.

The proof is given in Appendix 2I. The positive partial derivatives suggest that a larger coefficient of reduction efficiency leads to a higher optimal demand threshold and the expected switching time. This is because a larger r implies that less perishable agricultural product is saved from being wasted and disposed of by the blockchain-based SCIMS. As a result, it is economically rational for the retailer to defer the switching option.

Corollary 2.3: Given $\rho > \alpha$ and $\alpha - \frac{\sigma^2}{2} > 0$, $\frac{\partial D^*}{\partial I} > 0$, $\frac{\partial T^*}{\partial I} > 0$, $\frac{\partial D^*}{\partial C_b} > 0$, and $\frac{\partial T^*}{\partial C_b} > 0$.

The proof is given in Appendix 2J. Corollary 2.3 suggests that as the switching cost or the payment for using the blockchain-based SCIMS increases, the optimal demand threshold and the expected switching time increase. This makes economic sense because, under such circumstances, the retailer benefits less from the SCIMS switch, so there is less incentive for the retailer to switch. Therefore, the retailer will wait longer before exercising the switching option.

Corollary 2.4: Given $\rho > \alpha$ and $\alpha - \frac{\sigma^2}{2} > 0$, $\frac{\partial D^*}{\partial U} < 0$, $\frac{\partial T^*}{\partial U} < 0$, $\frac{\partial D^*}{\partial S} < 0$, and $\frac{\partial T^*}{\partial S} < 0$.

The proof is given in Appendix 2K. The interpretation of Corollary 2.4 is as follows. When the government provides the retailer with a higher fixed subsidy on the switching cost or a higher variable subsidy per unit demand, the retailer has a lower switching cost or a higher cash flow after switching. Either way, the retailer will be more eager to switch from an economic perspective, so the optimal demand threshold and expected switching time will decrease.

Numerical Study

In this section, the authors conduct a numerical study on romaine lettuce to further demonstrate the findings in the previous section. The parameter values and references are summarized in Table 2.5, where some parameter values are hypothetical due to the lack of numerical data.

Table 2.5 Parameters and Values

Parameter	**Value**	**References**
α	0.0505	Shahbandeh (2019); U.S. Census Bureau (2019); Method 3 in Croghan, Jackman, and Min's paper (2017)
σ	0.1202	
D_0	78,552 (lb at a day)	Population USA (2019); Shahbandeh, 2019)

Table 2.5 continued

Parameter	Value	References
P	0.94 ($/lb)	USDA (2019)
C	0.36 ($/lb)	USDA (2019)
w	0.137	ExerciseBike (2019)
C_b	133.33 ($/day)	IBM Cloud (2019)
ρ	0.0543	Damodaran (2019)
r	0.4	Hypothetical
I	1,000,000 ($)	Hypothetical
U	200,000 ($)	Hypothetical
S	0.05 ($/lb)	Hypothetical

The key numerical results in Table 2.6 show that, in the basic model where no subsidies are provided, the optimal demand threshold is 2,100,161 (lb at a day), and the corresponding expected switching time is 76 (day). With the presentence of two types of government subsidies, in the extended model, the optimal demand threshold is reduced to 625,047 (lb at a day), and correspondingly, the expected switching time is reduced to 48 (day). Also, the minimum demand level for the retailer to make a profit from the selling of the perishable product is reduced from 238 (lb at a day) to 218 (lb at a day) when the two government subsidies are provided.

Table 2.6 Numerical Results

Notation	Value (basic model - no subsidies)	Value (extended model - with subsidies)
β_1	1.0653	1.0653
A_1	2.8255	8.2255
D_{min}	238 (lb at a day)	218 (lb at a day)

Table 2.6 continued

Notation	Value (basic model - no subsidies)	Value (extended model - with subsidies)
D^*	2,100,161 (lb at a day)	625,047 (lb at a day)
T^*	76 (day)	48 (day)

Next, numerical sensitivity analysis is conducted on σ, α, and ρ, since their impact on D^* and T^* has not been analytically examined.

Figure 2.4 illustrates that as the demand becomes more volatile, the optimal demand threshold and the expected switching time increase, meaning that the exercise of the retailer's switching option should be deferred. This is because, with higher demand uncertainty, the flexibility to exercise the switching option at any time point becomes more valuable. Hence, it is economically rational for the retailer to hold the switching option longer and wait for more information.

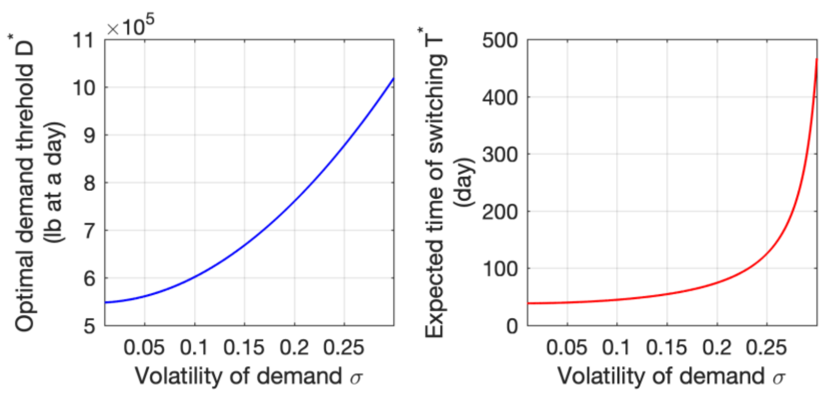

Figure 2.4 Variation of D^* and T^* with Respect to σ

In terms of the growth rate of demand, when it increases, the optimal demand threshold and the expected switching time decrease (see Figure 2.5). This is because when the retail customers' demand for the perishable product is rapidly growing, the retailer's benefit from using the blockchain-based SCIMS is amplified. Therefore, the retailer prefers to exercise the switching option earlier.

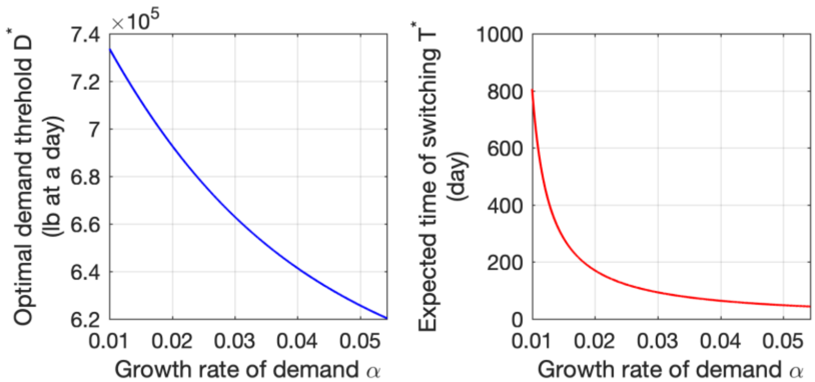

Figure 2.5 Variation of D^* and T^* with Respect to α

As shown in Figure 2.6, when the discount rate for money increases, the optimal demand threshold and the expected switching time increase. The reason is that, when money is heavily discounted, the retailer's loss due to wastage and disposal during recalls is trivial. Consequently, the retailer has less incentive to switch from the conventional SCIMS to the blockchain-based SCIMS.

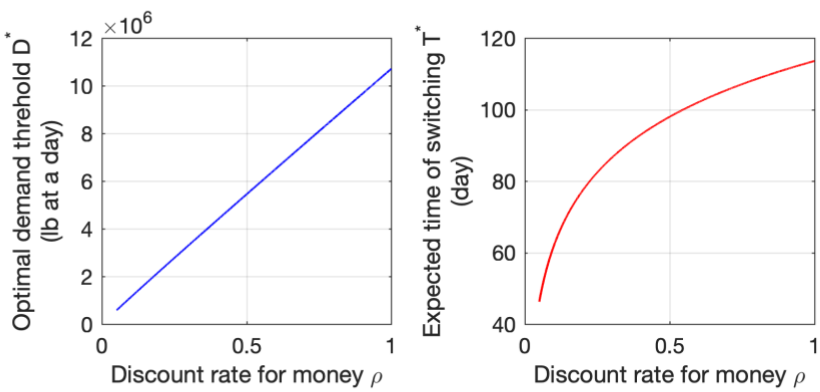

Figure 2.6 Variation of D^* and T^* with Respect to ρ

Although the magnitude of the partial derivative of D^* and T^* with respect to U and S have been given in the sensitivity analysis section, the authors include Figure 2.7 and Figure 2.8 to discuss the convexness and concaveness of these curves. Intuitively, the optimal demand threshold linearly decreases as the fixed subsidy on switching cost increases, and convex decreases as the variable subsidy per unit demand increases. Specifically, when the variable subsidy S increases from 0 to 0.1 (\$/lb), the optimal demand threshold D^* substantially decreased from 1.68×10^6(lb at a day) to 0.38×10^6 (lb at a day). However, when S increases from 0.3 (\$/lb) to 0.4 (\$/lb), D^* decreased from 0.15×10^6 (lb at a day) to 0.11×10^6 (lb at a day). This implies that, from a perspective of the optimal demand threshold reduction, a small amount of variable subsidy is more economically efficient than the fixed subsidy if the government expects retailers to rapidly switch to the blockchain-based SCIMS. On the other hand, the fixed subsidy is more viable than the variable subsidy when government anticipates an even switch among retailers.

As for the expected switching time, it is concave decreasing when the fixed subsidy increases and convex decreasing when the variable subsidy increases. This means that, regarding the expected switching time reduction, the fixed subsidy is more efficient at a higher level, while the variable subsidy is more efficient at a lower level.

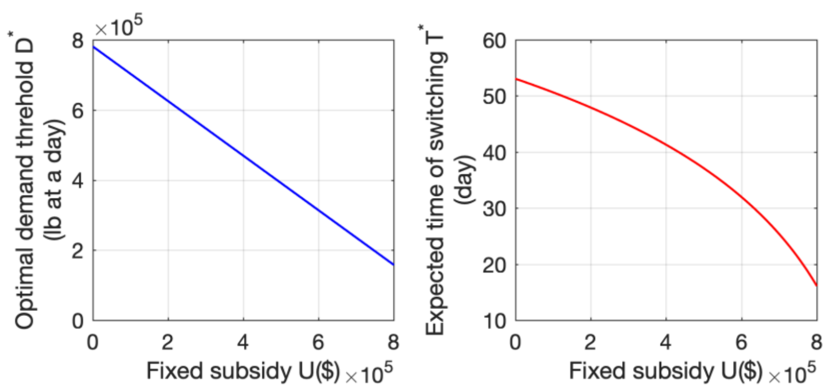

Figure 2.7 Variation of D^* and T^* with respect to U

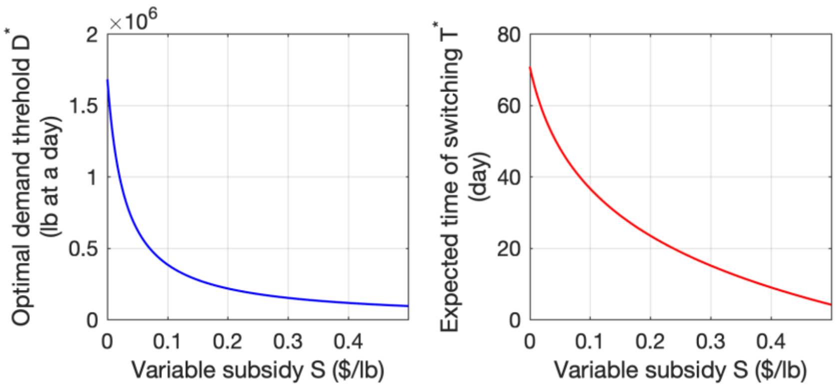

Figure 2.8 Variation of D^* and T^* with respect to S

Conclusions

This paper considers a retailer in a supply chain of a perishable agricultural product who faces a volatile retail customers' demand and decides when to switch to a blockchain-based SCIMS from a conventional SCIMS. The authors investigated how economically rational decisions can be made on such a switch from a real options perspective under the assumption that the retail customers' demand for a single perishable agricultural product follows a GBM process. Specifically, without/with the presentence of a fixed subsidy and a variable subsidy from the government, the authors constructed mathematical models and obtained the closed-form solutions of the demand thresholds for the retailer to optimally switch and the corresponding expected switching time. A series of managerial insights and policy implications are derived by analytically and numerically examining the impact of key parameters on the optimal demand threshold and the expected switching time. For instance, the retailer is recommended to defer the switching option when the customers' demand is volatile. Furthermore, from the government's perspective, a small amount of variable subsidy should be promoted if the government anticipates the retailers to rapidly switch to the blockchain-based SCIMS in a short time, while a fixed subsidy is recommended if an even pace of switch among retailers is expected. Also, the fixed subsidy is more efficient at a higher level than the variable subsidy, which is more efficient at a lower level.

The novelty of this paper is to show under what conditions a retailer can switch from a conventional SCIMS to a blockchain-based SCIMS and the expected time for the switch when the uncertain demand is characterized by a GBM process.

Limitations and Future Research

There are a few limitations in this paper which can be addressed in future research. First, the assumption that the blockchain-based SCIMS reduces the amount of wastage and disposal to r fraction of that using the conventional SCIMS (assumption 2.5) is based on qualitative inference and lacks quantitative data support. The authors anticipate quantitative data support to justify this assumption as the development of blockchain. Secondly, the demand is modeled as a GBM process, which indicates that the demand increases on average and fluctuates over time. Research can be expanded by modeling the demand as a jump-diffusion process considering that there can be a substantial reduction in the demand when recalls happen. Thirdly, besides the demand uncertainty, other uncertainties such as the uncertainties in the unit selling price and the technology innovations (e.g., blockchain may require updates or be replaced by a more advanced SCIMS in the future) can be incorporated into future research. Moreover, one can model the blockchain-based SCIMS switch decision from a perspective of other stakeholders, such as the wholesaler or the farm cooperative. Discussions can be expanded to the valuation of the blockchain-based system regarding other properties such as transparency, immutability, and irrefutability in various industries (e.g., financial, insurance, manufacturing industry).

Acknowledgement

The authors would like to thank Exploratory Research Projects Programs in the Department of Industrial and Manufacturing Systems Engineering and the College of Engineering at Iowa State University for funding.

The authors would also like to thank Dr. John Jackman for sharing his expertise in blockchain and stochastic optimal control theory and for providing constructive and developmental feedback.

References

Black, F., & Scholes, M. (1973). The pricing of options and corporate liabilities. *Journal of political economy*, *81*(3), 637-654.

Blissett, G. & Harreld, J.C. (2008). *Full Value Traceability*. Retrieved from http://www-935.ibm.com/services/at/bcs/pdf/wp-cons-traceability.pdf

Blockchain Guru. (2019, May 22). *Can Blockchain Technology Reduce Food Waste*? Retrieved from https://blockchainguru.ca/blog/f/can-blockchain-technology-reduce-food-waste

Boyle, P. P. (1977). Options: A monte carlo approach. *Journal of financial economics*, *4*(3), 323-338.

Cook, V. G. C., & Ali, A. (2010). Using net present value methods to evaluate quality improvement projects. *International Journal of Quality & Reliability Management*.

Cox, J. C., Ross, S. A., & Rubinstein, M. (1979). Option pricing: A simplified approach. *Journal of financial Economics*, *7*(3), 229-263.

Croghan, J., Jackman, J., & Min, K. J. (2017). Estimation of Geometric Brownian Motion Parameters for Oil Price Analysis. In *IIE Annual Conference. Proceedings* (pp. 1858-1863). Institute of Industrial and Systems Engineers (IISE).

Damodaran, A. (2019, January). *Cost of Capital by Sector (US)*. Retrieved from http://people.stern.nyu.edu/adamodar/New_Home_Page/datafile/wacc.htm

Dixit, R. K. & Pindyck, R. (1994). *Investment under uncertainty*. Princeton NJ, Princeton university press.

Elbel, B., Moran, A., Dixon, L. B., Kiszko, K., Cantor, J., Abrams, C., & Mijanovich, T. (2015). Assessment of a government-subsidized supermarket in a high-need area on household food availability and children’s dietary intakes. *Public health nutrition*, *18*(15), 2881-2890.

ExerciseBike. (2019). *Food Recalls Across the U.S.*. Retrieved from https://www.exercisebike.ca/food-recalls-by-state/

FAO (Food and Agricultural Organization of the United States). (2020). *Food Loss and Food Waste*. Retrieved from http://www.fao.org/food-loss-and-food-waste/en/

Guo, M., Liu, X. J., & Zhang, W. (2018). Using Blockchain Technology in Human Food Chain Provenance. *WIT Transactions on The Built Environment, 179*, 391-396.

Gupta, M. (2018). *Blockchain for Dummies*. Hoboken, NJ: John Wiley & Sons, Inc.

HHS (Health and Human Services). (2019, July 25). *HHS Awards Nearly $42 Million to Expand Health Information Technology In Health Centers Nationwide*. Retrieved from https://www.hhs.gov/about/news/2019/07/25/hhs-awards-nearly-42-million-to-expand-health-information-technology.html

IBM. (2018). *Focus on Food Freshness*. Retrieved from https://www.ibm.com/downloads/cas/QK0MVJNZ

IBM Cloud. (2019, September 6). *Pricing*. Retrieved from https://console.bluemix.net/docs/services/blockchain/howto/pricing.html#pricing

IBM Research. (2020). *Blockchain will prevent more food from going to waste.* Retrieved from https://www.research.ibm.com/5-in-5/harvest/

Kamilaris, A., Fonts, A., & Prenafeta-Boldύ, F. X. (2019). The rise of blockchain technology in agriculture and food supply chains. *Trends in Food Science & Technology, 91*, 640-652.

Luenberger, D. G. (1998). *Investment Science*. New York, NY: Oxford University Press.

Marin, M. P., Marin, I., & Vidu, L. (2019). Learning about the Reduction of Food Waste Using Blockchain Technology. In *INTED 2019 Proceedings* (pp. 3274-3277).

Miller, I., Miller, M., & Freund, J. E. (2014). *John E. Freund's mathematical statistics with applications*. Boston: Pearson.

Miller, L. T., & Park, C. S. (2002). Decision making under uncertainty—real options to the rescue?. *The engineering economist*, *47*(2), 105-150.

Mukherji, N., Rajagopalan, B., & Tanniru, M. (2006). A decision support model for optimal timing of investments in information technology upgrades. *Decision Support Systems*, *42*(3), 1684-1696.

Murto, P. (2007). Timing of investment under technological and revenue-related uncertainties. *Journal of Economic Dynamics and Control*, *31*(5), 1473-1497.

Population USA. (2019). *Houston Population 2019.* Retrieved from https://www.usapopulation.org/houston-population/

Schwartz, E. S., & Zozaya-Gorostiza, C. (2003). Investment under uncertainty in information technology: acquisition and development projects. *Management Science*, *49*(1), 57-70.

Shahbandeh, M. (2019, May 10). *Per capita consumption of fresh lettuce (romaine and leaf) in the United States from 2000 to 2018 (in pounds).* Retrieved from https://www.statista.com/statistics/257322/per-capita-consumption-of-fresh-lettuce-romaine-and-leaf-in-the-us/

Siddiqui, A., & Takashima, R. (2012). Capacity switching options under rivalry and uncertainty. *European Journal of Operational Research*, *222*(3), 583-595.

Sigman, K. (2006). *Geometric Brownian motion*. Retrieved from http://www.columbia.edu/~ks20/FE-Notes/4700-07-Notes-GBM.pdf

Takashima, R., & Yagi, K. (2009). Optimal investment timing and location under uncertainty. In *13th International Conference on Real Options*.

Tallon, P. P., Kauffman, R. J., Lucas, H. C., Whinston, A. B., & Zhu, K. (2002). Using real options analysis for evaluating uncertain investments in information technology: Insights from the ICIS 2001 debate. *Communications of the Association for Information Systems*, *9*(1), 9.

Tauer, L. W. (2006). When to get in and out of dairy farming: a real option analysis. *Agricultural and Resource Economics Review*, *35*(2), 339-347.

Tian, F. (2016, June). An agri-food supply chain traceability system for China based on RFID & blockchain technology. In *Service Systems and Service Management (ICSSSM), 2016 13th International Conference on* (pp. 1-6). IEEE.

Trigeorgis, L., & Tsekrekos, A. E. (2017). Real Options in Operations Research: A Review and Synthesis. *European Journal of Operational Research*.

U.S. Census Bureau. (2019, September 19). *Population of Houston City, TX*. Retrieved from https://www.google.com/publicdata/explore?ds=kf7tgg1uo9ude_&met_y=population&idim=place:4835000:4819000&hl=en&dl=en

USDA (United States Department of Agriculture). (2019, August 20). *Price Spreads from Farm to Consumer*. Retrieved from https://www.ers.usda.gov/data-products/price-spreads-from-farm-to-consumer/price-spreads-from-farm-to-consumer/

Walmart. (2018). *Walmart and Sam's Club to Require Real-Time, End-to-End Food Traceability with Blockchain*. Retrieved from https://corporate.walmart.com/media-library/document/leafy-greens-on-blockchain-press-release/_proxyDocument?id=00000166-0c4c-d96e-a3ff-8f7c09b50001

Walmart Food Safety & Health. (2018). *Fresh Leafy Greens New Walmart Food Traceability Initiative Questions and Answers.* Retrieved from https://corporate.walmart.com/media-library/document/leafy-greens-food-safety-traceability-requirements-faq/_proxyDocument?id=00000166-0c8e-dc77-a7ff-4dff95cb0001

Woo, J., Kim, E., Sung, T. E., Lee, J., Shin, K., & Lee, J. (2019). Developing an Improved Risk-Adjusted Net Present Value Technology Valuation Model for the Biopharmaceutical Industry. *Journal of Open Innovation: Technology, Market, and Complexity*, *5*(3), 45.

Wu, L. C., & Liou, F. M. (2011). A quantitative model for ERP investment decision: considering revenue and costs under uncertainty. *International Journal of Production Research*, *49*(22), 6713-6728.

Wu, L., Wu, L., and Wen, Y. (2010). "Interdisciplinary Research of Options Theory and Management Information Systems: Review, Research Issues, and Suggestions for Future Research," Industrial Management & Data Systems (110:3), pp. 433-452.

Yiannas, F. (2018). A New Era of Food Transparency Powered by Blockchain. *Innovations: Technology, Governance, Globalization*, *12*(1-2), 46-56.

Zhang, Y., Lee, S., & van de Ligt, J. L. G. (2016). *Blockchain Technology: What Is It?* Retrieved from https://vetmed.umn.edu/sites/vetmed.umn.edu/files/shmp_2018l19.46_blockchain_technology_part_1-sciencepage.pdf

Appendices

Appendix 2A. Proof of Proposition 2.1

Define $F_t = \ln(D_t)$. By Ito's Lemma, the total differential of function F_t is as follows (Dixit & Pindyck, 1994, p. 80):

$$dF_t = \frac{\partial F_t}{\partial t}dt + \frac{\partial F_t}{\partial D_t}dD_t + \frac{1}{2}\frac{\partial^2 F_t}{\partial {D_t}^2}(dD_t)^2$$

$$= \frac{1}{D_t}(\alpha D_t dt + \sigma D_t dz_t) + \frac{1}{2}\left(-\frac{1}{{D_t}^2}\right)(\alpha D_t dt + \sigma D_t dz_t)^2$$

$$= (\alpha dt + \sigma dz_t) - \frac{1}{2}(\alpha^2 dt^2 + \sigma^2 {dz_t}^2 + 2\alpha dt\sigma dz_t) \qquad (2A.1)$$

where $\frac{\partial F_t}{\partial t} = 0$ (because the function $F_t = \ln(D_t)$ has a steady state regardless of the value of t), $\frac{\partial F_t}{\partial D_t} = \frac{1}{D_t}$, and $\frac{\partial^2 F_t}{\partial {D_t}^2} = -\frac{1}{{D_t}^2}$. Since $dz_t = \epsilon\sqrt{dt}$, ${dz_t}^2 = \epsilon^2 dt$ and $dtdz_t = \epsilon dt^{\frac{3}{2}}$. Terms in

dt^2 and $dt^{\frac{3}{2}}$ go to zero faster than dt as it becomes infinitesimally small, so they can be ignored (Dixit & Pindyck, 1994, p. 80). Also, ${dz_t}^2 = \epsilon^2 dt \cong E(\epsilon^2)dt = \{Variance(\epsilon) + [E(\epsilon)]^2\}dt = (1 + 0^2)dt = dt$. Hence,

$$dF_t = (\alpha dt + \sigma dz_t) - \frac{1}{2}(\sigma^2 dt) = (\alpha - \frac{1}{2}\sigma^2)dt + \sigma dz_t \tag{2A.2}$$

Therefore, $\ln(D_t) = \ln(D_0) + (\alpha - \frac{1}{2}\sigma^2)t + \sigma z_t$, where D_0 is the value of D_t at time point 0. Stated otherwise, D_t is a lognormal process and can be written as $D_0 e^{(\alpha - \frac{1}{2}\sigma^2)t + \sigma z_t}$ (Luenberger, 1998, p. 308-309).

For a random variable $X \sim N(\mu, \sigma^2)$, the moment generating function (MGF) is as follows (Miller, Miller & Freund, 2014, p. 187):

$$M_X(s) = E(e^{sX}) = e^{\mu s + \frac{1}{2}\sigma^2 s^2}, -\infty < s < \infty \tag{2A.3}$$

For a random variable $F_t \sim N\left((\alpha - \frac{1}{2}\sigma^2)t, \sigma^2 t\right)$, the MGF is given by (Sigman, 2006, p. 3):

$$M_{F_t}(s) = E(e^{sF_t}) = e^{(\alpha - \frac{1}{2}\sigma^2)ts + \frac{1}{2}\sigma^2 ts^2}, -\infty < s < \infty \tag{2A.4}$$

Therefore, the expected value of D_t can be calculated by setting $s = 1$:

$$E(D_t) = E(D_0 e^{F_t}) = D_0 M_{F_t}(1) = D_0 e^{\left(\alpha - \frac{1}{2}\sigma^2\right)t + \frac{1}{2}\sigma^2 t} = D_0 e^{\alpha t} \tag{2A.5}$$

Appendix 2B. Proof of Proposition 2.2

Define $G_t = (1 + w)D_t$. By Ito's Lemma, the total differential of function G_t is given by

$$dG_t = \frac{\partial G_t}{\partial t}dt + \frac{\partial G_t}{\partial D_t}dD_t + \frac{1}{2}\frac{\partial^2 G_t}{\partial {D_t}^2}(dD_t)^2 = (1 + w)(\alpha D_t dt + \sigma D_t dz_t)$$

$$= \alpha[(1 + w)D_t]dt + \sigma[(1 + w)D_t]dz_t = \alpha G_t dt + \sigma G_t dz_t \tag{2B.1}$$

where $\frac{\partial G_t}{\partial t} = 0$ (because the function $G_t = (1 + w)D_t$ has a steady state regardless of the value of t), $\frac{\partial G_t}{\partial D_t} = 1 + w$, and $\frac{\partial^2 G_t}{\partial {D_t}^2} = 0$.

Hence, G_t, i.e., $(1 + w)D_t$, follows a GBM process with the same growth rate α and volatility σ as D_t.

Appendix 2C. Proof of Proposition 2.3

Similarly, define $H_t = (1 + rw)D_t$. By Ito's Lemma, the total differential of function H_t is given by

$$dH_t = \frac{\partial H_t}{\partial t} dt + \frac{\partial H_t}{\partial D_t} dD_t + \frac{1}{2}\frac{\partial^2 H_t}{\partial {D_t}^2}(dD_t)^2 = (1 + rw)(\alpha D_t dt + \sigma D_t dz_t)$$

$$= \alpha[(1 + rw)D_t]dt + \sigma[(1 + rw)D_t]dz_t = \alpha H_t dt + \sigma H_t dz_t \qquad (2C.1)$$

where $\frac{\partial H_t}{\partial t} = 0$ (because the function $H_t = (1 + rw)D_t$ has a steady state regardless of the value of t), $\frac{\partial H_t}{\partial D_t} = 1 + rw$, and $\frac{\partial^2 H_t}{\partial {D_t}^2} = 0$.

Hence, H_t, i.e., $(1 + rw)D_t$, follows a GBM process with the same growth rate α and volatility σ as D_t.

Appendix 2D. Proof of Equation (2.3)

$$V_2(D_t) = E\left\{\int_t^\infty e^{-\rho(x-t)}[PD_x - C(1 + rw)D_x - C_b]\, dx\right\}$$

$$= E\left\{\int_t^\infty e^{-\rho(x-t)}[P - C(1 + rw)]D_x\, dx\right\} - \int_t^\infty e^{-\rho(x-t)}\, C_b dx$$

$$= [P - C(1 + rw)]\int_t^\infty e^{-\rho(x-t)} E(D_x)\, dx - C_b \int_t^\infty e^{-\rho(x-t)}\, dx$$

$$= [P - C(1 + rw)]\int_t^\infty e^{-\rho(x-t)}\, D_t e^{\alpha(x-t)} dx - C_b \int_t^\infty e^{-\rho(x-t)}\, dx$$

$$= [P - C(1 + rw)]D_t \int_t^\infty e^{-(\rho-\alpha)(x-t)}\, dx - C_b \int_t^\infty e^{-\rho(x-t)}\, dx$$

$$= \left(-\frac{[P-C(1+rw)]D_t}{\rho-\alpha}\right) e^{-(\rho-\alpha)(x-t)}\Big|_t^\infty - \left(-\frac{C_b}{\rho}\right) e^{-\rho(x-t)}\Big|_t^\infty = \frac{[P-C(1+rw)]D_t}{\rho-\alpha} - \frac{C_b}{\rho} \qquad (2D.1)$$

Appendix 2E. Proof of Equation (2.8)

A particular solution to Equation (2.5) can be verified to be $V_1(D_t) = \frac{[P-C(1+w)]D_t}{\rho-\alpha}$ under a technical condition of $\rho - \alpha > 0$. Also, a homogeneous solution to Equation (2.5) can be written as $V_1(D_t) = A_1{D_t}^{\beta_1} + A_2{D_t}^{\beta_2}$ under a technical condition of $\alpha - \frac{\sigma^2}{2} > 0$, where $\beta_{1,2} = \left[\frac{\sigma^2}{2} - \alpha \pm \sqrt{\left(\frac{\sigma^2}{2} - \alpha\right)^2 + 2\rho\sigma^2}\right]/\sigma^2$ are the two roots of the fundamental quadratic equation $\mathbb{Q} = \frac{1}{2}\sigma^2\beta(\beta - 1) + \alpha\beta - \rho = 0$. It can be verified that $\beta_1 > 1$ and $\beta_2 < 0$ (Dixit and Pindyck's, 1994, p. 143). So, the general solution to Equation (2.5) is $V_1(D_t) = A_1{D_t}^{\beta_1} + A_2{D_t}^{\beta_2} + \frac{[P-C(1+w)]D_t}{\rho-\alpha}$, and A_1 and A_2 are constants to be determined.

The signs of constants A_1 and A_2 can be discussed as follows. Assuming A_1 is negative, since β_1 is greater than 1, when D_t goes to positive infinity, the term $A_1{D_t}^{\beta_1}$ goes to negative infinity. This is against economic implications as larger demand is supposed to bring the retailer with more profit and thus, contributes to a higher project value. Therefore, A_1 cannot be negative. Similarly, if A_2 is positive, when D_t is small and approaches to zero, the term $A_2{D_t}^{\beta_2}$ goes to positive infinity since β_2 is negative. This also violates the economic signification because smaller demand should contribute to lower profit as well as lower project value. Hence, A_2 cannot be positive. Conversely, if A_2 is negative, $\frac{\partial\left(A_2{D_t}^{\beta_2}\right)}{\partial D_t} = A_2\beta_2{D_t}^{\beta_2-1} < 0$, meaning that the project value decreases as the demand increases. This does not make economic sense since the project value should increase with an increase in the demand, so A_2 cannot be negative either. Since A_2 cannot be either positive or negative, it is required to be 0. Therefore, the general solution becomes $V_1(D_t) = A_1{D_t}^{\beta_1} + \frac{[P-C(1+w)]D_t}{\rho-\alpha}$.

Appendix 2F. Proof of Expected Switching Time

In Appendix 2A, the authors show that the change in F_t (the natural logarithm of D_t) is normally distributed with mean $\left(\alpha - \frac{1}{2}\sigma^2\right)t$ and variance of $\sigma^2 t$. Since the natural logarithm is a monotonically increasing function, the expected time for the retailer to optimally switch can be interpreted as the expected passage time from D_0 to D^*:

$$T^* = \frac{\ln D^* - \ln D_0}{\alpha - \frac{1}{2}\sigma^2} = \frac{\ln \frac{\left(\frac{C_b}{\rho}+I\right)(\rho-\alpha)\beta_1}{Cw(1-r)(\beta_1-1)} - \ln D_0}{\alpha - \frac{1}{2}\sigma^2} \tag{2F.1}$$

Appendix 2G. Proof of Equation (2.11)

$$V_2(D_t) = E\left\{\int_t^\infty e^{-\rho(x-t)}[PD_x - C(1+rw)D_x + SD_x - C_b]\,dx\right\}$$

$$= E\left\{\int_t^\infty e^{-\rho(x-t)}\,[P - C(1+rw) + S]D_x dx\right\} - \int_t^\infty e^{-\rho(x-t)} C_b\,dx$$

$$= [P - C(1+rw) + S]\int_t^\infty e^{-\rho(x-t)}\,E(D_x)dx - C_b\int_t^\infty e^{-\rho(x-t)}\,dx$$

$$= [P - C(1+rw) + S]\int_t^\infty e^{-\rho(x-t)}\,D_t e^{\alpha(x-t)} dx - C_b\int_t^\infty e^{-\rho(x-t)}\,dx$$

$$= [P - C(1+rw) + S]D_t\int_t^\infty e^{-(\rho-\alpha)(x-t)}\,dx - C_b\int_t^\infty e^{-\rho(x-t)}\,dx$$

$$= \left(-\frac{[P-C(1+rw)+S]D_t}{\rho-\alpha}\right)e^{-(\rho-\alpha)(x-t)}\Big|_t^\infty - \left(-\frac{C_b}{\rho}\right)e^{-\rho(x-t)}\Big|_t^\infty = \frac{[P-C(1+rw)+S]D_t}{\rho-\alpha} - \frac{C_b}{\rho} \tag{2G.1}$$

Appendix 2H. Proof of Corollary 2.1

By Equation (2.14), Equation (2.15) and technical conditions of $\rho > \alpha$ and $\alpha - \frac{\sigma^2}{2} > 0$,

$$\frac{\partial D^*}{\partial C} = -\frac{w(1-r)\left(\frac{C_b}{\rho}+I-U\right)(\rho-\alpha)\beta_1}{[Cw(1-r)+S]^2(\beta_1-1)} < 0 \tag{2H.1}$$

$$\frac{\partial T^*}{\partial C} = \frac{\partial T^*}{\partial D^*}\frac{\partial D^*}{\partial C} = -\frac{1}{\left(\alpha-\frac{1}{2}\sigma^2\right)D^*}\frac{w(1-r)\left(\frac{C_b}{\rho}+I-U\right)(\rho-\alpha)\beta_1}{[Cw(1-r)+S]^2(\beta_1-1)} = -\frac{1}{\left(\alpha-\frac{1}{2}\sigma^2\right)}\frac{w(1-r)}{[Cw(1-r)+S]} < 0 \tag{2H.2}$$

$$\frac{\partial D^*}{\partial w} = -\frac{C(1-r)\left(\frac{C_b}{\rho}+I-U\right)(\rho-\alpha)\beta_1}{[Cw(1-r)+S]^2(\beta_1-1)} < 0 \tag{2H.3}$$

$$\frac{\partial T^*}{\partial w} = \frac{\partial T^*}{\partial D^*}\frac{\partial D^*}{\partial w} = -\frac{1}{\left(\alpha-\frac{1}{2}\sigma^2\right)D^*}\frac{C(1-r)\left(\frac{C_b}{\rho}+I-U\right)(\rho-\alpha)\beta_1}{[Cw(1-r)+S]^2(\beta_1-1)} = -\frac{1}{\left(\alpha-\frac{1}{2}\sigma^2\right)}\frac{C(1-r)}{[Cw(1-r)+S]} < 0 \tag{2H.4}$$

Appendix 2I. Proof of Corollary 2.2

By Equation (2.14), Equation (2.15) and technical conditions of $\rho > \alpha$ and $\alpha - \frac{\sigma^2}{2} > 0$,

$$\frac{\partial D^*}{\partial r} = \frac{Cw\left(\frac{C_b}{\rho}+I-U\right)(\rho-\alpha)\beta_1}{[Cw(1-r)+S]^2(\beta_1-1)} > 0 \tag{2I.1}$$

$$\frac{\partial T^*}{\partial r} = \frac{\partial T^*}{\partial D^*}\frac{\partial D^*}{\partial r} = \frac{1}{(\alpha-\frac{1}{2}\sigma^2)D^*}\frac{Cw\left(\frac{C_b}{\rho}+I-U\right)(\rho-\alpha)\beta_1}{[Cw(1-r)+S]^2(\beta_1-1)} = \frac{1}{(\alpha-\frac{1}{2}\sigma^2)}\frac{Cw}{[Cw(1-r)+S]} > 0 \tag{2I.2}$$

Appendix 2J. Proof of Corollary 2.3

By Equation (2.14), Equation (2.15) and technical conditions of $\rho > \alpha$ and $\alpha - \frac{\sigma^2}{2} > 0$,

$$\frac{\partial D^*}{\partial I} = \frac{(\rho-\alpha)\beta_1}{[Cw(1-r)+S](\beta_1-1)} > 0 \tag{2J.1}$$

$$\frac{\partial T^*}{\partial I} = \frac{\partial T^*}{\partial D^*}\frac{\partial D^*}{\partial I} = \frac{1}{(\alpha-\frac{1}{2}\sigma^2)D^*}\frac{(\rho-\alpha)\beta_1}{[Cw(1-r)+S](\beta_1-1)} = \frac{1}{(\alpha-\frac{1}{2}\sigma^2)}\frac{1}{(\frac{C_b}{\rho}+I-U)} > 0 \tag{2J.2}$$

$$\frac{\partial D^*}{\partial C_b} = \frac{(\rho-\alpha)\beta_1}{\rho[Cw(1-r)+S](\beta_1-1)} > 0 \tag{2J.3}$$

$$\frac{\partial T^*}{\partial C_b} = \frac{\partial T^*}{\partial D^*}\frac{\partial D^*}{\partial C_b} = \frac{1}{(\alpha-\frac{1}{2}\sigma^2)D^*}\frac{(\rho-\alpha)\beta_1}{\rho[Cw(1-r)+S](\beta_1-1)} = \frac{1}{(\alpha-\frac{1}{2}\sigma^2)}\frac{1}{(\frac{C_b}{\rho}+I-U)\rho} > 0 \tag{2J.4}$$

Appendix 2K. Proof of Corollary 2.4

By Equation (2.14), Equation (2.15) and technical conditions of $\rho > \alpha$ and $\alpha - \frac{\sigma^2}{2} > 0$,

$$\frac{\partial D^*}{\partial U} = -\frac{(\rho-\alpha)\beta_1}{[Cw(1-r)+S](\beta_1-1)} < 0 \tag{2K.1}$$

$$\frac{\partial T^*}{\partial U} = \frac{\partial T^*}{\partial D^*}\frac{\partial D^*}{\partial U} = -\frac{1}{\left(\alpha-\frac{1}{2}\sigma^2\right)D^*}\frac{(\rho-\alpha)\beta_1}{[Cw(1-r)+S](\beta_1-1)} = -\frac{1}{(\alpha-\frac{1}{2}\sigma^2)}\frac{1}{(\frac{C_b}{\rho}+I-U)} < 0 \tag{2K.2}$$

$$\frac{\partial D^*}{\partial S} = -\frac{\left(\frac{C_b}{\rho}+I-U\right)(\rho-\alpha)\beta_1}{[Cw(1-r)+S]^2(\beta_1-1)} < 0 \tag{2K.3}$$

$$\frac{\partial T^*}{\partial S} = \frac{\partial T^*}{\partial D^*}\frac{\partial D^*}{\partial S} = -\frac{1}{\left(\alpha-\frac{1}{2}\sigma^2\right)D^*}\frac{\left(\frac{C_b}{\rho}+I-U\right)(\rho-\alpha)\beta_1}{[Cw(1-r)+S]^2(\beta_1-1)} = -\frac{1}{(\alpha-\frac{1}{2}\sigma^2)}\frac{1}{[Cw(1-r)+S]} < 0 \tag{2K.4}$$

CHAPTER 3. DECISION SUPPORT FOR ASPHALT ROAD RESURFACING UNDER MAINTENANCE COST UNCERTAINTY: A REAL OPTIONS APPROACH

Zhuoyi Zhao, Kyung Jo Min

Department of Industrial and Manufacturing Systems Engineering

Iowa State University

Modified from a manuscript submitted to *European Journal of Industrial Engineering (EJIE)*

Abstract

Resurfacing an asphalt road is a costly and irreversible but often necessary endeavor across many communities and regions. In this paper, under the assumption that the maintenance cost of a road follows a geometric Brownian motion (GBM) process, we construct and analyze a stochastic optimal control (a real options approach) model for a profit-maximizing decision-maker where the threshold in the maintenance cost to resurface the road is the decision variable. Furthermore, by a profit maximizer, we mean, for example, a private-sector company under a Public-Private Partnership over a road where its objective is to maximize profit. Given this framework of the model, we also mathematically derive the expected resurfacing interval, that is, how much time, on average, is between two consecutive resurfacing activities. In addition, we analytically and numerically illustrate key features of our model via analytical derivation and an extensive numerical example for managerial insights and economic implications.

Keywords: Geometric Brownian Motion (GBM), Real Options, Maintenance Cost Uncertainty, Decision Support, Road Resurfacing.

Introduction

The maintenance cost of asphalt roads has been substantially increasing (Tornquist, 2007, p. 1; PCA, 2012, pp. 7-8), where fluctuations are often observed. The escalation of the maintenance can be attributed to multiple factors, for instance, pavement aging (Ohio Auditor of

State, 2012, p. 7, slide 3), material prices such as asphalt (Tornquist, 2007, p. 4; PCA, 2012, p. 9), procurement policies of states' Department of Transportation (DOT) (PCA, 2012, p. 1), etc. In this article, we focus on the impact of pavement aging on the maintenance cost. Pavement aging leads to deterioration and is a complicated and uncertain process (Solatifar, 2021), which can explain the fluctuations in the maintenance cost evolution. Moreover, in literature such as Alqadhi et al. (2018), the road maintenance cost is modeled as a function of the serviceability index (Al-Mansour and Sinha, 1994), which can be further modeled as a function of the pavement condition index, International Roughness Index (IRI), (Gulen et al., 1994).

For a profit-maximizing decision-maker (e.g., a private-sector company under a Public-Private Partnership over a road where its objective is to maximize profit), resurfacing an asphalt road is a critical decision. Resurfacing a road implies placing a new layer over the existing pavement instead of replacing the entire roadway to extend the pavement life (Wisconsin Department of Transportation, n.d.; Thames Street Works, n.d.), upon which the pavement condition will be like new (Alqadhi et al., 2018). Considering the road maintenance cost reflects the pavement condition, the road maintenance cost is reduced to the new pavement level after resurfacing. The resurfacing decision is impacted by the maintenance cost uncertainty, which has not been addressed in the road resurfacing decision in the literature.

The resurfacing decision requires a careful study a priori as such a decision is costly and irreversible but often necessary endeavor across many communities and regions. Under such a framework, this article aims to provide economically rational decision support on when to resurface an asphalt road under maintenance cost uncertainty. Toward this goal, we

(1) Construct and analyze a stochastic optimal control (i.e., a real options approach) model where the threshold in the maintenance cost to resurface the road is the decision variable

assuming that the maintenance cost follows a geometric Brownian motion (GBM) process.

(2) Mathematically derive how much time, on average, is between two resurfacing activities.

(3) Analytically and numerically illustrate key features of our model via analytical derivation and an extensive numerical example for managerial insights and economic implications.

The remainder of this article is organized as follows. We first present a literature review on the pavement resurfacing and maintenance policy and the application of the real options approach to roads in Section 2. Next, in Section 3, we present the assumptions, followed by the formulation of the mathematical model for the resurfacing decision of an asphalt road and analytical sensitivity analysis of the optimal threshold of the maintenance cost and the expected resurfacing interval with respect to some parameter values. To further demonstrate our findings, we also conduct an extensive numerical example and perform numerical sensitivity analysis for managerial insights and economic implications in Section 4. Finally, conclusions and future research are discussed in Section 5.

Literature Review

Pavement Resurfacing and Maintenance Policy

One relevant literature stream is the optimal pavement resurfacing and maintenance policy. For instance, Lamptey et al. (2008) focused on preventive maintenance schedule optimization using an optimization-based decision support systems approach. The total agency and user costs were minimized by selecting the combination of treatment types and timings during the interval between resurfacing events. Gu et al. (2012) developed an analytical method to optimize pavement maintenance and resurfacing planning. Under the objective of minimizing the pavement lifecycle costs (including the user, maintenance, and resurfacing costs) over an infinite time horizon, the authors formulated the problem as a nonlinear mathematical program with continuous pavement state and continuous time and derived the optimality conditions. Reger et al. (2014) presented a framework under which greenhouse gas (GHG) emissions minimization was incorporated into the pavement resurfacing policy. In Alqadhi et al. (2018), the authors presented a case study of Interstate 465 in Indiana, USA, and evaluated the costs and benefits of the highway pavement resurfacing project from the perspective of agency, user, and community, respectively.

Moreover, some literature developed the optimal resurfacing policy based on a threshold structure. For instance, Li and Madanat (2002) solved the optimal frequency and intensity of pavement resurfacing under steady-state conditions over an infinite horizon. The optimal resurfacing strategy was based on a minimum serviceability level (or maximum roughness level), upon which the pavement should be resurfaced to its best state achievable. Ogwang et al. (2019) proposed a framework to estimate the relationship between GHG emissions due to pavement resurfacing activities and pavement cracking threshold policies. By cracking threshold, the authors meant the maximum percentage cracking level the pavement can reach, above which an asphalt overlay will be applied. The result of Monte Carlo simulation on variable population distributions (i.e., cracking level, underlying and surface layer thickness, environmental variables, and traffic loading), the authors found that within a planning horizon of 10 years, the optimal cracking threshold that minimizes the costs and the GHG emissions, respectively, are close to each other.

Application of the Real Options Approach to Roads

Derived from the financial engineering area, the real options approach has been applied to the infrastructure discipline since the early 2000s (Fawcett et al., 2015). Compared to the conventional deterministic valuation approaches, the real options approach incorporates the underlying uncertainties in the decision-making process. There are three methods in real options, analytical, lattice, and simulation, and each method has its advantages and disadvantages.

First, the analytical method gives precise optimal threshold and option value results. However, it has strict assumptions and requirements on input data, which are difficult to satisfy in the infrastructure problems (Fawcett et al., 2015). Hence, literature using the analytical method of the real options is not as common as using the other two methods in infrastructure decisions. One example of such literature is Galera and Soliño (2010), where the authors evaluated the highway concessions with a minimum traffic guarantee under traffic uncertainty and obtained the analytical solution for the value of the minimum traffic guarantee modeled as a European put option.

Secondly, the lattice method is more intuitive than the other two methods. However, the complexity rapidly increases when many periods are taken into consideration. For instance, Ashuri et al. (2011) evaluated the investments in toll road projects under a two-phase development plan within a real options-based framework. The authors used a binomial lattice method to model traffic uncertainty and determine optimal expansion time. Still, under the traffic uncertainty, Iyer and Sagheer (2011) modeled the traffic floor guarantee as a put option held by the concessionaire and the traffic ceiling guarantee as a call option held by the government. The authors constructed a binomial lattice for traffic and evaluated the value of the two options.

Lastly, the simulation method is commonly used when more than one uncertainty is considered despite its disadvantage in computational expensiveness. For instance, Zhao et al. (2004) considered the uncertainties of interdependent traffic demand, land price, and service quality. The authors developed a multistage stochastic model for decision-making in acquisition, expansion, and rehabilitation under these uncertainties and proposed a solution algorithm based on Monte Carlo simulation and least-squares regression. Brandao and Saraiva (2008) developed a minimum traffic guarantee real options model to assess the value of government guarantees where the traffic follows a GBM process, and so does the revenue. Assuming the option is exercised whenever the revenue is lower than the discounted minimum revenue guaranteed by the government, the value of the option can be determined through a Monte Carlo simulation of the traffic.

To our knowledge, the uncertainty of road maintenance cost has not been addressed in the resurfacing decision. Besides, the analytical method of the real options approach is rarely used in the literature related to decision-making on infrastructures. Under such circumstances, this article can fill in the gap in the literature by considering the road maintenance cost uncertainty in the resurfacing decision and proposing a threshold-based resurfacing policy using an analytical method of the real options approach.

Model Formulation and Analysis

We consider a profit-maximizing decision-maker such as a private-sector company that operates and maintains an asphalt-paved toll road under a Public-Private Partnership. Given that the maintenance cost increases on average and fluctuates over time, at any time point, the decision-maker has an option to resurface the road. The exercise of the resurfacing option implies a large sum of resurfacing cost and renewed road condition after resurfacing.

Assumptions

Before modeling the resurfacing decision, we propose the following critical assumptions to facilitate the formulation and analysis.

Assumption 3.1: *The road maintenance cost at year t (\$/lane-mile) C_t follows a GBM process.*

$$dC_t = \alpha C_t dt + \sigma C_t dz \tag{3.1}$$

where α (% per year; > 0) and σ (% per year; >0) are the instantaneous growth rate and the instantaneous volatility of the maintenance cost of the road, respectively. dt is the increment of time, and dz is the increment of a Wiener process, i.e., $dz = \varepsilon\sqrt{dt}$ where $\varepsilon \sim N(0, 1)$. In this article, we use % per unit time (year) to be consistent with the unit of instantaneous variance or volatility in the literature from the financial engineering area such as Carlos Dias & Pedro Vidal Nunes (2011, p. 234), Tse & Yang (2012, p. 533) and McDonald (2013, pp. 607-608).

Although there are numerous sources of empirical data on the maintenance cost of public roads, references that demonstrate what activities were included or excluded and maintenance cost data over consecutive periods are rare. In this article, we present our best finding, the maintenance cost data of an asphalt-paved county road, Co Rd 16 in Waseca County, MN, to demonstrate the evolution of maintenance cost despite it is not a toll road operated and maintained by a private company, and its length (2.6-mile) and average traffic (225 per day) are smaller than the scope of the road in our model (Rukashaza-Mukome et al., 2003; Jahren et al., 2005).

After extracting the values of cumulative maintenance cost ($/mile) from a line plot in the report using WebPlotDigitizer (Rohatgi, 2021), we obtain the annual maintenance cost by subtracting the cumulative maintenance cost of a year from that of the previous year. In the report (Rukashaza-Mukome et al., 2003), the maintenance activities that substantially contribute to the maintenance cost are snow and ice removal (21%), minor surface repair (17%), resurfacing (15%), bituminous treatment (12 %), and other maintenance activities (33%, activities not specified). Since resurfacing is the only type of treatment considered in our model, resurfacing and bituminous treatment should not be considered as part of the annual maintenance activities. Therefore, we keep snow and ice removal, minor surface repair, and other maintenance activities, which add up to 71% of the maintenance cost. We note the cost associated with smoothing surface (<1%), reshaping (<1%), dust treatment (~0%), surface treatment (~0%), and frost boils/patching (~0%) is excluded due to their low percentages in the maintenance cost.

With the above adjustment, the maintenance cost ($/lane-mile) is calculated by multiplying the annual maintenance cost by 71% and dividing by two since Co Rd 16 has two lanes. Figure 3.1 shows the evolution of maintenance cost, which increases on average and fluctuates over time and is characterized as a GBM process.

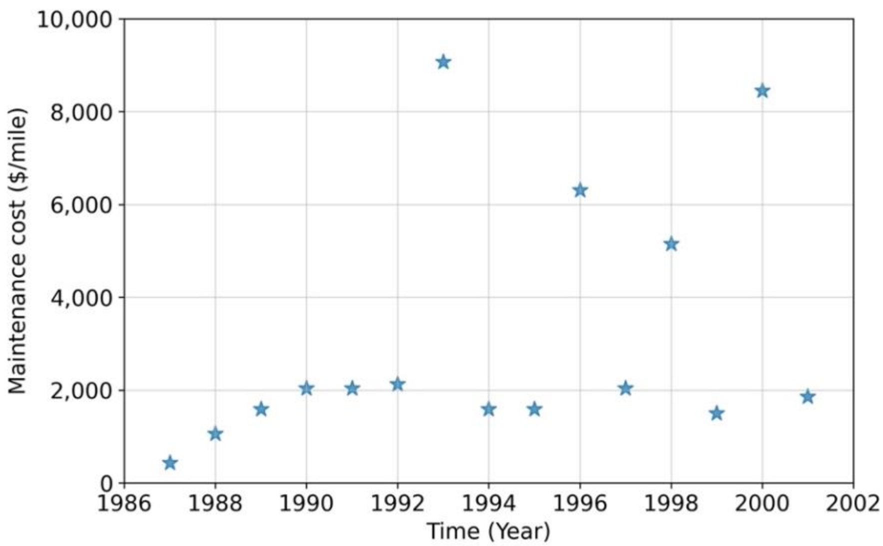

Figure 3.1 Maintenance cost of Co Rd 16

The GBM process assumption has been commonly applied in the literature while modeling decisions under uncertainties using a real options approach as it characters the trend where variables increase on average and fluctuate over time and facilitates the model formulation and analysis process. Even though some empirical data on the road maintenance cost may not support this assumption, alternative stochastic processes (e.g., Wiener process, Brownian motion with drift) can be applied.

Assumption 3.2: *Upon each resurfacing, the value of maintenance cost is reset to the initial value.*

IRI is a commonly used pavement condition index that typically ranges from 52 to 66 inches/mile for new asphalt highway pavements (FHWA, 2016) and increases as the pavement deteriorates. In a case study of interstate 465, IRI decreased from 142.5 inches/mile to 59.63 inches/mile after resurfacing (Alqadhi et al., 2018), which falls in IRI range of new pavement, implying that the road condition is as new after resurfacing. As previously mentioned, the road maintenance cost can be modeled as a function of IRI (Gulen et al., 1994; Al-Mansour and Sinha, 1994; Alqadhi et al., 2018) as it reflects the pavement condition, so it is reasonable to assume that the maintenance cost will be reset to the initial value upon each resurfacing.

Assumption 3.3: *Only one type of vehicle accesses the road (e.g., 2-axle).*

Assumption 3.4: *The decision-maker estimates the road maintenance cost at a year before implementing the maintenance and resurfaces the road if the estimated maintenance cost exceeds a certain level.*

Assumption 3.5: *The time it takes to resurface the road is ignored*.

Suppose the road has a length of K (mile), and the number of lanes is N (lane). The number of vehicles accessing the road in a year is denoted as D (vehicle), and the toll price is denoted as P (\$/vehicle, >0). At year t, the decision-maker collects revenue of PD (\$) from tolls and is responsible for a maintenance expenditure of NKC_t (\$), which gives a profit of $PD - NKC_t$.

Model Formulation

Before exercising the resurfacing option (i.e., when it is not optimal to resurface the road), the value of the project V obeys the Bellman optimality equation in Equation (3.2). The value of the project V (i.e., the value of the road) is equal to the summation of the discounted cash flow generated by the road and the value of the resurfacing option.

$$\rho V dt = (PD - NKC_t)dt + E[dV] \quad (3.2)$$

where ρ (% per year) denotes the discount rate for money. Equation (3.2) states that the total return of this project while holding the resurfacing option consists of the profit generated from the project plus the expected future appreciation in the value of the project.

After applying Ito's Lemma on dV, it can be verified that the Bellman optimality equation yields the following second-order differential equation.

$$\frac{1}{2}\sigma^2 {C_t}^2 \frac{\partial^2 V}{\partial {C_t}^2} + \alpha C_t \frac{\partial V}{\partial C_t} - \rho V + (PD - NKC_t) = 0 \quad (3.3)$$

To solve the differential equation, we first note that, under a technical condition of $\rho - \alpha > 0$ (Dixit & Pindyck, 1994), a particular solution can be verified to be:

$$V(C_t) = \frac{PD}{\rho} - \frac{NKC_t}{\rho - \alpha} \quad (3.4)$$

Secondly, under a technical condition of $\alpha - \frac{\sigma^2}{2} > 0$ (Dixit & Pindyck, 1994), a homogeneous solution can be verified to be:

$$V(C_t) = A_1 {C_t}^{\beta_1} + A_2 {C_t}^{\beta_2} \quad (3.5)$$

where A_1 and A_2 are constants to determine, and $\beta_{1,2} = \frac{1}{2} - \frac{\alpha}{\sigma^2} \pm \sqrt{\left(\frac{\alpha}{\sigma^2} - \frac{1}{2}\right)^2 + \frac{2\rho}{\sigma^2}}$. It can be verified that $\beta_1 > 1$ and $\beta_2 < 0$ (see Dixit & Pindyck, 1994, pp. 142–143 for details).

With the particular and homogenous solutions, the general solution to Equation (3.3) is given by $V(C_t) = A_1 {C_t}^{\beta_1} + A_2 {C_t}^{\beta_2} + \frac{PD}{\rho} - \frac{NKC_t}{\rho - \alpha}$. When C_t becomes very small, the value of the resurfacing option should be worthless. However, with a negative β_2, ${C_t}^{\beta_2}$ goes to ∞ as C_t goes to 0. Hence, the constant multiplying this term, A_2, should be zero. Because of this, we should exclude the negative power term of C_t by setting $A_2 = 0$, which gives the following:

$$V(C_t) = A_1 {C_t}^{\beta_1} + \frac{PD}{\rho} - \frac{NKC_t}{\rho - \alpha} \tag{3.6}$$

The function of the project value is subject to the following boundary conditions:

$$V(C^*) = V(C_0) - NKI \tag{3.7}$$

$$V'(C^*) = 0 \tag{3.8}$$

where C^* is the optimal threshold of maintenance cost at which point the road is resurfaced, C_0 is the initial value of maintenance cost, and I ($/lane-mile) is the resurfacing cost (material and labor costs). Equation (3.7), the value matching condition, states that the value of the project just before resurfacing is equal to the value of the project just after resurfacing minus the resurfacing cost. Equation (3.8), the smooth pasting condition, ensures the slope of the left-hand side and the right-hand side of the value matching condition, Equation (3.7), are equal at the optimal threshold C^*.

From the smooth pasting condition, Equation (3.8), A_1 can be analytically solved as follows:

$$A_1 = \frac{NK}{(\rho - \alpha)\beta_1 {C^*}^{\beta_1 - 1}} \tag{3.9}$$

Substituting the expression of A_1 into the value matching condition, Equation (3.7), it can be verified that the value of C^* satisfies the following equation.

$$(\beta_1 - 1){C^*}^{\beta_1} - \beta_1[C_0 + (\rho - \alpha)I]{C^*}^{\beta_1 - 1} + {C_0}^{\beta_1} = 0 \tag{3.10}$$

Equation (3.10) can be further simplified by dividing ${C_0}^{\beta_1}$ from both sides:

$$(\beta_1 - 1)\lambda^{\beta_1} - \beta_1 \left[1 + \frac{(\rho - \alpha)I}{C_0}\right] \lambda^{\beta_1 - 1} + 1 = 0 \tag{3.11}$$

where $\lambda = \frac{C^*}{C_0}$, $\lambda > 1$. λ is defined as the ratio of the optimal threshold to resurface the road over the initial value of the maintenance cost. Although the value of λ cannot be analytically solved, it can be computationally solved by software such as Excel and MATLAB. The value of C^* can be obtained using $C^* = \lambda C_0$, and correspondingly, the value of A_1 can be obtained using Equation (3.9) and the value of the project can be obtained using Equation (3.6).

The reason we solve the ratio λ as well as the optimal threshold C^* is that both ratio and threshold are used while evaluating the conditions of infrastructures. For instance, Bridge Health Index (BHI) is a bridge performance measure based on the condition of the bridge element and assessed from an element level inspection and calculated as the ratio of current value over the initial value of all bridge elements (Adams & Kang, 2009, pp. i, iii, and 3-5). It varies from 0% (worst possible condition) to 100% (best possible condition), providing an intuitive measure for bridge engineers, legislators, and the public as it is expressed as a percentage value. Meanwhile, thresholds are also used to indicate a condition upon which corrective or preventive treatment is needed on the pavement (Elkins et al., 2013a, pp. 14-17). One example of such thresholds is the pavement present serviceability rating (PSR), where resurfacing is triggered when the pavement PSR falls below a minimum tolerable condition based on highway functional classification (Elkins et al., 2013b, pp. 53-54). With the pavement condition evaluated and literature that investigates the relationship between the maintenance cost and the pavement condition (e.g., Gulen et al., 1994; Al-Mansour and Sinha, 1994; Alqadhi et al., 2018, and Adams et al. 2007), the threshold of pavement condition triggering the resurfacing can be converted to the threshold of maintenance cost.

Consequently, the expected resurfacing interval, i.e., how much time, on average, is between two consecutive resurfacing activities, $E[T^*]$ can be calculated as follows (Dixit & Pindyck, 1994, p. 71, p. 81).

$$E[T^*] = \frac{\ln C^* - \ln C_0}{\alpha - \frac{1}{2}\sigma^2} = \frac{\ln\left(\frac{C^*}{C_0}\right)}{\alpha - \frac{1}{2}\sigma^2} = \frac{\ln(\lambda)}{\alpha - \frac{1}{2}\sigma^2} \tag{3.12}$$

Analytical Sensitivity Analysis

The model involves nine parameters, where four of them (the toll price P, the number of vehicles accessing the road in a year D, the number of lanes N, the length of the road K) have no impact on the resurfacing decision. In other words, the optimal threshold of the maintenance cost to resurface the road C^* and the expected resurfacing interval $E[T^*]$ are insensitive to these four parameters.

On the other hand, the rest five parameters impact the resurfacing decision. Under technical conditions $\rho - \alpha > 0$ and $\alpha - \frac{1}{2}\sigma^2 > 0$ (Dixit & Pindyck, 1994), we conduct analytical sensitivity analysis with respect to the resurfacing cost I, the initial value of the maintenance cost C_0, and the volatility of the maintenance cost σ, respectively. The sensitivity analysis with respect to the growth rate of the maintenance cost α and the discount rate for money ρ are numerically examined because the signs of derivatives cannot be straightforwardly determined.

Proposition 3.1: $\frac{\partial C^*}{\partial I} > 0$, $\frac{\partial E[T^*]}{\partial I} > 0$ *(see Appendix 3A for proof).*

An increase in the resurfacing cost leads to a higher optimal threshold of maintenance cost to resurface the road and a longer expected resurfacing interval. The economic sense behind it is when resurfacing is costly, the decision-maker has less incentive to exercise the resurfacing option. As a result, the exercise of the resurfacing option will be deferred, and the expected resurfacing interval will be prolonged.

Proposition 3.2: $\frac{\partial C^*}{\partial C_0} > 0$, $\frac{\partial E[T^*]}{\partial C_0} < 0$ *(see Appendix 3B for proof).*

A higher initial maintenance cost results in a higher optimal threshold of maintenance cost to resurface the road but a shorter expected resurfacing interval. This is because, with a higher initial maintenance cost, the benefit of exercising the resurfacing option is undermined, which makes it economically rational for the decision-maker to hold the resurfacing option longer and defer its exercise. Meanwhile, starting from a higher initial maintenance cost, the decision-maker is less likely to maintain a long expected resurfacing interval.

Proposition 3.3: $\frac{\partial C^*}{\partial \sigma} > 0, \frac{\partial E[T^*]}{\partial \sigma} > 0$ *(see Appendix 3C for proof).*

As the volatility of the maintenance cost increases, the optimal threshold of maintenance cost to resurface the road increases, and so as the expected resurfacing interval. The reason is that when the maintenance cost becomes more volatile, as time progresses, it may favor the decision-maker, which motivates the decision-maker to postpone the exercise of the resurfacing option to wait for more information on the evolution of the volatile maintenance cost. Consequently, the expected resurfacing interval will be prolonged.

Numerical Example

Parameter Values and Numerical Results

In this section, we use Chicago Skyway as a benchmark and conduct a numerical example. The parameter values are a mix of real, estimated, and hypothetical values depending on the availability of the values, as summarized in Table 3.1 with the explanation and justification presented in Appendix 3D.

Table 3.1 Parameter values

Parameter	**Value**	**Source**
Growth rate of the maintenance cost α	0.04 per year	Hypothetical
Volatility of the maintenance cost σ	0.02 per year	Hypothetical
Initial value of maintenance cost C_0	30,000 $/lane-mile	Hypothetical
Discount rate for money ρ	0.05 per year	Hypothetical

Table 3.1 continued

Parameter	**Value**	**Source**
Number of lanes of the road *N*	6 lanes	Wikipedia (2021)
Length of the road *K*	7.8 miles	FHWA (n.d.)
Toll price *P*	4.50 $/vehicle	Bipartisan Policy Center (2005)
Number of vehicles accessing the road in a year *D*	15,055,885 vehicles	
Resurfacing cost *I*	102,267 $/lane-mile	FHWA (2014); Asphalt Paving Nashville (2018); Eosso Brothers Paving (n.d.); Georgiev (n.d.), HomeGuide (2020), Beiler Brothers Asphalt (n.d.),

Substituting the parameter values in Table 3.1 into the analytical model in the previous section, we obtain the numerical results in Table 3.2. Specifically, we first obtain the value of β_1, with which and Equation (3.11), we can obtain the value of the ratio of the optimal threshold over the initial value of the maintenance cost λ, 1.633. Correspondingly, the optimal threshold of maintenance cost to resurface the road is 48,991 ($/lane-mile), and the expected resurfacing interval is 12.323 years. The value of A_1 can also be calculated, which leads to the value of the project as follows:

$$V(C_t) = 256.224\, C_t^{1.248} + 1{,}355{,}029{,}650 - 4{,}680\, C_t \tag{3.13}$$

Table 3.2. Numerical results

Notation	**Value**
β_1	1.248
λ	1.633
C^*	48,990.994 $/lane-mile
$E[T^*]$	12.323 years
A_1	256.224

Numerical Sensitivity Analysis

First, the relationship of C^* and $E[T^*]$ with respect to α are shown in Figure 3.2, from which we observe that as the growth rate of the maintenance cost increases, the optimal threshold increases while the expected resurfacing interval decreases. This makes economic sense because as the maintenance cost grows faster, the decision-maker has less incentive to resurface the road, considering that the maintenance cost will continue to grow rapidly after resurfacing. Meanwhile, the decision-maker is unlikely to maintain a long expected resurfacing interval because the maintenance cost will rise to a high level soon.

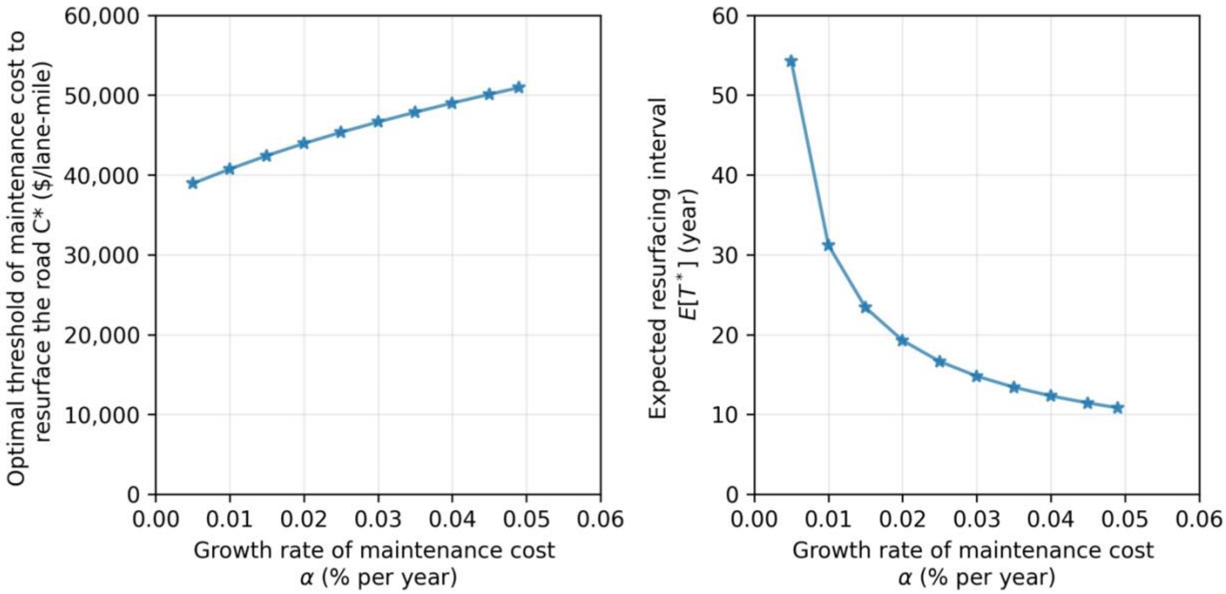

Figure 3.2 Relationship of C^* and $E[T^*]$ with respect to α

Secondly, the relationship of C^* and $E[T^*]$ with respect to ρ are shown in Figure 3.3, from which we observe that when the discount rate for money increases, both the optimal threshold and the expected resurfacing interval increase. The economic implication is that when maintenance cost is heavily discounted as time progresses, the decision-maker prefers to postpone the road resurfacing because the maintenance cost becomes a lighter burden. Consequently, the expected resurfacing interval will be prolonged.

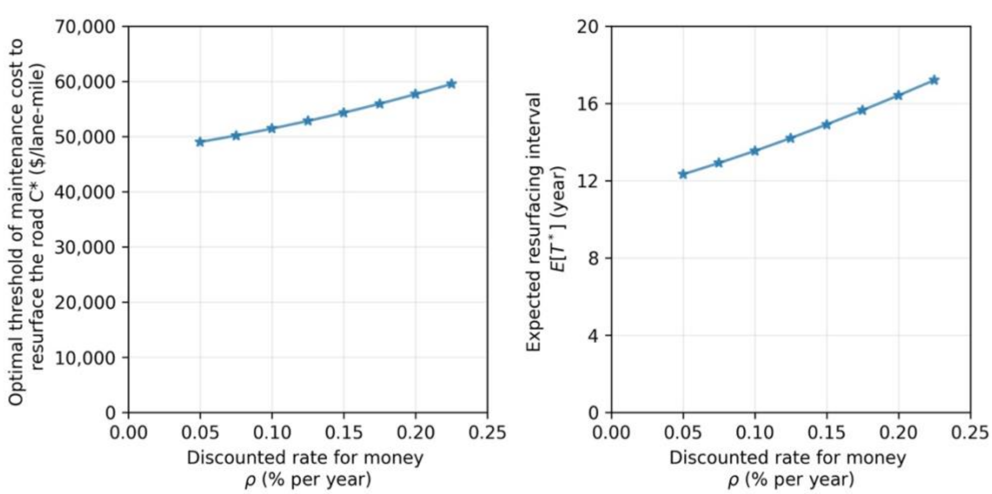

Figure 3.3 Relationship of C^* and $E[T^*]$ with respect to ρ

Simulation

Next, we conduct a Monte Carlo simulation 100,000 times to simulate the maintenance cost with a lease term of 100 years (referring to the fact that Chicago Skyway was leased for 99 years), where the core uncertainty is a standard normal distribution. The sample paths of the simulated maintenance cost are shown in Figure 3.4, which visualizes the evolution of the maintenance cost under the threshold-based resurfacing policy. That is, the maintenance cost starts increasing on average and fluctuating over time from an initial value of 30,000 ($/lane-mile). Every time it reaches the optimal threshold, 48,991 ($/lane-mile), the road is resurfaced, upon which the maintenance cost is reset to its initial value. Furthermore, for each simulation path, we calculate the total discounted profits by summing the discounted profit in each year within a lease term of 100 years using continuous compounding. The total discounted profits have a mean of 1,339.657 (million $) and a standard deviation of 0.695 (million $).

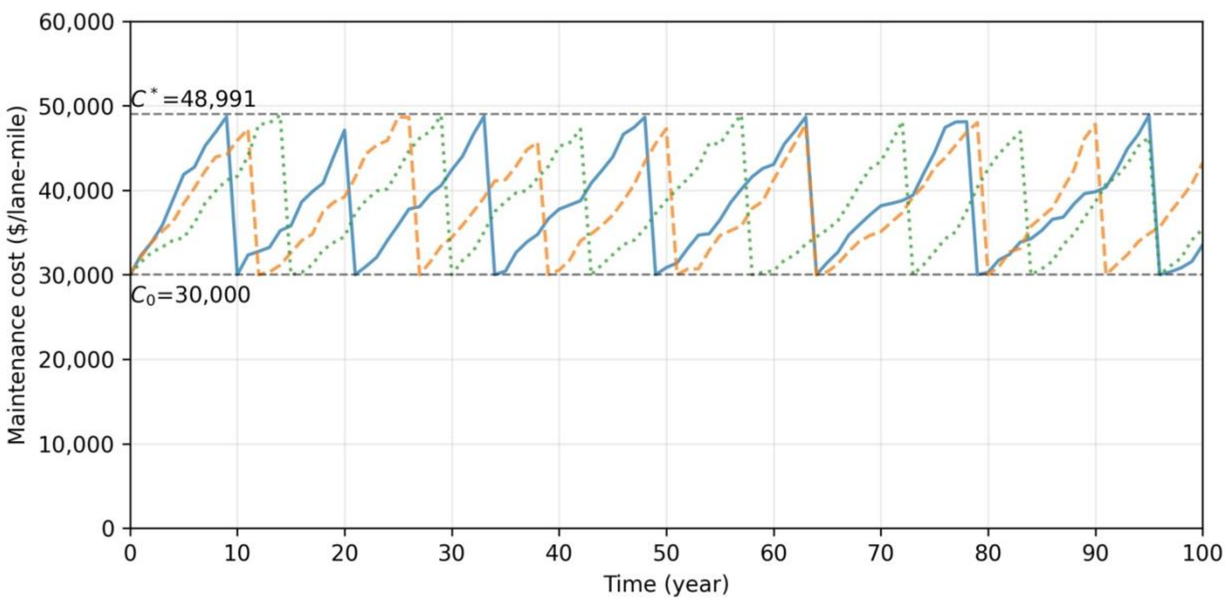

Figure 3.4 Sample paths of simulated maintenance cost

Alternatively, suppose the decision-maker resurfaces the road under an interval-based policy, by which we mean the road is resurfaced every k years (where k is an integer value between 0 and the lease term, in this case, 100), regardless of the road maintenance cost level at the time of resurfacing. We calculate the total discounted profits within a lease term of 100 years using the same approach for each k as the threshold-based resurfacing policy. The relationship between the average total discounted profits and the resurfacing interval is shown in Figure 3.5 where the light blue area depicts a 90% confidence interval. The results imply that the average total discounted profits are maximized (1,339.081 million \$) when the road is resurfaced every 12 years, which is close to the expected resurfacing interval under the threshold-based policy, 12.323 years.

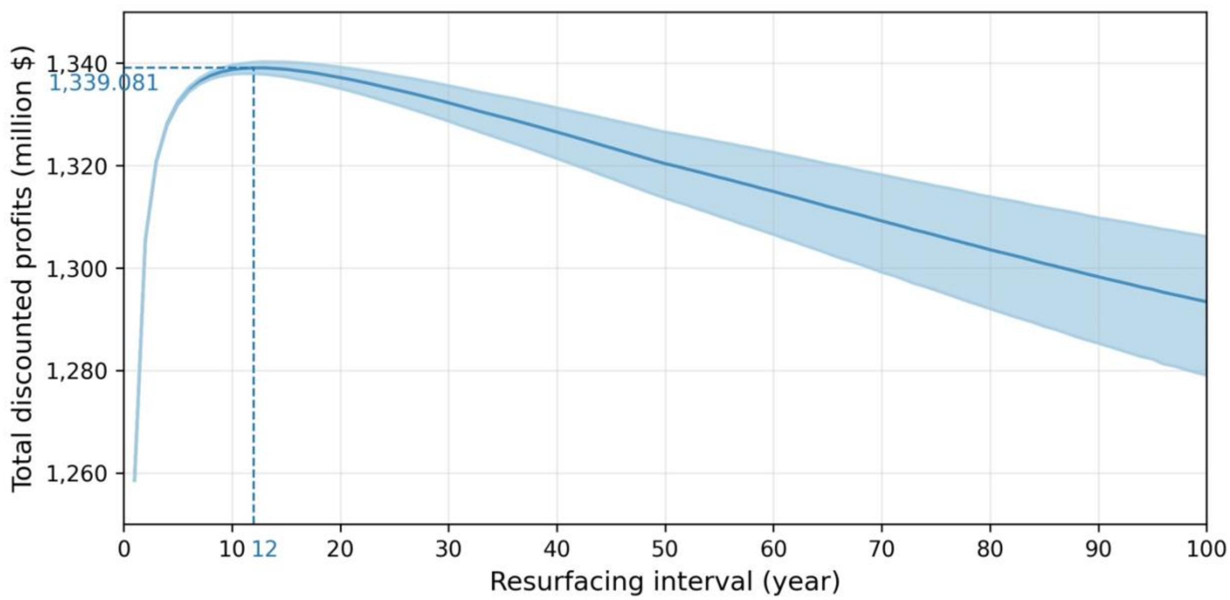

Figure 3.5 Relationship between total discounted profits and resurfacing interval

Despite the closeness in the (expected) resurfacing intervals under the two resurfacing policies, the average discounted profits under the threshold-based policy is 0.576 (million \$) higher than that under the interval-based policy. We also note that for the threshold-based policy, analytically deriving and numerically solving the optimal threshold of maintenance cost of resurfacing give a precise result of optimal threshold and the expected resurfacing interval. On the other hand, for the interval-based policy, solving the optimal resurfacing interval using simulation is computationally expensive, and the computational expensiveness depends on the granularity of the resurfacing intervals.

Conclusions

In this article, under the assumption that the maintenance cost of an asphalt road follows a GBM process, we constructed and analyzed the resurfacing decision using a real options approach for a profit-maximizing decision-maker. We computationally solved the optimal threshold in the maintenance cost to resurface the road and obtained the expected resurfacing interval. We also derived managerial insights and economic implications by examining the impact of parameters on the resurfacing decision through analytical and numerical sensitivity analyses.

Specifically, we analytically showed that (1) when it costs more money to resurface the road, the decision-maker should defer the road resurfacing, which implies a longer expected resurfacing interval; (2) with a higher initial road maintenance cost, the decision-maker should defer the road resurfacing and maintain a shorter expected resurfacing interval; (3) as the road maintenance cost becomes more volatile, the road resurfacing should be deferred, and the expected resurfacing interval should be extended.

Moreover, from the numerical sensitivity analyses, we observe that (1) when the maintenance cost grows faster, it is beneficial to defer the road resurfacing and shorten the expected resurfacing interval; (2) when money becomes heavily discounted as time progresses, it is suggested to postpone the road resurfacing and prolong the expected resurfacing interval. Furthermore, through the simulation of the maintenance cost, we obtained the total discounted profits within the lease term. The results indicate that the average total discounted profits under the interval-based policy are maximized at an interval close to the expected resurfacing interval under the threshold-based policy. However, the average total discounted profits under the threshold-based policy slightly surpass that under the interval-based policy.

Our article is original in the following three aspects. First, applying the analytical method of the real options approach is rare in decision-making on infrastructures. Although the analytical method requires strict assumptions compared to the binomial lattice and the simulation methods, it leads to precise results guiding the resurfacing decision under uncertainties. Secondly, this article is the first attempt to address the maintenance cost uncertainty in the resurfacing decision, although the operation and maintenance cost uncertainty has been commonly considered in other decisions, e.g., the exit and entry decisions for a renewable power site (Min et al., 2012) and replacement decision for heavy mobile equipment (Richardson et al., 2013). Thirdly, besides the optimal threshold of the maintenance cost to resurface the road, we also derive the ratio of the optimal threshold to resurface the road over the initial value of the maintenance cost to indicate the condition to optimally resurface the road, which is also unique in the literature.

Our research can stimulate a series of threads of future research. For instance, one can extend the decision support from a profit-maximizing decision maker to a non-profit decision maker with objectives such as minimizing the cost. Moreover, other uncertainties in the resurfacing decision can be taken into consideration, such as traffic demand, which has been modeled as a GBM process in the literature such as Zhao et al. (2004), Galera and Soliño (2010). Furthermore, one can relax our assumption that only one type of vehicle accesses the road by incorporating the impact of heavy vehicles on the maintenance cost. There has been discussion on heavy trucks causing more road deterioration than passenger cars (Gibby et al., 1990), which may further raise the maintenance cost. On a larger scale, one can model multiple decisions under uncertainties, e.g., the decisions to resurface, reconstruct the road, and apply preventive surface treatment to the road (e.g., Zhao & Min, 2021).

Statements and Declarations

The authors have no competing interests to declare that are relevant to the content of this article.

References

Adams, T. M., & Kang, M. M. (2009). Sensitivity analysis of bridge health index to element failure and element conditions (No. MRUTC 08-07).

Adams, T. M., Sokolowski, D., Juni, E., & Kannan, K. (2007, August). Routine Highway Maintenance: Relationship between Cost and Condition. In *Proceedings of the 2007 Mid-Continent Transportation Research Symposium, Ames, Iowa*.

Al-Mansour, A., & Sinha, K. C. (1994). Economic analysis of effectiveness of pavement preventive maintenance. *Transportation Research Record*, (1442).

Alqadhi, S., Ghahari, S. A., Chen, S., Volovski, M., & Woldemariam, W. (2018). Costs and benefits of highway resurfacing: a case study of Interstate 465 in Indiana, USA. *Infrastructure Asset Management*, *5*(2), 45–55. https://doi.org/10.1680/jinam.17.00036

Ashuri, B., Lu, J., & Kashani, H. (2011). A real options framework to evaluate investments in toll road projects delivered under the two-phase development strategy. *Built Environment Project and Asset Management*, *1*(1), 14–31. https://doi.org/10.1108/20441241111143759

Asphalt Paving Nashville. (2018, May 30). *Asphalt Resurfacing/Overlay*. Retrieved November 21, 2021, from https://www.asphaltpavingnashville.com/tennessee-pavement-contractor/asphalt-resurfacing-overlay-parking-lot-and-road

Beiler Brothers Asphalt. (n.d.). *Asphalt Paving Pricing*. Retrieved November 21, 2021, from https://www.asphaltpaving-pa.com/pricing/

Bipartisan Policy Center. (2005). *Infrastructure Case Study: Chicago Skyway Bridge*. https://bipartisanpolicy.org/download/?file=/wp-content/uploads/2016/10/BPC-Infrastructure-Chicago-Skyway-Bridge.pdf

Brandao, L. E. T., & Saraiva, E. (2008). The option value of government guarantees in infrastructure projects. *Construction Management and Economics*, *26*(11), 1171–1180. https://doi.org/10.1080/01446190802428051

Carlos Dias, J., & Pedro Vidal Nunes, J. (2011). Pricing real options under the constant elasticity of variance diffusion. *Journal of Futures Markets, 31*(3), 230-250.

Dixit, A. K., & Pindyck, R. S. (1994). *Investment under Uncertainty*. Princeton University Press.

Elkins, G. E., Rada, G. R., Groeger, J., & Visintine, B. A. (2013a). *Pavement remaining service interval implementation guidelines* (No. FHWA-HRT-13-050). United States. Federal Highway Administration. Office of Infrastructure Research and Development.

Elkins, G. E., Thompson, T., Groeger, J., Visintine, B. A., & Rada, G. R. (2013b). *Reformulated pavement remaining service life framework* (No. FHWA-HRT-13-038). United States. Federal Highway Administration. Office of Infrastructure Research and Development.

Eosso Brothers Paving. (n.d.). *A Handy FAQ on Pavement Resurfacing and Reconstruction*. Retrieved November 21, 2021, from https://www.ebpave.com/pavement-faqs/

Fawcett, W., Urquijo, I. R., Krieg, H., Hughes, M., Mikalsen, L., & Gutiérrez, S. R. R. (2015). Cost and Environmental Evaluation of Flexible Strategies for a Highway Construction Project under Traffic Growth Uncertainty. *Journal of Infrastructure Systems*, *21*(3), 05014006. https://doi.org/10.1061/(asce)is.1943-555x.0000230

Federal Highway Administration (FHWA). (n.d.). *FHWA - Center for Innovative Finance Support - Project Profiles*. Retrieved November 21, 2021, from https://www.fhwa.dot.gov/ipd/project_profiles/il_chicago_skyway.aspx

Federal Highway Administration (FHWA). (2014, October 15). *Mitigation Strategies For Design Exceptions - Safety | Federal Highway Administration*. Retrieved November 21, 2021, from https://safety.fhwa.dot.gov/geometric/pubs/mitigationstrategies/chapter3/3_lanewidth.cfm

Federal Highway Administration (FHWA). (2016, June). *Tech Brief: Measuring and Specifying Pavement Smoothness*. https://www.fhwa.dot.gov/pavement/pubs/hif16032.pdf

Galera, A. L. L., & Soliño, A. S. (2010). A Real Options Approach for the Valuation of Highway Concessions. *Transportation Science*, *44*(3), 416–427. https://doi.org/10.1287/trsc.1090.0299

Georgiev, G. Z. (n.d.). *Asphalt Calculator*. GIGAcalculator. Retrieved November 21, 2021, from https://www.gigacalculator.com/calculators/asphalt-calculator.php

Gibby, R., Kitamura, R., & Zhao, H. (1990). Evaluation of truck impacts on pavement maintenance cost. *Transportation Research Record*, *1262*, 48-56.

Gu, W., Ouyang, Y., & Madanat, S. (2012). Joint optimization of pavement maintenance and resurfacing planning. *Transportation Research Part B: Methodological*, *46*(4), 511–519. https://doi.org/10.1016/j.trb.2011.12.002

Gulen, S., Woods, R., Weaver, J., & Anderson, V. L. (1994). Correlation of present serviceability ratings with international roughness index. *Transportation Research Record*, *1435*, 27.

HomeGuide. (2020, December 17). *How much does asphalt cost?* Retrieved November 21, 2021, from https://homeguide.com/costs/asphalt-prices

Iyer, K., & Sagheer, M. (2011). A real options based traffic risk mitigation model for build-operate-transfer highway projects in India. *Construction Management and Economics*, *29*(8), 771–779. https://doi.org/10.1080/01446193.2011.597412

Jahren, C. T., Smith, D., Thorius, J., Rukashaza-Mukome, M., White, D., & Johnson, G. (2005, January). *Economics of Upgrading an Aggregate Road* (MN/RC-2005-09). Local Road Research Board (LRRB). https://www.lrrb.org/pdf/200509.pdf

Lamptey, G., Labi, S., & Li, Z. (2008). Decision support for optimal scheduling of highway pavement preventive maintenance within resurfacing cycle. *Decision Support Systems*, *46*(1), 376–387. https://doi.org/10.1016/j.dss.2008.07.004

Li, Y., & Madanat, S. (2002). A steady-state solution for the optimal pavement resurfacing problem. *Transportation Research Part A: Policy and Practice*, *36*(6), 525–535. https://doi.org/10.1016/s0965-8564(01)00020-9

Marathe, R. R., & Ryan, S. M. (2005). On the validity of the geometric Brownian motion assumption. *The Engineering Economist*, *50*(2), 159-192.

McDonald, R. L. (2013). *Derivatives markets* (3rd edition). Pearson.

Min, K. J., Lou, C., & Wang, C. H. (2012). An Exit and Entry Study of Renewable Power Producers: A Real Options Approach. *The Engineering Economist*, *57*(1), 55–75. https://doi.org/10.1080/0013791x.2011.651566

Ohio Auditor of State. (2012). *Are Your Road Dollars Struggling to Keep Up With Deterioration?* https://ohioauditor.gov/trainings/lgoc/2012/Are%20Your%20Road%20Dollars%20Struggling%20to%20Keep%20Up%20with%20Deterioration.pdf

Ogwang, A., Madanat, S., & Horvath, A. (2019). Optimal Cracking Threshold Resurfacing Policies in Asphalt Pavement Management to Minimize Costs and Emissions. *Journal of Infrastructure Systems*, *25*(2), 04019003. https://doi.org/10.1061/(asce)is.1943-555x.0000469

Portland Cement Association (PCA). (2012, February). *The New Paving Realities: The Impact of Asphalt Cost Escalator Clauses on State Finances*. Portland Cement Association (PCA) Market Intelligence. http://www2.cement.org/econ/pdf/escalator_report_2-27-12.pdf

Reger, D., Madanat, S., & Horvath, A. (2014). Economically and environmentally informed policy for road resurfacing: tradeoffs between costs and greenhouse gas emissions. *Environmental Research Letters*, *9*(10), 104020. https://doi.org/10.1088/1748-9326/9/10/104020

Richardson, S., Kefford, A., & Hodkiewicz, M. (2013). Optimised asset replacement strategy in the presence of lead time uncertainty. *International Journal of Production Economics*, *141*(2), 659–667. https://doi.org/10.1016/j.ijpe.2012.10.006

Rohatgi, A. (2021, August). *WebPlotDigitizer*. WebPlotDigitizer. Retrieved November 21, 2021, from https://automeris.io/WebPlotDigitizer

Ross, S. M. (2011). *An elementary introduction to mathematical finance*. Cambridge University Press.

Ross, S. M. (2014). *Introduction to probability models (11th edition)*. Academic press.

Rukashaza-Mukome, M. C., Thorius, J. M., Jahren, C. T., Johnson, G. D., & White, D. J. (2003, August). Cost comparison of treatments used to maintain or upgrade aggregate roads. In *Proceedings of the 2003 Mid-Continent Transportation Research Symposium. Ames, Iowa*.

Solatifar, N. (2021). Analysis of Uncertainties in Deterioration Process of Asphalt Pavements based on Roughness Index Using LTPP Data. *Amirkabir Journal of Civil Engineering*, *53*(4), 1-1. https://doi.org/10.22060/CEEJ.2019.16072.6116

Thames Street Works. (n.d.). *What is Road Resurfacing?* Retrieved November 21, 2021, from https://www.thbuk.co.uk/what-is-road-resurfacing/

Tornquist, D. (2007, September). *Growth in Highway Construction and Maintenance Costs* (CR-2007-079). Federal Highway Administration. https://www.oig.dot.gov/sites/default/files/Growth_in_Highway_Construction_and_Maintenance_Costs_Final.pdf

Tse, Y. K., & Yang, T. T. (2012). Estimation of high-frequency volatility: An autoregressive conditional duration approach. *Journal of Business & Economic Statistics*, *30*(4), 533-545.

Wikipedia. (2021, October 25). *Interstate 90 in Illinois*. Wikipedia. Retrieved November 21, 2021, from https://en.wikipedia.org/wiki/Interstate_90_in_Illinois

Wisconsin Department of Transportation. (n.d.). *Highway Improvement Type Definitions*. Retrieved November 21, 2021, from https://wisconsindot.gov/Documents/doing-bus/local-gov/astnce-pgms/highway/tools/definitions.pdf

Zhao, T., Sundararajan, S. K., & Tseng, C. L. (2004). Highway Development Decision-Making under Uncertainty: A Real Options Approach. *Journal of Infrastructure Systems*, *10*(1), 23–32. https://doi.org/10.1061/(asce)1076-0342(2004)10:1(23)

Zhao, Z., & Min, K. J. (2021). Preventive Surface Treatment Decision on Asphalt Road under Maintenance Cost Uncertainty. In *IISE Annual Conference. Proceedings* (pp. 1183-1188). Institute of Industrial and Systems Engineers (IISE).

Appendices

Appendix 3A. Proof of Proposition 1

Let $f=(\beta_1-1){C^*}^{\beta_1}-\beta_1[C_0+(\rho-\alpha)I]{C^*}^{\beta_1-1}+{C_0}^{\beta_1}$, it can be verified that

$$\frac{\partial f}{\partial C^*}=\frac{(\beta_1-1)\left({C^*}^{\beta_1}-{C_0}^{\beta_1}\right)}{C^*}>0 \tag{3A.1}$$

$$\frac{\partial f}{\partial I}=-\beta_1(\rho-\alpha){C^*}^{\beta_1-1}<0 \tag{3A.2}$$

By implicit function theorem,

$$\frac{\partial C^*}{\partial I}=-\frac{\partial f/\partial I}{\partial f/\partial C^*}=-\frac{-\beta_1(\rho-\alpha){C^*}^{\beta_1-1}}{\frac{(\beta_1-1)\left({C^*}^{\beta_1}-{C_0}^{\beta_1}\right)}{C^*}}=\frac{\beta_1(\rho-\alpha){C^*}^{\beta_1}}{(\beta_1-1)\left({C^*}^{\beta_1}-{C_0}^{\beta_1}\right)}>0 \tag{3A.3}$$

By Equation (3.12), we have $\frac{\partial E[T^*]}{\partial C^*}=\frac{1}{\left(\alpha-\frac{1}{2}\sigma^2\right)C^*}>0$. By chain rule, $\frac{\partial E[T^*]}{\partial I}=\frac{\partial E[T^*]}{\partial C^*}\frac{\partial C^*}{\partial I}>$

0.

Appendix 3B. Proof of Proposition 2

With the expression of f, it can be verified that

$$\frac{\partial f}{\partial C_0}=-\beta_1\left({C^*}^{\beta_1-1}-{C_0}^{\beta_1-1}\right)<0 \tag{3B.1}$$

By implicit function theorem,

$$\frac{\partial C^*}{\partial C_0}=-\frac{\partial f/\partial C_0}{\partial f/\partial C^*}=-\frac{-\beta_1\left({C^*}^{\beta_1-1}-{C_0}^{\beta_1-1}\right)}{\frac{(\beta_1-1)\left({C^*}^{\beta_1}-{C_0}^{\beta_1}\right)}{C^*}}=\frac{\beta_1\left({C^*}^{\beta_1-1}-{C_0}^{\beta_1-1}\right)C^*}{(\beta_1-1)\left({C^*}^{\beta_1}-{C_0}^{\beta_1}\right)}>0 \tag{3B.2}$$

From Equation (3.12), we have $\frac{\partial E[T^*]}{\partial C_0}=-\frac{1}{\left(\alpha-\frac{1}{2}\sigma^2\right)C_0}<0$. Meanwhile, C^* is also a

function of C_0. By chain rule, we have

$$\frac{\partial E[T^*]}{\partial C_0}=\frac{\partial E[T^*]}{\partial C_0}+\frac{\partial E[T^*]}{\partial C^*}\frac{\partial C^*}{\partial C_0}=-\frac{1}{\left(\alpha-\frac{1}{2}\sigma^2\right)C_0}+\frac{1}{\left(\alpha-\frac{1}{2}\sigma^2\right)C^*}\frac{\beta_1\left({C^*}^{\beta_1-1}-{C_0}^{\beta_1-1}\right)C^*}{(\beta_1-1)\left({C^*}^{\beta_1}-{C_0}^{\beta_1}\right)}$$

$$= -\frac{1}{\left(\alpha - \frac{1}{2}\sigma^2\right)} \frac{\beta_1 C^{*\beta_1 - 1}(\rho - \alpha) I}{(\beta_1 - 1)\left(C^{*\beta_1} - C_0{}^{\beta_1}\right) C_0} < 0 \tag{3B.3}$$

Appendix 3C. Proof of Proposition 3

With the expression of f, it can be verified that

$$\frac{\partial f}{\partial \beta_1} = \frac{C^{*\beta_1} - C_0{}^{\beta_1} - \beta_1 C_0{}^{\beta_1}(\ln C^* - \ln C_0)}{\beta_1} \tag{3C.1}$$

Let $g(C) = C^{\beta_1} - \beta_1 C_0{}^{\beta_1} \ln C$. We have

$$\frac{dg(C)}{dC} = \beta_1 C^{\beta_1 - 1} - \beta_1 C_0{}^{\beta_1} \frac{1}{C} = \frac{\beta_1\left(C^{\beta_1} - C_0{}^{\beta_1}\right)}{C} > 0 \tag{3C.2}$$

Since $C^* > C_0$, $g(C^*) > g(C_0)$, i.e., $C^{*\beta_1} - \beta_1 C_0{}^{\beta_1} \ln C^* > C_0{}^{\beta_1} - \beta_1 C_0{}^{\beta_1} \ln C_0$, which is equivalent to $C^{*\beta_1} - C_0{}^{\beta_1} + \beta_1 C_0{}^{\beta_1}(\ln C_0 - \ln C^*) > 0$. Hence, $\frac{\partial f}{\partial \beta_1} > 0$.

Next, it can be verified that

$$\frac{\partial \beta_1}{\partial \sigma} = \left(\frac{2\alpha}{\sigma^3}\right)\left\{1 - \frac{\left(\frac{\alpha}{\sigma^2} - \frac{1}{2}\right) + \frac{\rho}{\alpha}}{\sqrt{\left(\frac{\alpha}{\sigma^2} - \frac{1}{2}\right)^2 + \frac{2\rho}{\sigma^2}}}\right\} \tag{3C.3}$$

Under technical conditions $\rho - \alpha > 0$ and $\alpha - \frac{1}{2}\sigma^2 > 0$, $\frac{\left(\frac{\alpha}{\sigma^2} - \frac{1}{2}\right) + \frac{\rho}{\alpha}}{\sqrt{\left(\frac{\alpha}{\sigma^2} - \frac{1}{2}\right)^2 + \frac{2\rho}{\sigma^2}}} > 0$ and

$\left(\frac{\left(\frac{\alpha}{\sigma^2} - \frac{1}{2}\right) + \frac{\rho}{\alpha}}{\sqrt{\left(\frac{\alpha}{\sigma^2} - \frac{1}{2}\right)^2 + \frac{2\rho}{\sigma^2}}}\right)^2 = \frac{\left(\frac{\alpha}{\sigma^2} - \frac{1}{2}\right)^2 + \left(\frac{\rho}{\alpha}\right)^2 + 2\left(\frac{\alpha}{\sigma^2} - \frac{1}{2}\right)\frac{\rho}{\alpha}}{\left(\frac{\alpha}{\sigma^2} - \frac{1}{2}\right)^2 + \frac{2\rho}{\sigma^2}} = 1 + \frac{\frac{\rho}{\alpha^2}(\rho - \alpha)}{\left(\frac{\alpha}{\sigma^2} - \frac{1}{2}\right)^2 + \frac{2\rho}{\sigma^2}} > 1$. Therefore, $\frac{\left(\frac{\alpha}{\sigma^2} - \frac{1}{2}\right) + \frac{\rho}{\alpha}}{\sqrt{\left(\frac{\alpha}{\sigma^2} - \frac{1}{2}\right)^2 + \frac{2\rho}{\sigma^2}}} > 1$.

Consequently, $\frac{\partial \beta_1}{\partial \sigma} < 0$.

By chain rule, $\frac{\partial f}{\partial \sigma} = \frac{\partial f}{\partial \beta_1}\frac{\partial \beta_1}{\partial \sigma} < 0$. Then by implicit function theorem, $\frac{\partial C^*}{\partial \sigma} = -\frac{\partial f/\partial \sigma}{\partial f/\partial C^*} > 0$. Furthermore, by chain rule, $\frac{\partial E[T^*]}{\partial \sigma} = \frac{\partial E[T^*]}{\partial \sigma} + \frac{\partial E[T^*]}{\partial C^*}\frac{\partial C^*}{\partial \sigma} > 0$ because $\frac{\partial E[T^*]}{\partial \sigma} = \frac{\sigma(\ln C^* - \ln C_0)}{\left(\alpha - \frac{1}{2}\sigma^2\right)^2} > 0$, $\frac{\partial E[T^*]}{\partial C^*} = \frac{1}{\left(\alpha - \frac{1}{2}\sigma^2\right)C^*} > 0$ and $\frac{\partial C^*}{\partial \sigma} > 0$.

Appendix 3D. Justification of Parameter Values

In the numerical example, Chicago Skyway is used as a benchmark of the road in our model. It was leased by the City of Chicago to the Skyway Concession Company (SCC) in 2005 for 99 years, and Calumet Concession Partners LLC assumed the remaining lease until 2104 in 2015 (FHWA, n.d.).

Chicago Skyway is 7.8 miles long (FHWA, n.d.) and has three lanes in each direction (Wikipedia, 2021), so we have the length of the road K = 7.8 miles and the number of lanes N = 2 * 3 = 6. Besides, given that the toll price of Chicago Skyway for 2-axle vehicles in 2015 was $4.50 (Bipartisan Policy Center, 2005, 1st Figure), we have the toll price P = 4.50 $ per vehicle. In addition, with the average daily traffic of 41,249 vehicles in 2013 (Bipartisan Policy Center, 2005, p.2), we have the number of vehicles accessing the road in a year D = 41,249 * 365 = 15,055,885 vehicles.

The resurfacing cost I of an asphalt road is estimated based on a scale of one mile (5,280 ft) in length by one lane (typically 12 ft, FHWA, 2014, 3rd Table) in width. Suppose the resurfacing requires an asphalt layer of 2 inches (0.167 ft) thick (Asphalt Paving Nashville, 2018; Eosso Brothers Paving, n.d.). The total volume of asphalt is 5280 ft * 12 ft * 0.167 ft = 10,581 ft^3. With a standard density of asphalt of 145 lb/ft^3 (Georgiev, n.d.), the weight of asphalt is given by 145 lb/ft^3 * 10,581 ft^3 = 1,534,245 lb = 767 ton. Considering the asphalt price varies from 40 to 80 $/ton (HomeGuide, 2020), the asphalt price is estimated to be the mean of the price range, (40+80) / 2 = 60 $/ton. Hence, the cost of asphalt needed for resurfacing is 60 $/ton * 767 ton = 46,020 $. In addition, material cost only accounts for a portion of the overall resurfacing cost. Due to a lack of relevant data, we use the percentage of the material cost in the driveway installation prices as an approximation. As the material cost typically takes 30% - 60%

of the total cost (material, labor, and equipment) in the driveway installation prices (Beiler Brothers Asphalt, n.d.), we estimate the percentage of material cost in resurfacing cost to be the mean of the percentage range, (30% + 60%) / 2 = 45%. Therefore, the resurfacing cost I is estimated to be 46,020 $ / 45% = 102,267 ($/lane-mile).

CHAPTER 4. DECISION SUPPORT FOR CONVERSION FROM A CONVENTIONAL ROOF TO A COOL ROOF UNDER ENERGY PRICE UNCERTAINTIES: A REAL OPTIONS APPROACH

Zhuoyi Zhao, Kyung Jo Min

Department of Industrial and Manufacturing Systems Engineering

Iowa State University

Modified from a manuscript submitted to *The Engineering Economist (TEE)*

Abstract

For a commercial building that consumes electricity for cooling and natural gas for heating, converting the current conventional roof to a cool roof has been observed in numerous warmer regions domestically and globally. Such efforts will lead to not only lower electricity consumption but also higher natural gas consumption. In this paper, under the assumption that the building's electricity consumption sufficiently exceeds its natural gas consumption, we aim to provide decision support for the roof conversion for profit-maximizing decision-makers (e.g., commercial building owners). Specifically, in the basic model, we assume that the electricity price follows a geometric Brownian motion (GBM) process, and the natural gas price is characterized as a constant multiple of the electricity price, and analytically solve for the optimal electricity price threshold to implement roof conversion and the corresponding expected time. In the extended model, we value the roof conversion option using the Least Squares Monte Carlo simulation (i.e., using Least Squares to estimate the expected payoff from continuation with current energy prices and obtain the option value via Monte Carlo simulation). We then construct and analyze numerical examples to investigate how parameter values impact the roof conversion decisions, and derive managerial insights and economic implications.

Keywords: Real Options, Energy Price Uncertainty, Geometric Brownian Motion, Correlation, Least Squares Monte Carlo Simulation.

Introduction

A cool roof is a roof with high solar reflection (ability to reflect sunlight) and high thermal emittance (ability to emit thermal radiation), which improves building energy efficiency (Gao et al., 2014). Cool materials on the surface of cool roofs reflect solar radiation and reject solar heat gains at the building surfaces, which results in reduced heat transferred to the internal space by conduction (Kolokotroni et al., 2013). As a result, cool roofs reduce the need for cooling in summer but increase the need for heating in winter (Heat Island Group, 2022).

As demonstrated by numerous experimental and computational studies, cool roofs reduce the energy demand of buildings in cooling-dominated climates (Kolokotroni et al., 2013). There were concerns that cool roofs increase heating energy consumption due to lower solar radiation absorption, and the heating penalties may exceed the cooling savings. However, research has shown that cool roofs in cold climates can also save energy expenditure, especially under the effect of snow (e.g., Hosseini & Akbari, 2016).

In this paper, we consider a commercial building that consumes electricity for cooling and natural gas for heating (U.S. EIA, 2021d, p. 28), where its electricity consumption sufficiently exceeds its natural gas consumption. The commercial building is currently equipped with a conventional roof, but the profit-maximizing decision-maker has an option to convert the conventional roof to a cool roof so as to improve energy efficiency and reduce utility bills. The roof conversion will reduce electricity consumption but increase natural gas consumption (Akbari et al., 1999).

This endeavor is costly yet irreversible and made under the uncertainties of electricity and natural gas prices. The electricity and natural gas prices increase on average and fluctuate over time (U.S. EIA, 2021c; U.S. EIA, 2022b), and a correlation relationship between them is also observed (Lukes, 2021; U.S. EIA, 2021a; Pressler, 2022) because natural gas is used for power generation (Maribu et al., 2007).

Under such a framework, we aim to provide decision support for the conversion from a conventional roof to a cool roof under the uncertainties of electricity and natural gas prices. Specifically, in a basic model, we characterize the electricity price as a geometric Brownian motion (GBM) process and the natural gas price as a constant multiplied by the electricity price. We mathematically construct and analyze the roof conversion model using a real options approach and analytically derive the optimal electricity price threshold to implement the roof conversion and the expected time. To demonstrate how our model can be applied and how locations impact the roof conversion decision, we conduct a numerical example for retail stores in the Northeast and the South of the United States using publicly available data (or estimated and hypothetical data when not available) with justifications. We obtain the optimal electricity price threshold and the corresponding expected time and numerically examine the impact of parameter values on the optimal threshold and the expected time.

In an extended model, a more general and complicated case, we model the electricity the natural gas prices as correlated GBM processes. Under a real options framework, we apply the Least Squares Monte Carlo simulation to obtain the value of the roof conversion option by way of a numerical example. Following that, the numerical example for retail stores in the Northeast and the South of the United States is extended to obtain the value of the roof conversion option. Through numerical sensitivity analysis, we show how the value of the roof conversion option is impacted when the parameter values change.

The rest of this paper is organized as follows. In Section 2, we review the literature on cool roofs and the application of the real options approach involving correlated uncertainties. Next, in Section 3 (basic model), we construct and analyze the roof conversion model and analytically solve for the optimal electricity price threshold to implement the roof conversion, followed by a numerical example and sensitivity analysis. Next, in Section 4 (extended model), we obtain the value of the roof conversion option using the Least Squares Monte Carlo simulation via a numerical example and perform sensitivity analysis. In Section 5, the discussion section, we first demonstrate the connection between the basic model and the extended model via a numerical example and discuss the choice of distributions in simulation. Finally, we summarize our findings and discuss the limitations and future research in Section 6.

Literature Review

Cool Roofs

Much experimental and computational literature has quantitatively investigated the energy saving of cool roofs in different countries and regions (e.g., Akbari et al., 1999; Kolokotroni et al., 2013; Paolini et al., 2014; Feng et al., 2022). Moreover, Guo et al. (2020) integrated the cool roof and night ventilation and evaluated the thermal performance, energy savings, and thermal comfort improvement. A multi-objective optimization approach was applied to optimize the annual cooling energy use and thermal comfort performance.

However, to the authors' knowledge, the decision support from an economic perspective for converting a conventional roof to a cool roof under energy price uncertainties has not been addressed in the existing literature.

Application of Real Options under Correlated Uncertainties

Derived from financial engineering, the real options approach has been applied in decision-making under uncertainties in various industries. In this section, we present a review of the literature on the applications of real options where the underlying uncertainties follow correlated uncertainties (e.g., correlated GBM processes) and group the literature by methods, i.e., analytical, lattice, and simulation.

First, literature using the analytical method of the real options approach can be further divided into two streams. The first stream of literature derives the optimal thresholds of the random variables as the decision variables. For instance, Dockendorf & Paxson (2013) developed real options models to value an operating asset with the flexibility to choose between two commodity outputs (e.g., ammonia and urea). The two commodity prices were assumed to follow correlated GBM processes. The authors derived quasi-analytical solutions to the optimal thresholds of the commodity prices to switch from producing one commodity output to the other. The second stream of literature uses the ratio between two random variables as the decision variable. For instance, in an investment entry problem in Dixit and Pindyck (1994, pp. 207-211), the revenue and the investment cost were assumed to follow correlated GBM processes. The authors used the ratio of revenue over the investment cost as the decision variable and derived the closed-form solution to the optimal ratio as the free boundary between waiting and investment. Similarly, in the entry and exit problem of ethanol firms in Schmit et al. (2011), the revenue and cost were assumed to follow correlated GBM processes. The authors also used the ratio of revenue over cost as the decision variable and proposed the boundary conditions with which the optimal ratio to entry and exit can be numerically solved.

The second method in the real options approach is the lattice. For instance, Wang and Min (2006) developed and analyzed a real options model for general interrelated projects. The authors derived lattices to approximate the interrelated continuous processes for the evolution of project values and options and provided a backward dynamic programming model for optimal sequential decision-making upon options and illustrated via a numerical example of electric power generation planning. Moreover, Elias et al. (2018) assessed the value of retrofitting carbon capture and storage technology (post-combustion and oxy-fuel combustion) to an existing natural gas-fired base-load power plant in a deregulated electricity market. The price uncertainties of electricity and natural gas were characterized as correlated Mean Reverting (MR) processes, and their movements were modeled through lattices.

The third method using a real options approach is the Least Squares Monte Carlo simulation, a simple yet powerful approach developed by Longstaff and Schwartz (2001) to approximate the value of American options by simulation. Cortazar et al. (2008) valuated a copper mine using Least Squares Monte Carlo simulation under the correlated uncertainties of the commodity spot price, the demeaned convenience yield, and the expected long-term spot price return. Moreover, Abadie and Chamorro (2017) addressed the valuation of the options to delay investment and the option to abandon a producing field in crude oil production using Least Squares Monte Carlo simulation where the spot price, long-term price, and spot price volatility are uncertain and correlated with each other. In addition, Maeda and Watts (2019) assessed the economic valuation of wind farms and analyzed the effect of incorporating the uncertainty of the levelized cost of energy in the valuation on top of the electricity price uncertainty.

Basic Model

To facilitate the formulation and analysis, we propose the following assumptions.

Assumption 4.1: *The time granularity is a year, and the seasonal pattern of the energy consumption for cooling and heating is not considered.*

Assumption 4.2: *The commercial building consumes electricity for cooling and natural gas for heating, and the consumption is constant. Moreover, the electricity consumption sufficiently exceeds its natural gas consumption.*

Assumption 4.3: *The conversion from a conventional roof to a cool roof reduces the annual electricity consumption from* D_C *(kWh) to* $(1 - \theta_C)D_C$ *(kWh), where* $0 \leq \theta_C \leq 1$.

Assumption 4.4: *The conversion from a conventional roof to a cool roof increases the annual natural gas consumption from* D_H *(kWh) to* $(1 + \theta_H)D_H$ *(kWh), where* $0 \leq \theta_H < \frac{\theta_C D_C}{D_H}$.

Assumptions 4.3 and 4.4 are backed up by references investigating the energy consumption change due to roof conversion (e.g., Akbari et al., 1999). The requirement of $\theta_H < \frac{\theta_C D_C}{D_H}$ is equivalent to $\theta_C D_C > \theta_H D_H$. This implies that the electricity consumption reduction exceeds the natural gas consumption increase after the roof conversion, so the decision-maker is incentivized to convert a conventional roof to a cool roof.

We also note that despite the typical unit for natural gas consumption being British Thermal Unit (BTU) or therm, we unify the unit of electricity and natural gas consumption to be kWh for ease of formulation and analysis.

Assumption 4.5: *The time to convert a conventional roof to a cool roof is negligible and assumed to be 0.*

Assumption 4.6: *After converting a conventional roof to a cool roof, the cool roof will be used forever.*

Energy Price Modeling

Multiple factors impact energy prices, e.g., fuel costs, power plant availability and costs, generation sources availability, transmission and distribution system, variations in electricity demand, weather conditions, regulations, etc. (U.S. EIA, 2021a). Especially, the market-driven energy prices in deregulated markets, where consumers can switch among different providers (Electric Choice, 2022), are more volatile as the deregulation exposes the inherent volatility of energy prices (Klitgaard & Reddy, 2000). In the literature, electricity and natural gas prices have been commonly modeled as GBM processes (e.g., Zambujal-Oliveir, 2013, Santos et al., 2014, Hach & Spinler, 2016).

Assumption 4.7: *The electricity price C_t ($/kWh) can be characterized as a geometric Brownian motion (GBM) process:*

$$dC_t = \alpha_C C_t dt + \sigma_C C_t dz_C \tag{4.1}$$

where α_C (% per year; > 0) and σ_C (% per year; >0) are the instantaneous growth rate and the instantaneous volatility of electricity price, respectively. dt is the increment of time, and dz_C is the increment of a Wiener process. That is, $dz_C = \varepsilon_C \sqrt{dt}$ where $\varepsilon_C \sim N(0, 1)$. The time granularity is a year.

Figure 4.1 shows that from 2001 to 2016, the average commercial electricity price in Illinois (a deregulated electricity market) increased in general and fluctuated over time (U.S. EIA, 2021c). Variables with such a trend are commonly modeled as a GBM process in the decision-making under uncertainties using a real options approach as it can characterize the trend and facilitate the model formulation and analysis. To verify the plausibility of assuming that the electricity price follows a GBM process, we test the electricity price data against the normality, stationary, and independence tests. The results indicate no evidence to reject such an assumption.

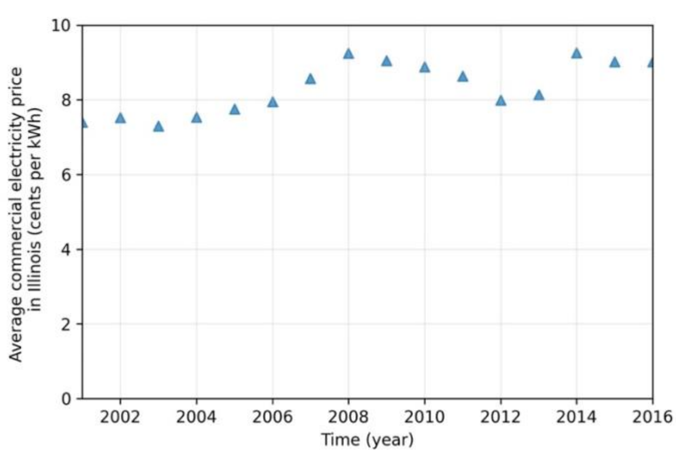

Figure 4.1 Average commercial electricity price in Illinois from 2001 to 2016 (U.S. EIA, 2021c)

Assumption 4.8: The relationship between the natural gas price H_t (\$/kWh) and the electricity price is characterized by Equation (4.2) where λ is a constant which denotes the ratio of natural gas price over electricity price.

$$H_t = \lambda C_t \tag{4.2}$$

The approximation in the relationship between electricity and natural gas prices is backed up by the rule of thumb in the literature. For instance, CenterPoint Energy (n.d.) states that natural gas prices are consistently two to three times lower than electricity prices even when a range of electricity prices is considered. Besides, a dimensionless value representing the ratio of the electricity cost rate to the natural gas cost rate is used in the problem of an optimal energy management of cogeneration system for combined cooling, heating, and power production (Kong et al., 2005).

With Equations (4.1) and (4.2), it can be verified that

$$dH_t = \alpha_C H_t dt + \sigma_C H_t dz_C \tag{4.3}$$

which implies that H_t also follows a GBM process with the same growth rate α_C and volatility σ_C as C_t (see Appendix 4A for proof). The assumption that the natural gas price follows a GBM process aligns with the price evolution. As can be observed from Figure 4.2, the average commercial natural gas price in Illinois (a deregulated natural gas market) increases in general and fluctuates over time between 1990 and 2020 (U.S. EIA, 2022b). We also verify the plausibility of assuming the natural gas price follows a GBM process through statistical tests, and the results indicate no evidence to reject such an assumption.

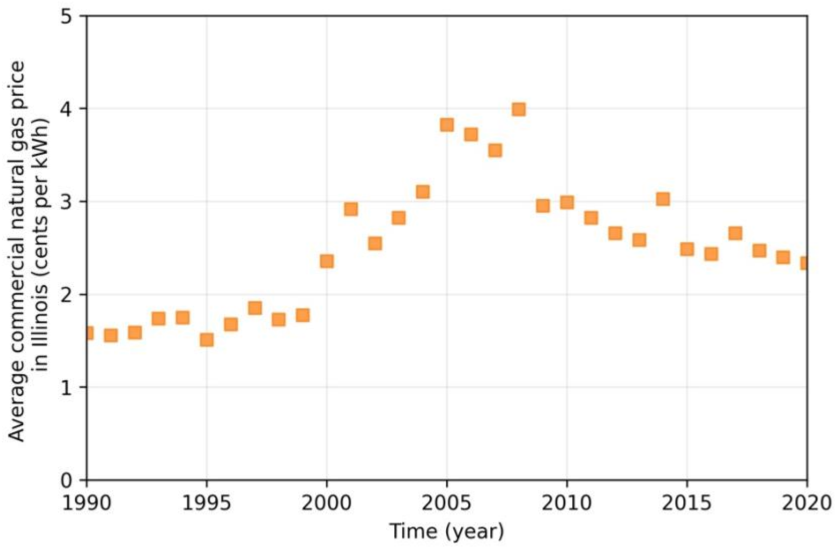

Figure 4.2 Average commercial natural gas price in Illinois from 1990 to 2020 (U.S. EIA, 2022b)

We also note that in the basic model, the natural gas price is a function of the electricity price, which simplifies the model to only one GBM process, the electricity price. Since the electricity increases on average and fluctuates over time, the decision-maker is incentivized to exercise the roof conversion option.

Model Formulation

The decision-maker collects revenue of R (\$) generated from the operation of the commercial building and is responsible for an operating expense excluding energy costs M (\$) (e.g., janitorial/maintenance, real estate, and other taxes, administrative/benefits, and insurance/services) and the electricity and natural gas expenditures. Correspondingly, the profit flows of while using a conventional roof π_{convl} and while using a cool roof π_{cool} are given by:

$$\pi_{convl} = R - M - (D_C + D_H\lambda)C_t \tag{4.4}$$

$$\pi_{cool} = R - M - [(1 - \theta_C)D_C + (1 + \theta_H)D_H\lambda]C_t \tag{4.5}$$

To ensure that the total energy cost decreases after the roof conversion, we require that $D_C C_t + D_H H_t > (1-\theta_C) D_C C_t + (1+\theta_H) D_H H_t$, which is equivalent to $\lambda < \frac{\theta_C D_C}{\theta_H D_H}$ in the basic model.

While using a conventional roof, the value of the project V_{convl} is the value of the commercial building given that a conventional roof is currently used, and there is a future potential to switch to a cool roof. It is equal to the summation of the discounted cash flow generated from the operation while using a conventional roof plus the value of the option to switch to a cool roof (Dixit & Pindyck, 1994, pp. 187-188). During the operation while using a conventional roof, V_{convl} follows the Bellman optimality equation:

$$\rho V_{convl} dt = \pi_{convl} dt + E[dV_{convl}] \tag{4.6}$$

where ρ (% per year; >0) is the discount rate for money. Equation (4.6) implies that the total return of the project consists of the profit generated from the operation plus the expected future appreciation in the value of the project.

After applying Ito's Lemma on dV_{convl}, the following second-order differential equation is yielded:

$$\frac{1}{2}{\sigma_C}^2 {C_t}^2 \frac{\partial^2 V_{convl}}{\partial {C_t}^2} + \alpha_C C_t \frac{\partial V_{convl}}{\partial C_t} - \rho V_{convl} + \pi_{convl} = 0 \tag{4.7}$$

It can be verified that under technical conditions of $\rho - \alpha_C > 0$ and $\alpha_C - \frac{{\sigma_C}^2}{2} > 0$ (Dixit & Pindyck, 1994), the general solution to Equation (4.7) is given by:

$$V_{convl}(C_t) = A_1 {C_t}^{\beta_1} + \frac{R-M}{\rho} - \frac{(D_C + D_H \lambda) C_t}{\rho - \alpha_C} \tag{4.8}$$

where $\beta_1 = \frac{1}{2} - \frac{\alpha_C}{{\sigma_C}^2} + \sqrt{\left(\frac{\alpha_C}{{\sigma_C}^2} - \frac{1}{2}\right)^2 + \frac{2\rho}{{\sigma_C}^2}} > 1$, and A_1 is the constant coefficient for the homogenous terms to be determined.

Considering that numerous literature calls for a conversion from a conventional roof to a cool roof, but a reverse conversion has been rarely mentioned in the existing literature, the decision-maker has no option to switch from a cool roof to a conventional roof. While using a cool roof, the value of the project V_{cool} is the value of the commercial building, given that a cool roof is currently used, which is equal to the discounted cash flow generated from the operation of the commercial building, as given in Equation (4.9).

$$V_{cool}(C_t) = \frac{R-M}{\rho} - \frac{[(1-\theta_C)D_C+(1+\theta_H)D_H\lambda]C_t}{\rho-\alpha_C} \tag{4.9}$$

Equation (4.7) is subject to the following two boundary conditions:

$$V_{convl}(C^*) = V_{cool}(C^*) - I \Rightarrow$$

$$A_1 C^{*\beta_1} + \frac{R-M}{\rho} - \frac{(D_C+D_H\lambda)C^*}{\rho-\alpha_C} = \frac{R-M}{\rho} - \frac{[(1-\theta_C)D_C+(1+\theta_H)D_H\lambda]C^*}{\rho-\alpha_C} - I \tag{4.10}$$

$$V_{convl}'(C^*) = V_{cool}'(C^*) \Rightarrow A_1\beta_1 C^{*\beta_1-1} - \frac{(D_C+D_H\lambda)}{\rho-\alpha_C} = -\frac{[(1-\theta_C)D_C+(1+\theta_H)D_H\lambda]}{\rho-\alpha_C} \tag{4.11}$$

where C^* is the optimal threshold of electricity price at which point a conversion from a conventional roof to a cool roof should be implemented, and I (\$) is the cost to transit from a conventional roof to a cool roof.

Equation (4.10) is the value-matching condition, which states that at the optimal threshold of electricity price, the value of the project under a conventional roof is equal to the value of the project under a cool roof minus the cost to transit a conventional roof to a cool roof. Equation (4.11) is the smooth-pasting condition, which requires that the slope of the left-hand side and the right-hand side of Equation (4.10) equal at C^*.

First, from the smooth-pasting condition of Equation (4.11), we can analytically solve for A_1, which can be verified to be:

$$A_1 = \frac{\theta_C D_C - \theta_H D_H \lambda}{(\rho-\alpha_C)\beta_1 C^{*\beta_1-1}} \tag{4.12}$$

Next, we substitute the expression of A_1 into the value-matching condition of Equation (4.10). The closed-form solution to C^* can be verified to be:

$$C^* = \frac{I(\rho-\alpha_C)\beta_1}{(\theta_C D_C - \theta_H D_H \lambda)(\beta_1 - 1)} \tag{4.13}$$

Correspondingly, the expected time of roof conversion is given by (Dixit & Pindyck, 1994):

$$E[T^*] = \frac{\ln C^* - \ln C_0}{\alpha_C - \frac{\sigma_C{}^2}{2}} = \frac{\ln \frac{I(\rho-\alpha_C)\beta_1}{(\theta_C D_C - \theta_H D_H \lambda)(\beta_1 - 1)} - \ln C_0}{\alpha_C - \frac{\sigma_C{}^2}{2}} \tag{4.14}$$

Analytical Sensitivity Analysis

Among the nine parameters that appear in the expressions of C^* and $E[T^*]$. By deriving the derivatives of C^* and $E[T^*]$ with respect to seven of them (σ_C, λ, D_C, θ_C, D_H, θ_H, and I), we analytically examined how they impact the roof conversion decision under technical conditions $\rho - \alpha > 0$ and $\alpha - \frac{1}{2}\sigma^2 > 0$ (Dixit & Pindyck, 1994). For the rest two (α_C and ρ), we will numerically examine their impact on the roof conversion decision since the signs of the derivatives of C^* and $E[T^*]$ with respect to them cannot be determined.

Proposition 4.1: $\frac{\partial C^*}{\partial \sigma_C} > 0,\ \frac{\partial E[T^*]}{\partial \sigma_C} > 0.$

Proposition 4.1 implies that as the volatility of electricity price increases, the optimal threshold and the expected time for roof conversion increase. The reason is that when the electricity price becomes more uncertain, the electricity price might become in favor of the decision-maker as time progresses, so the decision-maker prefers to postpone the exercise of the roof conversion option.

Proposition 4.2: $\frac{\partial C^*}{\partial \lambda} > 0, \frac{\partial E[T^*]}{\partial \lambda} > 0.$

Proposition 4.2 indicates that when the ratio of natural gas price to electricity price increases, the optimal threshold and the expected time for roof conversion increase. This makes sense because a higher ratio means a higher natural gas price given a particular electricity price level, which discourages the decision-maker from exercising the roof conversion option because the roof conversion will increase the natural gas consumption.

Proposition 4.3: $\frac{\partial C^*}{\partial D_C} < 0, \frac{\partial E[T^*]}{\partial D_C} < 0; \frac{\partial C^*}{\partial D_H} > 0, \frac{\partial E[T^*]}{\partial D_H} > 0.$

Proposition 4.3 states that the optimal threshold and the expected time for roof conversion decrease as the electricity consumption increases and increase as the natural gas consumption increases. Given that the roof conversion will decrease the electricity consumption and increase the natural gas consumption, the decision-maker is encouraged to exercise the roof conversion option when the electricity consumption is higher and discouraged from exercising it when the natural gas consumption is higher.

Proposition 4.4: $\frac{\partial C^*}{\partial \theta_C} < 0, \frac{\partial E[T^*]}{\partial \theta_C} < 0; \frac{\partial C^*}{\partial \theta_H} > 0, \frac{\partial E[T^*]}{\partial \theta_H} > 0.$

Proposition 4.4 implies that the optimal threshold and the expected time for roof conversion decrease as the percentage reduction in electricity consumption after the roof conversion increases and increase as the percentage increase in natural gas consumption after the roof conversion increases. This makes economic sense because the roof conversion is more economically rational when the cool roof results in more electricity consumption saving and less natural gas consumption penalty.

Proposition 4.5: $\frac{\partial C^*}{\partial I} > 0, \frac{\partial E[T^*]}{\partial I} > 0.$

Proposition 4.5 is straightforward, which suggests that when the conversion from a conventional roof to a cool roof becomes more costly, the decision-maker prefers to wait longer before exercising the roof conversion option, so the optimal threshold and the expected time for roof conversion both increase.

Numerical Example and Sensitivity Analysis

In this section, we conduct a numerical example of one-story retail stores in the Northeast and the South of the United States. The conversion from a conventional roof to a cool roof can be implemented by applying cool roof coating on the existing built-up roof. By built-up roof, we mean the roof with asphalt-coated glass fiber (a material consisting of numerous extremely fine fibers of glass) mat cap sheet surfaced with mineral granules (small compact particles) (GAFGLAS, 2016). As for the cool roof coating, they are white or special reflective pigments that reflect sunlight (U.S. Department of Energy, 2010). The reason that applying cool roof coating to the built-up roof reflects more sunlight is not because of the white color but because the prime pigment, such as Titanium Dioxide (TiO_2), increases sunlight's reflection. Explanation on why TiO_2 reflects more sunlight is provided in Appendix 4B.

The common parameter values are presented in Table 4.1, and the parameter values that vary on location are presented in Table 4.2. Most parameter values are from publicly available data, and some are estimated or from hypothetical data when the public data is unavailable. Justifications for parameter values are provided in Appendix 4C.

Table 4.1 Common parameter values

Parameter (Unit)	**Value**	**Source**
Growth rate of electricity price α_C (per year)	0.0145	U.S. EIA (2021c); Croghan et al. (2017)
Volatility of electricity price σ_C (per year)	0.0520	
Initial value of electricity price C_0 (\$/kWh)	0.0740	U.S. EIA (2021c)

Table 4.1 continued

Parameter (Unit)	**Value**	**Source**
Discount rate for money ρ (per year)	0.02995	CNBC (2022)
Ratio of natural gas price over electricity price λ	0.3657	U.S. EIA (2021c); U.S. EIA (2022b); CenterPoint Energy (n.d.)
Cost to convert a conventional roof to a cool roof I ($)	40,000	Hypothetical

Table 4.2 Parameter values upon locations

Parameter (Unit)	**Northeast**	**South**	**Source**
Annual electricity consumption D_C (kWh)	448,000	570,500	U.S. EIA (2016a)
Annual natural gas consumption D_H (kWh)	266,924	160,580	U.S. EIA (2016b)
Percentage reduction in electricity consumption after roof conversion θ_C	0.04	0.03	Akbari et al. (1999)
Percentage increase in natural gas consumption after roof conversion θ_H	0.06	0.01	

With the above parameter values, we obtain the numerical results in Table 3. For the retail store in the Northeast, the optimal electricity price threshold to convert from a conventional roof to a cool roof is 10.79 cents/kWh, which on average, occurs in 28.65 years. The value of the roof conversion option at time 0 is $ 21,572. Meanwhile, for the retail store in the South, the optimal electricity price threshold for roof conversion is 7.87 cents/kWh, which is expected to occur in 4.70 years. The value of the roof conversion option at time 0 is $ 39,301.

The numerical results suggest that the conversion from a conventional roof to a cool roof is expected to occur sooner in the South than in the Northeast and that the roof conversion option is more valuable in the South than in the Northeast. This makes sense considering the electricity consumption is relatively higher than the natural gas consumption in the South than that in the Northeast, and explains why cool roofs are observed more often in the South than in the Northeast.

Table 4.3 Numerical results

Description	**Northeast**	**South**
β_1	1.9048	1.9048
A_1	3,074,664	5,601,284
Optimal electricity price threshold for roof conversion C^* ($/kWh)	0.1079	0.0787
Expected roof conversion time $E[T^*]$ (year)	28.65	4.70
Value of the roof conversion option at time 0 $A_1 {C_0}^{\beta_1}$ ($)	21,572	39,301

Figures 4.3 and 4.4 show the variation of C^* and $E[T^*]$ with respect to α_C and ρ respectively. In both figures, we observe that the optimal electricity price threshold to convert the conventional roof to a cool roof for the retail store in the Northeast is higher than that for the retail store in the South, similarly for the corresponding expected time.

From Figure 4.3, we observe that as the growth rate of the electricity price increases, the optimal electricity price threshold and the corresponding expected time decrease. This makes sense because when the electricity price grows faster, the decision-maker is incentivized to convert the conventional roof to a cool roof sooner, as the latter one is more energy efficient.

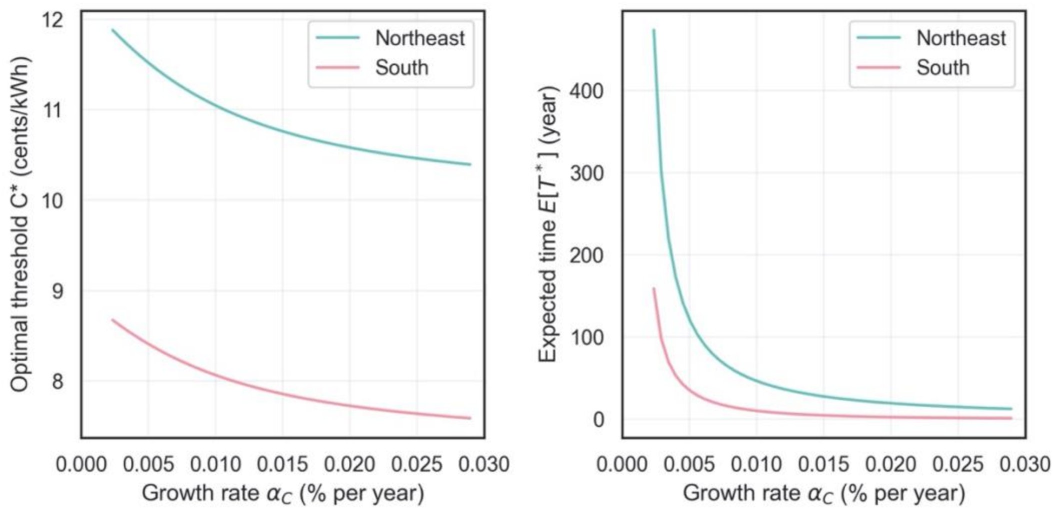

Figure 4.3 Variation of C^* and $E[T^*]$ with respect to α_C

As shown in Figure 4.4, when the discount rate for money increases, the optimal electricity price threshold and the expected conversion time increase. This also makes sense because the decision-maker is inclined to postpone the conversion to a cool roof as the future cost becomes more heavily discounted.

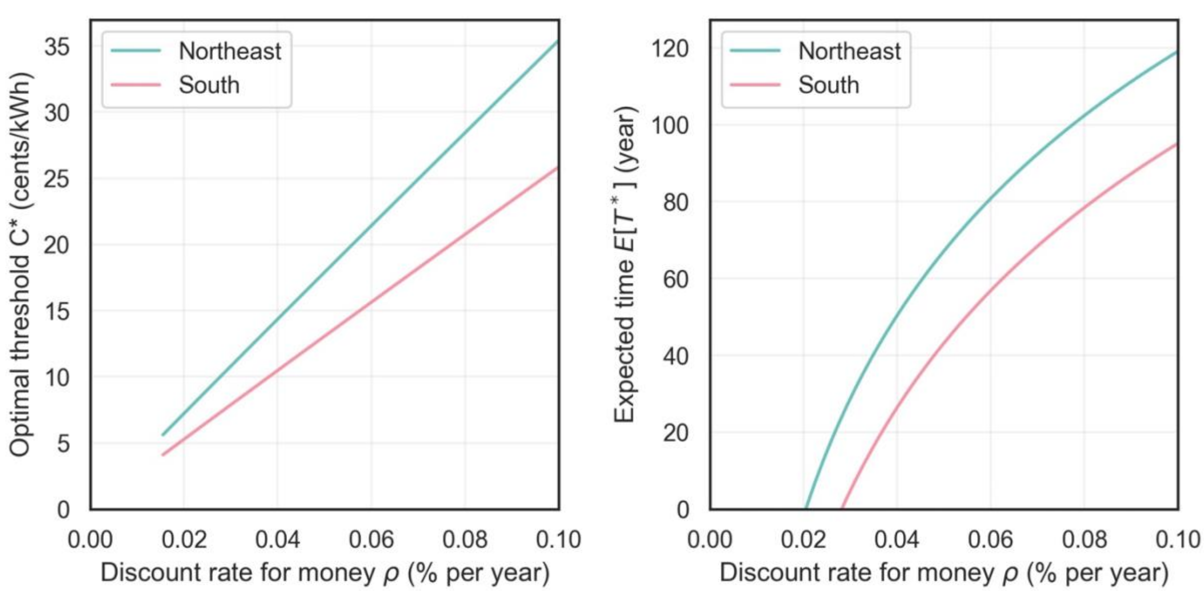

Figure 4.4 Variation of C^* and $E[T^*]$ with respect to ρ

Extended Model

In this section, we extend the basic model to a more general and complicated case where the electricity and the natural gas prices follow correlated GBM processes. Assumptions 4.1 to 4.5 in the basic model still hold in the extended model.

Energy Price Modeling

Assumption 4.9: *The electricity price C_t ($/kWh) can be characterized as a geometric Brownian motion (GBM) process:*

$$dC_t = \alpha_C C_t dt + \sigma_C C_t dz_C \tag{4.15}$$

where α_C (% per year; > 0) and σ_C (% per year; >0) are the instantaneous growth rate and the instantaneous volatility of electricity price, respectively. dt is the increment of time, and dz_C is the increment of a Wiener process. That is, $dz_C = \varepsilon_C \sqrt{dt}$ where $\varepsilon_C \sim N(0, 1)$. The time granularity is a year.

Assumption 4.10: *The natural gas price at year t, H_t ($/kWh), follows a GBM process:*

$$dH_t = \alpha_H H_t dt + \sigma_H H_t dz_H \tag{4.16}$$

where α_H (% per year; > 0) and σ_H (% per year; >0) are the instantaneous growth rate and the instantaneous volatility of natural gas price, respectively. dt is the increment of time, and dz_H is the increment of a Wiener process. That is, $dz_H = \varepsilon_H \sqrt{dt}$, where $\varepsilon_H = r_{CH}\varepsilon_C + \sqrt{1 - {r_{CH}}^2}\varepsilon_0$. r_{CH} is the constant correlation coefficient between the uncertainty incorporated in the change of C_t and H_t, $\varepsilon_0 \sim N(0, 1)$, and ε_C and ε_0 are uncorrelated (Sigman, 2007; Liatard, 2022). It can be verified that $E[\varepsilon_C \varepsilon_H] = r_{CH}$. See Appendix 4D for proof.

The correlation relationship between electricity and natural gas prices has been well documented in the literature (e.g., U.S. EIA, 2021a; Pressler, 2022) because natural gas is used for power generation (Maribu et al., 2007). Lukes (2021) found a correlation between the electricity and natural gas prices in more than 33 different markets in the United States over 15 years. The correlation varied from 0.81 to 0.96 and remained stable over time, where 0 indicates no correlation and 1 indicates a perfect correlation.

The basic model is a special case of the extended model from a perspective of energy price modeling. First, the electricity price modeling remains the same in both models, i.e., a GBM process. As for the natural gas price modeling, in the basic model, Equation (4.3) can be verified, where $dH_t = \alpha_C H_t dt + \sigma_C H_t dz_C$. In the extended model, with $\alpha_H = \alpha_C$, $\sigma_H = \sigma_C$, and $r_{CH} = 1$, Equation (4.16) becomes Equation (4.17) as follows, which is the same as Equation (4.3). In other words, when the natural gas price shares the same growth rate and volatility of the electricity price, and the electricity and natural gas prices are perfectly correlated, the extended model in the extended model becomes that in the basic model.

$$dH_t = \alpha_H H_t dt + \sigma_H H_t \left(r_{CH}\varepsilon_C + \sqrt{1 - {r_{CH}}^2}\varepsilon_0\right)\sqrt{dt}$$

$$= \alpha_C H_t dt + \sigma_C H_t\left(1\varepsilon_C + \sqrt{1 - 1^2}\varepsilon_0\right)\sqrt{dt} = \alpha_C H_t dt + \sigma_C H_t \varepsilon_C \sqrt{dt} \tag{4.17}$$

Model Formulation

The profit flows while using a conventional roof and a cool roof are as follows.

$$\pi_{convl} = R - M - D_C C_t - D_H H_t \tag{4.18}$$

$$\pi_{cool} = R - M - (1 - \theta_C)D_C C_t - (1 + \theta_H)D_H H_t \tag{4.19}$$

The net energy cost saving due to the conversion from a conventional roof to a cool roof at time t is hence given by $\pi_{cool} - \pi_{convl}$, i.e., $\theta_C D_C C_t - \theta_H D_H H_t$.

The objective function can be formulated as follows:

$$\max_{T^*} E\left\{\int_0^{T^*} e^{-\rho t}\,(R - M - D_C C_t - D_H H_t)dt - Ie^{-\rho T^*} + \int_{T^*}^{\infty} e^{-\rho t}[R - M - (1 - \theta_C)D_C C_t - (1 + \theta_H)D_H H_t]dt\right\} \tag{4.20}$$

T^* is the optimal time of roof conversion that maximizes the expected value of discounted profit.

In the extended model, the electricity and natural gas prices both increase on average with a correlation relationship, so the electricity cost saving may not always exceed the natural gas cost penalty. This suggests that converting a conventional roof to a cool roof may or may not result in a positive net energy cost saving, meaning that the roof conversion option is not guaranteed to exist in the analytical model. In addition, a reverse conversion (converting a cool roof to a conventional roof) has rarely been addressed in the literature, so it is impractical to assume the existence of the option for such a reverse conversion. These two reasons differentiate our roof conversion problem from Dockendorf and Paxson (2013), where continuous switching is allowed from producing one commodity output to the other, and quasi-analytical solutions to the commodity prices for alternate switching are derived.

We also consider using the ratio of correlated GBM processes as the decision variable (e.g., Dixit and Pindyck, 1994, pp. 207-211; Schmit et al., 2011). Using this approach, the project value has to be written as a function of the ratio, where the ratio is the only decision variable, and the optimal decision only depends on the ratio. However, in our roof conversion problem, we are modeling from a profit maximization perspective, besides the energy costs, the revenue and the operation expense should also be included in the project value. As a result, the project value cannot be converted to a function where the ratio is the only decision variable, so the ratio approach does not apply to our problem either.

As for the lattice method, the computation complexity substantially increases when more than one GBM process is considered, especially when the GBM processes are correlated.

Finally, we use the Least Squares Monte Carlo simulation to valuate the roof conversion option as the decision support, which was originally proposed by Longstaff and Schwartz (2001) and has been used in option evaluation when analytical and lattice methods are not applicable. They used Least Squares to estimate the expected payoff to the option holder from continuation with the current stock price and approximate the value of American options by Monte Carlo simulation. We extend its application to the valuation of the roof conversion option and achieve it by way of a numerical example. That is, we use Least Squares to estimate the expected payoff from continuation with the current electricity and natural gas prices and obtain the value of the roof conversion option by Monte Carlo simulation.

GBM Discretization

Let us denote the modeling horizon as L (year), and the discrete time index as k ($k = 0, 1, 2, \dots, L-1$). With Δt (e.g., $\Delta t = 1$), the continuous GBM processes of energy prices in the extended model, Equations (4.15) and (4.16), can be discretized as follows (Luenberger, 1997, p. 311):

$$C_{k+1} - C_k = \alpha_C C_k \Delta t + \sigma_C C_k \varepsilon_{Ck} \sqrt{\Delta t} \tag{4.21}$$

$$H_{k+1} - H_k = \alpha_H H_k \Delta t + \sigma_H H_k \left(r_{CH} \varepsilon_{Ck} + \sqrt{1 - {r_{CH}}^2} \varepsilon_{0k} \right) \sqrt{\Delta t} \tag{4.22}$$

where ε_{Ck}'s are independent and identically distributed random variables that follow a standard normal distribution, and the same for ε_{0k}'s. For each k, ε_{Ck} and ε_{0k} are uncorrelated.

Net Energy Cost Saving

The net energy cost saving from year k to year L when the roof conversion option is exercised in year k is denoted as N_k.

When $k = L$, N_k (or N_L) is given by:

$$N_L = \theta_C D_C C_L - \theta_H D_H H_L \tag{4.23}$$

At year k ($k < L$), only the energy prices from year 0 to year k are known, but energy prices from year $k+1$ to time L are unknown. However, the expectation of energy prices in year $k+1$, …, L can be estimated by taking the average of the simulated energy prices in year $k+1$, …, L, respectively. That is, for any year i ($i = k+1, \dots, L$), the expected value of electricity price at year i is given by $E[C_i] = \frac{1}{n}\sum_{j=1}^{n} C_i^j$ where j is the path index ($j = 1, 2, 3, \dots, n$, n is the number of paths simulated). Similarly for the expected natural gas price in year i, $E[H_i] = \frac{1}{n}\sum_{j=1}^{n} H_i^j$.

Correspondingly, if the roof conversion option is exercised in year k, the expected net energy cost saving from year k to year L is calculated as the net energy cost saving in year k plus the expected net energy cost saving from year $k+1$ to year L discounted to year k as follows.

$$E[N_k] = \theta_C D_C C_k - \theta_H D_H H_k + \sum_{i=k+1}^{L} (\theta_C D_C E[C_i] - \theta_H D_H E[H_i]) e^{-\rho(i-k)} \quad (4.24)$$

Exercise Value and Continuation Value

As discussed in literature such as Longstaff and Schwartz (2001) and Abadie and Chamorro (2017), the decision on whether to exercise the option depends on the exercise value and the continuation value evaluated at the time of making the decision.

In year L, the exercise value is the net energy cost if the option is exercised in year L minus the cost to covert a conventional roof to a cool roof, i.e., $N_L - I$. The continuation value (the value of holding the option) is zero because the option is not obligated to be exercised and expires after the end of the modeling horizon. The roof conversion option should be exercised if $N_L - I > 0$. The payoff in L is the maximum of the exercise value and the continuation value:

$$V_L = \max\{N_L - I, 0\} \quad (4.25)$$

In year k ($k < L$), the exercise value is the expected net energy cost if the option is exercised in year k minus the cost to covert a conventional roof to a cool roof, i.e., $E[N_k] - I$.

The decision-maker must decide whether to exercise the roof conversion option immediately or continue holding it until year $k + 1$. The option should be exercised if exercising immediately is more valuable than the expected value from holding (Abadie & Chamorro, 2017), which calls for estimating the continuation value. For this purpose, we regress the payoff in year $k + 1$ if the option is not exercised in year k discounted to year k on the degree 2 polynomial in the energy prices at time k (C_k and H_k). That is,

$$E[e^{-\rho\Delta t}V_{k+1}(C_k, H_k)] = a_0 + a_1C_k + a_2H_k + a_3C_k^2 + a_4C_kH_k + a_5H_k^2 \quad (4.26)$$

With the in-the-money paths (i.e., $E[N_k] - I > 0$), we apply least squares Monte Carlo simulation to obtain the numerical estimate of the coefficients a_0, a_1, …, a_5 to estimate the continuation value in year k. The payoff in year k is hence given by:

$$V_k = \max\{E[N_k] - I, E_k[e^{-\rho}V_{k+1}(C_k, H_k)|C_k, H_k]\} \quad (4.27)$$

Only in-the-money paths are included in the Least Squares regression because it “allows us to better estimate the conditional expectation function in the region where exercise is relevant and significantly improves the efficiency of the algorithm” (Longstaff & Schwartz, 2001).

Using backward induction, we can obtain the optimal strategy for exercising the roof conversion option by maximizing the option value at each time along each path. Correspondingly, the option value in year 0 for the path is given by:

$$V_0 = \max\{E[N_0] - I, E_0[e^{-\rho\Delta t}V_1(C_0, H_0)|C_0, H_0]\} \quad (4.28)$$

In the end, we calculate the average option value across all paths as the value of the roof conversion option.

Numerical Example and Sensitivity Analysis

In this section, we conduct the numerical example to obtain the value of the roof conversion option for the retail stores in the Northeast and the South using the Least Squares

Monte Carlo simulation described above. Specifically, we simulate the electricity and natural gas prices with the additional parameter values in Table 4.4, besides the parameter values used in the numerical example of the basic model. The core uncertainty is a standard normal distribution, and the number of paths simulated is 1,000. A smaller value is used for the cost to convert a conventional roof to a cool roof, \$25,000, to generate a positive option value with a modeling horizon of 55 years. The modeling horizon is set to be 55 years is used considering that the lifespan of a commercial building ranges from 50 to 60 years on average without the need for major repairs or renovations and can last longer depending on the preservation techniques and the way the building is utilized (BCI Construction, 2021; Shingobee, 2021). This value is close to the average age of commercial buildings in the United States at the end of 2021, 53.03 years (Feldstein, 2022).

Table 4.4 Additional parameter values used in the numerical example of the extended model

Parameter	**Value**	**Source**
Growth rate of natural gas price α_H (per year)	0.0207	U.S. EIA (2022b), Croghan, et al. (2017)
Volatility of natural gas price σ_H (per year)	0.1248	
Initial value of natural gas price H_0 (\$/kWh)	0.0292	U.S. EIA (2022b)
Correlation coefficient r_{CH}	0.91	Lukes (2021)

One trial of simulated electricity and natural gas prices is shown in Figure 4.5, where both energy prices increase on average and fluctuate over time, and positively correlation can be observed. The triangles connected by a solid blue line depict the electricity prices, and the squares connected by a dashed orange line depict the natural gas prices.

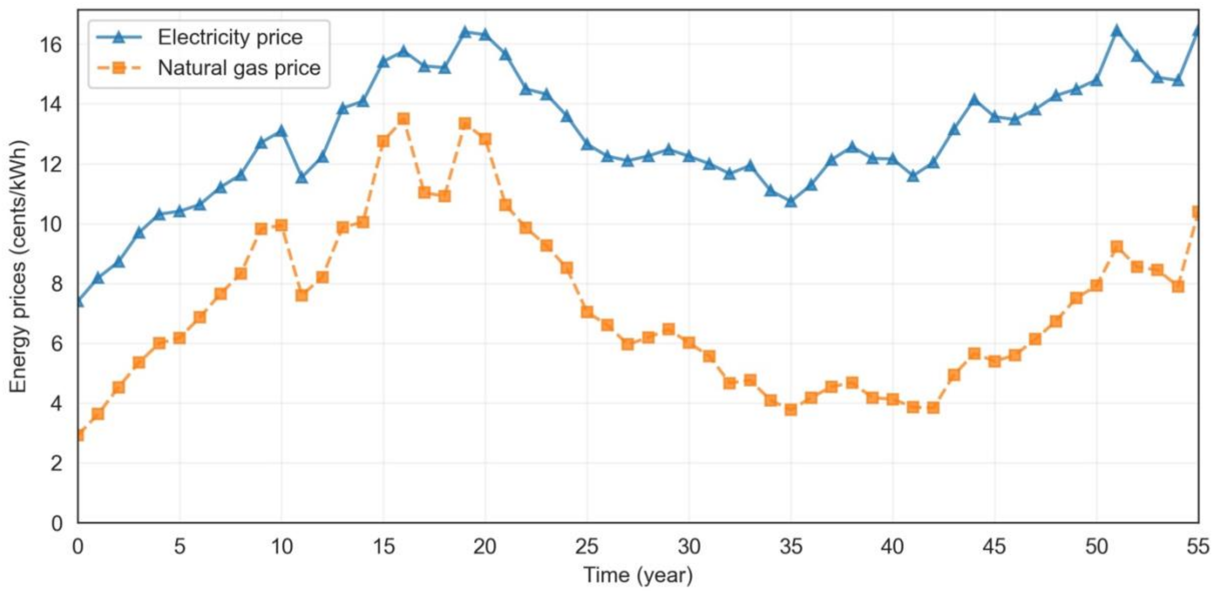

Figure 4.5 One trial of simulated electricity and natural gas prices

The option values for the retail stores in the Northeast are in the South are $4,398 (standard deviation of $27) and $20,289 (standard deviation of $58), respectively, which indicates that the value of the option for the retail store in the South is much higher than that in the Northeast. This makes economic sense given the difference in the electricity and natural gas consumption and the percentage change in the energy consumption after converting from a conventional roof to a cool roof between the Northeast and the South under the impact of location.

To examine how the value of the roof conversion option changes with respect to the parameter values, we perform numerical sensitivity analysis for the numerical example and summarize our observations as follows.

To begin with, it is straightforward that a higher cost to convert a conventional roof to a cool roof I results in a lower option value. Meanwhile, the value of the roof conversion option decreases as the discount rate for money ρ increases (see Figure 4.6). This makes economic sense because when money is heavily discounted as time progresses, the present value of the future energy cost is lower, under which circumstance the roof conversion option is less valuable.

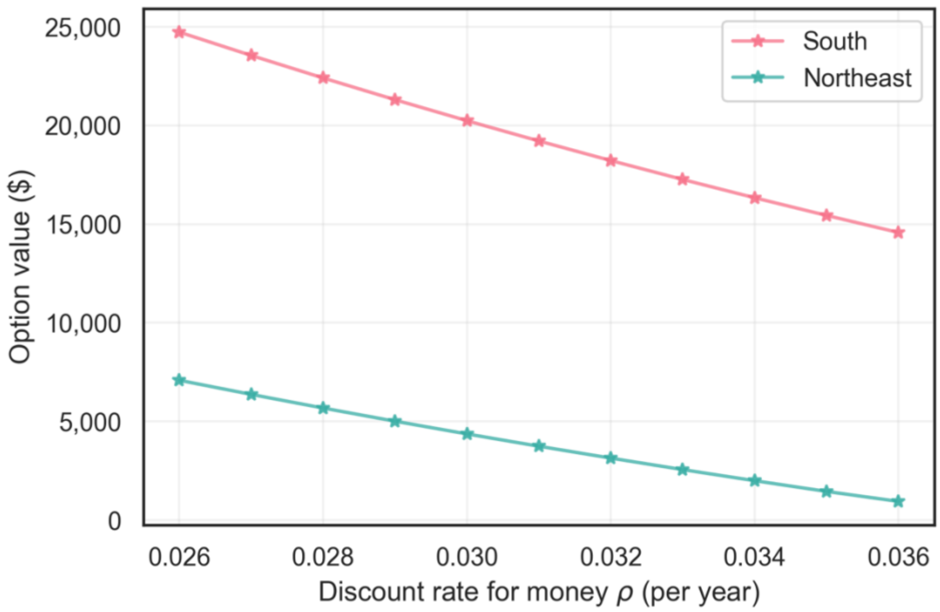

Figure 4.6 Variation of the option value with respect to ρ

Moreover, energy consumption also impacts the roof conversion option's value. Specifically, the option value increases as the annual electricity consumption D_C increases and decreases as the annual natural gas consumption D_H increases. Regarding the energy consumption saving or penalty, the option value increases with the percentage reduction in electricity consumption θ_C and decreases with the percentage increase in natural gas consumption θ_H.

We also observe that the option value increases with the initial value C_0 or the growth rate α_C of the electricity price and decreases with the initial value H_0 or the growth rate α_H of the natural gas price. This makes economic sense because the roof conversion option is more valuable when the electricity price is higher and is less valuable when the natural gas price is higher.

Figure 4.7 shows the variation of the option value with respect to the volatility of energy prices. We observe that the option value increases with the electricity price volatility σ_C and decreases with the volatility of the natural gas price σ_H. Considering that the roof conversion reduces electricity consumption but increases natural gas consumption, it makes sense that the roof conversion option is more valuable when the electricity price becomes more volatile and is less valuable when the natural gas price becomes more volatile.

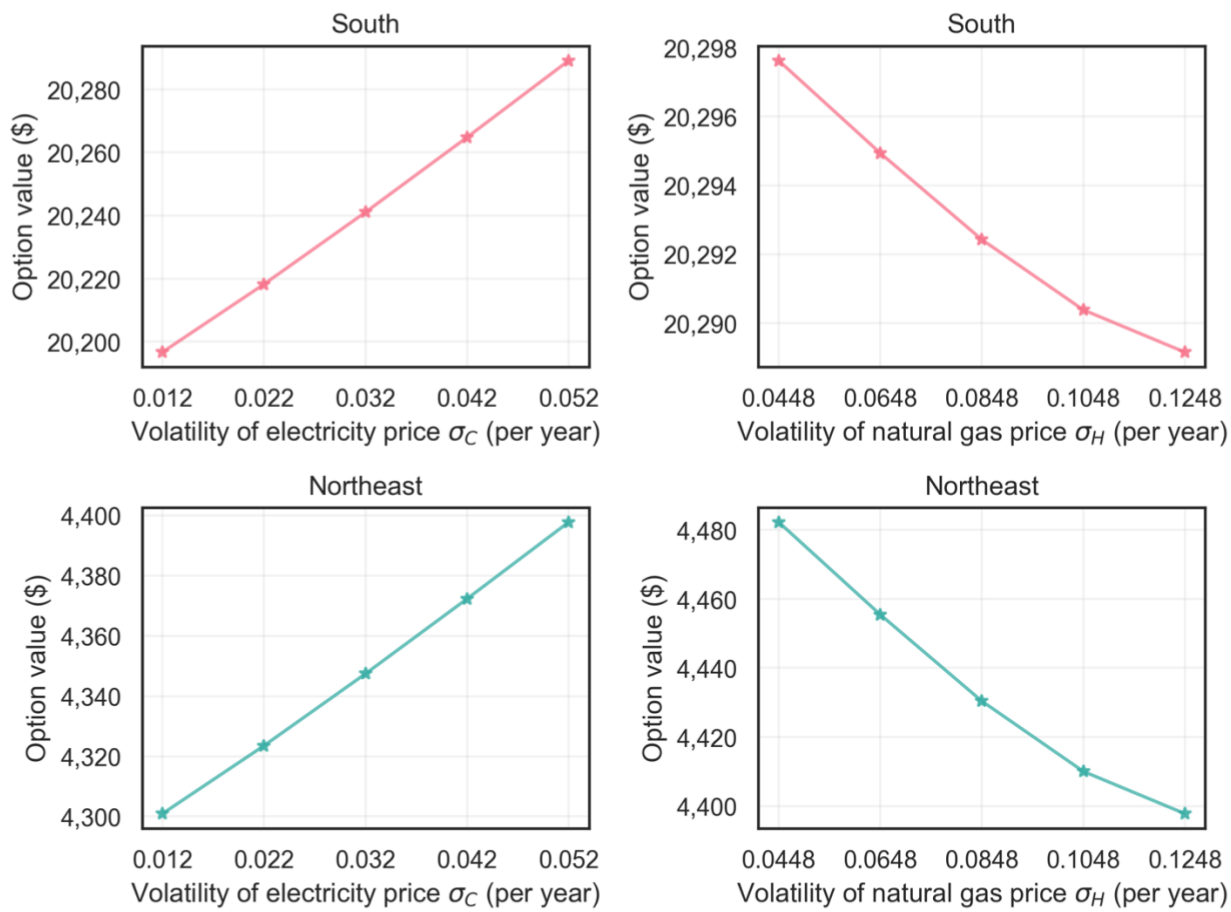

Figure 4.7 Variation of the option value with respect to σ_C and σ_H

The variation of option value with respect to the correlation coefficient r_{CH} between 0 and 1 is shown Figure 4.8. We note that despite the correlation coefficient between two random variables can vary between -1 and 1, we did not find references indicating a negative correlation coefficient between the electricity and natural gas prices, e.g., between 0.81 and 0.96 (Lukes, 2021). We observe that as the correlation coefficient increases, the option value first decreases and then increases, and the option value is the lowest when r_{CH} is around 0.5. The economic implication is as follows. As the correlation coefficient increases from 0 (uncorrelated) to around 0.5 (moderately correlated), with an increasing electricity price, an increasing natural gas price undermines the net energy cost saving after the roof conversion, so the roof conversion option becomes less valuable. However, when the correlation coefficient continues to increase from 0.5 (moderately correlated) to 1 (perfectly correlated), the positive correlation relationship between the electricity and natural gas prices is so strong that the natural gas price can be approximated as a constant multiplied by the electricity price (e.g., the basic model). In such a case, the conversion to a cool roof is more likely to result in a net energy cost saving, so the roof conversion option becomes more valuable.

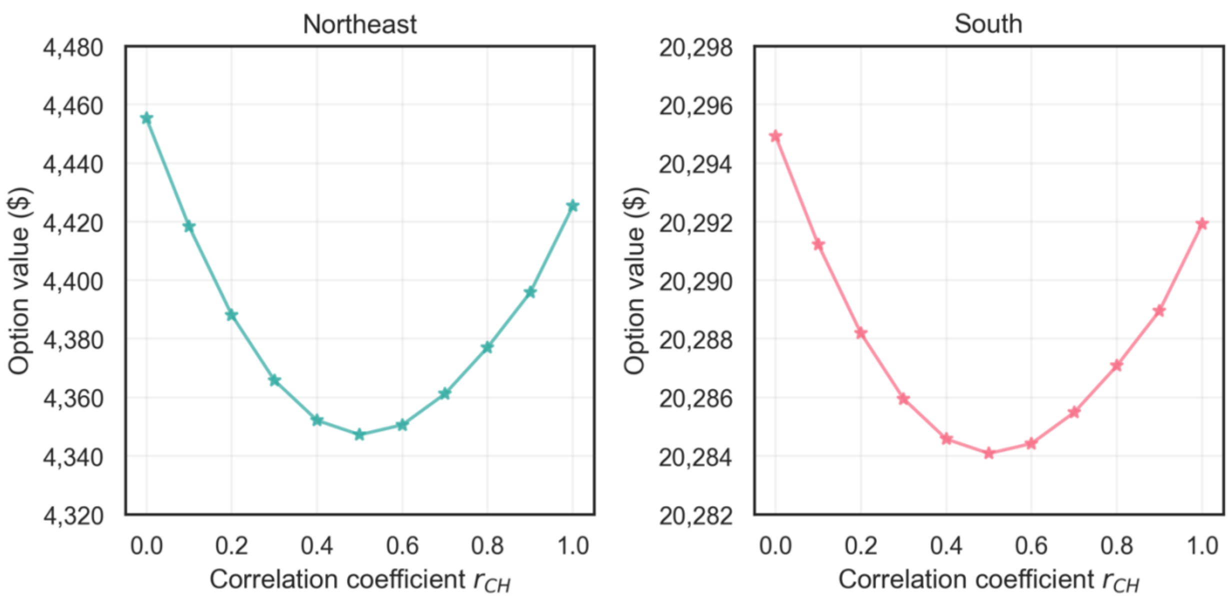

Figure 4.8 Variation of the option value with respect to r_{CH}

Discussion

Connection between Basic Model and Extended Model via Numerical Example

In this subsection, we present the connection between the basic model and the extended model via a numerical example. As previously demonstrated in the energy price modeling in the extended model, the natural gas price in the extended model becomes that in the basic model when $\alpha_H = \alpha_C$, $\sigma_H = \sigma_C$, and $r_{CH} = 1$. We also note that in the basic model, after converting a conventional roof to a cool roof, the cool roof is assumed to be used forever, while in the extended model, a finite modeling horizon is required to apply the simulation approach. Hence, the value of the roof conversion option in the extended model should converge to that in the basic model when the modeling horizon increases and approaches positive infinity, as shown in Figure 4.9. That is, as the modeling horizon in the extended model increases, the option value first rapidly increases, and then the increasing speed slows down and converges to the option value in the basic model when the modeling horizon is longer than 300 years ($21,572 in the Northeast and $39,299 in the South respectively).

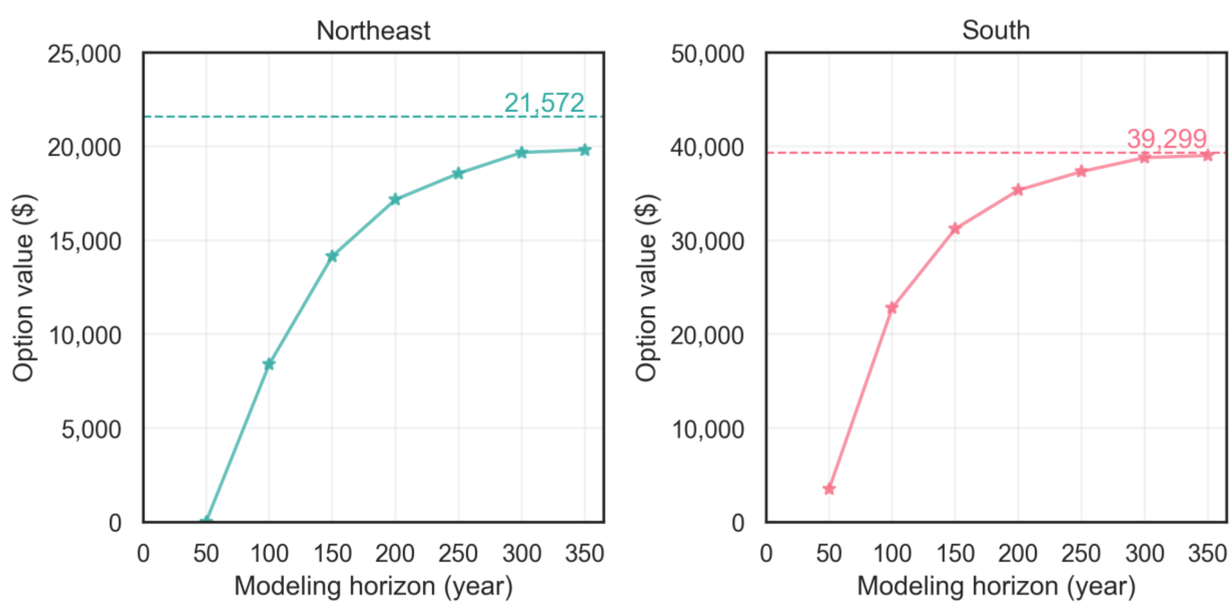

Figure 4.9 Variation of the option value with respect to modeling horizon

Choice of Distributions in Simulation

Simulation has been widely used to quantify uncertainties in various problems. The advantage of simulation is that it provides insights when complex stochastic behavior is present (Chick, 2001). However, its disadvantage is that the simulation output is sensitive to the input distributions (Lipton et al., 1995). This calls for selecting appropriate input distribution to characterize the underlying uncertainties, as failing to do so can contribute to misleading simulation output and irrational decisions (Chick, 2001). The simulated data sets should resemble reality so that the results can be generalized to real situations with credibility (Burton et al., 2006).

In the context of energy prices, there has been a dispute between the GBM process and MR process in modeling the uncertainty of energy prices. Some references model the uncertain energy prices as GBM processes (e.g., Zambujal-Oliveir, 2013, Santos et al., 2014, and Hach & Spinler, 2016), while others model the uncertain energy prices as MR processes (e.g., Mayer et al., 2015; Borovkova & Schmeck, 2017; Elias et al., 2018).

The definition of the GBM process has been extensively discussed in the previous sections. For a random variable X_t that follows a GBM process such that $dX_t = \alpha X_t dt + \sigma X_t dz$, where $dz = \varepsilon\sqrt{dt}$, $\varepsilon \sim N(0,\ 1)$. It can be verified that $E[X_t] = X_0 e^{\alpha t}$ and $Var[X_t] = X_0^2 e^{2\alpha t}\left(e^{\sigma^2 t} - 1\right)$ (Wu & Buyya, 2015). When $t \to \infty$, $E[X_t] \to \infty$, $Var[X_t] \to \infty$.

As for the MR process, it characterizes the mean-reverting behavior observed in the evolution of random variables over time (Barlow, 2002). The simplest form of the MR process is the Ornstein-Uhlenbeck process, such that $Y_t = log(X_t)$, $dY_t = \eta(\bar{Y} - Y_t)dt + \sigma dz$, where Y_t is the log of the value X_t, η the mean reversion coefficient, $\bar{Y}$ the log of the long-term mean value,

$dz = \varepsilon\sqrt{dt}$, $\varepsilon \sim N(0,\ 1)$. It can be verified that $E[Y_t] = \bar{Y} + (Y_0 - \bar{Y})e^{-\eta t}$ and $Var[Y_t] = \frac{\sigma^2}{2\eta}(1 - e^{-2\eta t})$ (Pinto et al., 2007). When $t \to \infty$, $E[Y_t] \to \bar{Y}$, $Var[Y_t] \to \frac{\sigma^2}{2\eta}$.

Mathematically, the main difference in the definition between the GBM and MR processes is the drift. Specifically, the drift in GBM process is a constant, while the drift in MR process is a function of the current value. That is, the drift in MR process is positive when the current value is lower than the long-term mean value and is negative when the current value is higher than the long-term mean value. Furthermore, when $t \to \infty$, the expected value and the variance of the GBM process both approach positive infinity, while the expected value and variance of the MR process are bounded (Pinto et al., 2007).

In addition, the prices of commodities (e.g., oil, copper, and others that are related to their long-term marginal production costs) fluctuate randomly in the short run in the short term (Boonpramote, n.d.), and it may be possible and appropriate to use GBM models in the short run (Pinto et al., 2007). However, in the long run, commodity prices tend to revert to the long-term mean (Nomikos & Andriosopoulos, 2012; Boonpramote, n.d.).

Despite this, in an investigation on the behavior of the oil, coal, and natural gas prices in the United States, Pindyck (1999) found that the prices are mean reverting, but the rate of mean reversion is slow over the long run, so the oil price can be treated as a GBM for the purposes of making investment decisions. It is also noted that in the investment decisions where energy prices are the key stochastic variables, a GBM formulation is unlikely to lead to large errors in the long-term investment valuation (Pindyck, 2001).

As explained in Metcalf and Hassett (1995), the expected cumulative investment after some time is the same under GBM and MR formulation due to two effects that work in opposite directions and offset each other, the variance effect and the realized price effect. The variance effect means that a higher reversion speed in the MR process reduces the long-run variance, resulting in increasing investment. The realized price effect means that the increasing volatility of the GBM process means higher trigger price levels may be achieved, which induces a greater investment. Hence, the additional tractability and intuitive nature of results under GBM formulation can be acquired at a very low cost in terms of realism.

Based on the above findings and that the statistics test results indicate no evidence to reject the assumptions that the average commercial electricity and natural gas prices in Illinois (U.S. EIA, 2021c; U.S. EIA, 2022b) follow GBM processes, we continue modeling the electricity and natural gas prices as GBM processes in the extended model. As an extension to this discussion and future research, we will apply the Least Squares Monte Carlo simulation to valuate the roof conversion option when the energy prices are modeled as correlated MR processes with realistic estimate of parameter values and compare it with the option value under GBM formulation.

Conclusions

In this paper, we considered a commercial building that consumes electricity for cooling and natural gas for heating, where its electricity consumption sufficiently exceeds its natural gas consumption. Using a real options approach, we provided decision support for the conversion from a conventional roof to a cool roof under the uncertainties of electricity and natural gas prices. Managerial insights and economic implications were derived through sensitivity analyses and numerical examples.

Specifically, in the basic model where we characterize the electricity price as a GBM process and the natural gas price as a constant multiplied by the electricity price, we constructed and analyzed a real options model and analytically solved for the optimal electricity price threshold for roof conversion and the expected time. From analytical sensitivity analysis, we found that (1) when the electricity price becomes more uncertain, the decision-maker should postpone the roof conversion; and (2) with a higher ratio of the natural gas price over the electricity price, the decision-maker should delay the roof conversion. In a numerical example of the retail stores in the Northeast and the South of the United States, the numerical results indicated that the roof conversion should be implemented in the South earlier than in the Northeast, which explains why cool roofs are more commonly applied in the South than in the Northeast. We also numerically observed that the roof conversion should be expedited when the electricity price grows faster and postponed when money becomes heavily discounted as time progresses.

In the extended model, where the electricity and natural gas prices followed correlated GBM processes, we obtained the value of the roof conversion option using the Least Squares Monte Carlo simulation via a numerical example. The numerical results indicated that the roof conversion option is more valuable in the South than in the Northeast. We also observed that (1) the roof conversion option becomes less valuable when the discount rate for money is higher, (2) the roof conversion option is more valuable when the electricity price becomes more volatile, and is less valuable when the natural gas price becomes more volatile, and (3) given a positive correlation between the electricity and natural gas prices, the value of the roof conversion option first decreases and then increases as the correlation coefficient increases.

There are numerous directions for future research. For instance, it is worthwhile to investigate the value of the roof conversion option when the energy prices are modeled as MR processes (e.g., Mayer et al., 2015; Borovkova & Schmeck, 2017; Elias et al., 2018) and the difference between the option values under the GBM and MR assumptions. In addition, one can relax the assumption on the fixed energy consumption and incorporate the energy consumption uncertainties into the roof conversion problem, as addressed in literature (e.g., Marathe & Ryan, 2005; Djauhari et al., 2020). In terms of the method used to estimate the expected payoff from continuation with the current electricity and natural gas prices, one can also incorporate the variance into the regression using the Weighted Least Squares method. Moreover, our models can be extended to other economic conversion decisions under energy price uncertainties toward sustainability, such as heating pump selection and conversion.

Disclosure Statement

The authors report there are no competing interests to declare.

References

Abadie, L. M., & Chamorro, J. M. (2017). Valuation of real options in crude oil production. *Energies*, *10*(8), 1218.

Akbari, H., Konopacki, S., & Pomerantz, M. (1999). Cooling energy savings potential of reflective roofs for residential and commercial buildings in the United States. *Energy*, *24*(5), 391-407.

Barlow, M. T. (2002). A diffusion model for electricity prices. *Mathematical finance*, *12*(4), 287-298.

BCI Construction. (2021, November 26). Which Factors Determine the Lifespan of a Building? Retrieved from https://bciconstruction.us/which-factors-determine-the-lifespan-of-a-building/#:~:text=The%20lifespan%20of%20a%20commercial,not%20suited%20for%20significant%20adaptation.

Borovkova, S., & Schmeck, M. D. (2017). Electricity price modeling with stochastic time change. *Energy Economics*, *63*, 51-65.

Boonpramote, T. (n.d.) Stochastic Processes. Retrieved from http://pioneer.netserv.chula.ac.th/~btitisak/AIT_DA_23Stochastic.pdf

Burton, A., Altman, D. G., Royston, P., & Holder, R. L. (2006). The design of simulation studies in medical statistics. *Statistics in medicine*, *25*(24), 4279-4292.

CenterPoint Energy. (n.d.). Natural Gas and Electricity. Retrieved from https://www.centerpointenergy.com/en-us/Services/Pages/natural-gas-electricity-cost-comparison.aspx?sa=mn&au=bus#:~:text=As%20illustrated%2C%20even%20when%20a,to%20cost%20%241.77%20per%20therm

Chick, S. E. (2001). Input distribution selection for simulation experiments: Accounting for input uncertainty. *Operations Research*, *49*(5), 744-758.

CNBC. (2022). U.S. 30 Year Treasury. Retrieved from https://www.cnbc.com/quotes/US30Y Accessed on July 25, 2022.

Croghan, J., Jackman, J., & Min, K. J. (2017). Estimation of geometric Brownian motion parameters for oil price analysis. In *IIE Annual Conference. Proceedings* (pp. 1858-1863). Institute of Industrial and Systems Engineers (IISE).

Cortazar, G., Gravet, M., & Urzua, J. (2008). The valuation of multidimensional American real options using the LSM simulation method. *Computers & Operations Research*, *35*(1), 113-129.

Dixit, R. K., Dixit, A. K., & Pindyck, R. S. (1994). *Investment under uncertainty*. Princeton university press.

Djauhari, M. A., Asrah, N. M., Li, L. S., Djakaria, I., Badruzzaman, S. T. A. I. K., & KM10, J. R. S. (2020). Forecasting model of electricity consumption in Malaysia: A geometric Brownian motion approach. *Solid State Technology*, *63*(3), 40-46.

Dockendorf, J., & Paxson, D. (2013). Continuous rainbow options on commodity outputs: what is the real value of switching facilities? *The European Journal of Finance*, *19*(7-8), 645-673.

Electric Choice. (2022, February 3). Deregulated Energy Markets. Retrieved from https://www.electricchoice.com/map-deregulated-energy-markets/

Elias, R. S., Wahab, M. I. M., & Fang, L. (2018). Retrofitting carbon capture and storage to natural gas-fired power plants: A real-options approach. *Journal of Cleaner Production*, *192*, 722-734.

Feldstein, S. A. (2022). Age of U.S. Commercial Buildings. Retrieved from https://www.commbuildings.com/ResearchComm.html

Feng, J., Saliari, M., Gao, K., & Santamouris, M. (2022). On the cooling energy conservation potential of super cool roofs. *Energy and Buildings*, *264*, 112076.

GAFGLAS. (2016, August). Mineral-Surfaced Cap Sheet. Retrieved from https://www.gaf.com/en-us/document-library/documents/productdocuments/commercialroofingsystemsdocuments/builtuproofingdocuments/gafglasdocuments/burcapsheetdocuments/gafglasmineralsurfacedcapsheetdocuments/Data_Sheet__GAFGLAS_MineralSurfaced_Cap_Sheet.pdf

Gao, Y., Xu, J., Yang, S., Tang, X., Zhou, Q., Ge, J., ... & Levinson, R. (2014). Cool roofs in China: Policy review, building simulations, and proof-of-concept experiments. *Energy Policy*, *74*, 190-214.

Guo, R., Gao, Y., Zhuang, C., Heiselberg, P., Levinson, R., Zhao, X., & Shi, D. (2020). Optimization of cool roof and night ventilation in office buildings: A case study in Xiamen, China. *Renewable Energy*, *147*, 2279-2294.

Hach, D., & Spinler, S. (2016). Capacity payment impact on gas-fired generation investments under rising renewable feed-in—A real options analysis. *Energy Economics*, *53*, 270-280.

Hosseini, M., & Akbari, H. (2016). Effect of cool roofs on commercial buildings energy use in cold climates. *Energy and Buildings*, *114*, 143-155.

Isaac Physics. (n.d.). Reflection and Refraction. Retrieved from https://isaacphysics.org/concepts/cp_reflection_and_refraction

Klitgaard, T., & Reddy, R. (2000). Lowering electricity prices through deregulation. *Available at SSRN 730107*.

Kohl's. (2019, March 7). Updates on Kohl's Store Optimization Initiatives. Retrieved from https://corporate.kohls.com/news/archive-/2018/march/store-optimization

Kolokotroni, M., Gowreesunker, B. L., & Giridharan, R. (2013). Cool roof technology in London: An experimental and modelling study. *Energy and Buildings*, *67*, 658-667.

Kong, X. Q., Wang, R. Z., & Huang, X. H. (2005). Energy optimization model for a CCHP system with available gas turbines. *Applied Thermal Engineering*, *25*(2-3), 377-391.

Liatard, M. (2022). Correlated Wiener Processes. Retrieved from http://question-player.com/index.php?p=Blog&t=correlated-wiener-processes&target=69bc347c65b2a91a2b872779ab30d7c7&lang=en

Lipton, J., Shaw, W. D., Holmes, J., & Patterson, A. (1995). Selecting input distributions for use in Monte Carlo simulations. *Regulatory toxicology and pharmacology*, *21*(1), 192-198.

Longstaff, F. A., & Schwartz, E. S. (2001). Valuing American options by simulation: a simple least-squares approach. *The review of financial studies*, *14*(1), 113-147.

Lukes, T. (2021). Electricity vs. Natural Gas Generation - Utility Costs, Price Correlation, and How to Save Your Facility Money. Retrieved from https://unisonenergy.com/insight/electric-and-gas-price-correlation-means-your-cogeneration-savings-will-stay-stable/

Luenberger, D. G. (1997). Investment science. *OUP Catalogue*.

Maeda, M., & Watts, D. (2019). The unnoticed impact of long-term cost information on wind farms' economic value in the USA.–A real option analysis. *Applied energy*, *241*, 540-547.

Marathe, R. R., & Ryan, S. M. (2005). On the validity of the geometric Brownian motion assumption. *The Engineering Economist*, *50*(2), 159-192.

Maribu, K. M., Galli, A., & Armstrong, M. (2007). Valuation of Spark-spread Options with Mean Reversion and Stochastic Volatility. *Int. J. Electron. Bus. Manag.*, *5*(3), 173-181.

Mayer, K., Schmid, T., & Weber, F. (2015). Modeling electricity spot prices: combining mean reversion, spikes, and stochastic volatility. *The European Journal of Finance*, *21*(4), 292-315.

Metcalf, G. E., & Hassett, K. A. (1995). Investment under alternative return assumptions comparing random walks and mean reversion. *Journal of Economic Dynamics and control*, *19*(8), 1471-1488.

Metric Conversions. (2018, July 22). Therms (US) to Kilowatt-hours conversion. Retrieved from https://www.metric-conversions.org/energy-and-power/therms-us-to-kilowatt-hours.htm

Neal, S.L. (2010, February 8). Light at Interfaces. Retrieved from http://www1.udel.edu/chem/sneal/sln_tchng/CHEM620/CHEM620/Chi_4._Light_at_Interfaces.html

Nomikos, N., & Andriosopoulos, K. (2012). Modelling energy spot prices: Empirical evidence from NYMEX. *Energy Economics*, *34*(4), 1153-1169.

Paolini, R., Zinzi, M., Poli, T., Carnielo, E., & Mainini, A. G. (2014). Effect of ageing on solar spectral reflectance of roofing membranes: Natural exposure in Roma and Milano and the impact on the energy needs of commercial buildings. *Energy and Buildings*, *84*, 333-343.

Pindyck, R. S. (1999). The long-run evolutions of energy prices. *The energy journal*, *20*(2).

Pindyck, R. S. (2001). The dynamics of commodity spot and futures markets: a primer. *The energy journal*, *22*(3).

Pinto, C. B., Brandão, L., & Hahn, W. J. (2007, June). Modeling switching options using mean reverting commodity price models. In *11th International Conference on Real Options* (pp. 6-9).

Pressler, M. (2022, February 18). Average US Electricity Costs & The Effect of Energy Deregulation. Retrieved from https://quickelectricity.com/average-electricity-prices-and-deregulation/

Santos, L., Soares, I., Mendes, C., & Ferreira, P. (2014). Real options versus traditional methods to assess renewable energy projects. *Renewable Energy*, *68*, 588-594.

Shingobee. (2021, March 24). What Is the Lifespan of a Commercial Building? – Ask the Expert. Retrieved from http://www.shingobee.com/About-Us/News/entryid/191/what-is-the-lifespan-of-a-commercial-building-ask-the-expert

Sigman, K. (2007). Simulating normal (Gaussian) random variables with applications to simulating Brownian motion and geometric Brownian motion in one and two dimensions. Retrieved from http://www.columbia.edu/~ks20/4703-Sigman/4703-07-Notes-BM-GBM-I.pdf

Schmit, T. M., Luo, J., & Conrad, J. M. (2011). Estimating the influence of US ethanol policy on plant investment decisions: A real options analysis with two stochastic variables. *Energy Economics, 33*(6), 1194-1205.

U.S. Department of Energy. (2010, July). Guidelines for Selecting Cool Roofs. Retrieved from https://www1.eere.energy.gov/buildings/publications/pdfs/corporate/coolroofguide.pdf

U.S. Energy Information Administration (EIA). (2013, July 3). Energy sources have changed throughout the history of the United States. Retrieved from https://www.eia.gov/todayinenergy/detail.php?id=11951

U.S. Energy Information Administration (EIA). (2016a, May). Commercial Buildings Energy Consumption Survey (CBECS) - Table C15. Electricity consumption and conditional energy intensity by Census region, 2012. Retrieved from https://www.eia.gov/consumption/commercial/data/2012/c&e/cfm/c15.php

U.S. Energy Information Administration (EIA). (2016b, May). Commercial Buildings Energy Consumption Survey (CBECS) - Table C25. Natural gas consumption and conditional energy intensity by Census region, 2012. Retrieved from https://www.eia.gov/consumption/commercial/data/2012/c&e/cfm/c25.php

U.S. Energy Information Administration (EIA). (2021a, April 12). Electricity explained - Factors affecting electricity prices. Retrieved from https://www.eia.gov/energyexplained/electricity/prices-and-factors-affecting-prices.php

U.S. Energy Information Administration (EIA). (2021b, June 1). What are Ccf, Mcf, Btu, and therms? How do I convert natural gas prices in dollars per Ccf or Mcf to dollars per Btu or therm? Retrieved from https://www.eia.gov/tools/faqs/faq.php?id=45&t=8#:~:text=One%20thousand%20cubic%20feet%20(Mcf,1.037%20MMBtu%2C%20or%2010.37%20therms.

U.S. Energy Information Administration (EIA). (2021c, September 15). Electricity Detailed State Data - Average Price by State by Provider (EIA-861). Retrieved from https://www.eia.gov/electricity/data/state/

U.S. Energy Information Administration (EIA). (2021d, September). 2018 Commercial Buildings Energy Consumption Survey. Retrieved from https://www.eia.gov/consumption/commercial/

U.S. Energy Information Administration (EIA). (2022b, January 31). Illinois Price of Natural Gas Sold to Commercial Consumers. Retrieved from https://www.eia.gov/dnav/ng/hist/n3020il3a.htm

Wang, C. H., & Min, K. J. (2006). Electric power generation planning for interrelated projects: a real options approach. *IEEE Transactions on Engineering Management*, *53*(2), 312-322.

Wang, S., & Zhang, J. (2014). Effect of titanium dioxide (TiO2) on largely improving solar reflectance and cooling property of high density polyethylene (HDPE) by influencing its crystallization behavior. *Journal of Alloys and Compounds*, *617*, 163-169.

Wu, C., & Buyya, R. (2015). Cloud Data Centers and Cost Modeling, Geometric Brownian Motion. Retrieved from https://www.sciencedirect.com/topics/computer-science/geometric-brownian-motion

Zambujal-Oliveira, J. (2013). Investments in combined cycle natural gas-fired systems: A real options analysis. *International Journal of Electrical Power & Energy Systems*, *49*, 1-7.

Appendices

Appendix 4A. H_t in Basic Model Follows a GBM Process

Following Dixit & Pindyck (1994, pp. 79-80), with Ito's Lemma, it can be verified that:

$$dH_t = \frac{\partial H_t}{\partial t} dt + \frac{\partial H_t}{\partial C_t} dC_t + \frac{1}{2}\frac{\partial^2 H_t}{\partial {C_t}^2}(dC_t)^2 \tag{4A.1}$$

Since $H_t = \lambda C_t$, we have $\frac{\partial H_t}{\partial C_t} = \lambda$, and $\frac{\partial^2 H_t}{\partial {C_t}^2} = 0$. With $\frac{\partial H_t}{\partial t} = 0$ (Dixit & Pindyck, 1994, p. 80) and $dC_t = \alpha_C C_t dt + \sigma_C C_t dz_C$, dH_t becomes

$$dH_t = \lambda(\alpha_C C_t dt + \sigma_C C_t dz_C) = \alpha_C(\lambda C_t)dt + \sigma_C(\lambda C_t)dz_C = \alpha_C H_t dt + \sigma_C H_t dz_C \tag{4A.2}$$

which implies that H_t also follows a GBM process with the same growth rate α_C and volatility σ_C as C_t.

Appendix 4B. Explanation on Why TiO_2 Reflects More Sunlight

Before demonstrating why TiO_2 reflects more sunlight, we first introduce the concept of the refractive index. The refractive index of a medium, n_{medium}, is defined as the ratio of the speed of light in vacuum c_{vacuum} to the speed of light in that medium c_{medium} as follows (Isaac Physics, n.d.):

$$n_{medium} = \frac{c_{vacuum}}{c_{medium}} \tag{4B.1}$$

The refractive index of different medium can be verified such as $n_{air} \approx n_{vacuum} = 1.00$, $n_{asphalt} = 1.63$, and $n_{TiO_2} \approx 2.70$ (Wang & Zhang, 2014).

Next, we discuss the relationship between refractive indices and reflectance. In the case of normal incidence, the ray path is perpendicular (normal) to the surface, meaning the angle of incidence is 0. In such a case, the reflectance is defined as

$$reflectance = \left(\frac{n_1 - n_2}{n_1 + n_2}\right)^2 \tag{4B.2}$$

where n_1 and n_2 are the refractive indices of two media (Neal, 2010).

When the sunlight perpendicularly hits the surface of asphalt from the air, the reflectance is:

$$reflectance_{air-asphalt} = \left(\frac{1.63 - 1.00}{1.63 + 1.00}\right)^2 = 0.057 = 5.7\% \tag{4B.3}$$

Similarly, when the sunlight perpendicularly hits the surface of TiO_2 from the air, the reflectance is:

$$reflectance_{air-TiO_2} = \left(\frac{2.70 - 1.00}{2.70 + 1.00}\right)^2 = 0.21 = 21\% \tag{4B.4}$$

Hence, the percentage of sunlight reflected when it perpendicularly hits the surface of TiO_2 is much higher than that when it perpendicularly hits the surface of the asphalt.

We assume the conversion from a conventional roof to a cool roof is implemented by applying cool roof coating on the existing built-up roof. We approximate the refractive index of asphalt as the refractive index of the conventional roof because the built-up roof contains an asphalt-coated glass fiber mat cap sheet. We also approximate the refractive index of TiO_2 as the refractive index of cool roof coating. The above explanation and calculation explain why the sunlight is reflected more when cool roof coating is applied on the built-up roof.

Appendix 4C. Justification on Parameter Values

The value of the discount rate for money ρ is estimated from the 30-year treasury yield as of July 25, 2022, 2.9950% (CNBC, 2022).

With the average commercial electricity prices in U.S. EIA (2021c) and natural gas prices in U.S. EIA (2022b) between 2001 and 2016, we calculate the ratio of natural gas price over electricity price, as shown in Table 4C.1. The ratios have a mean of 0.3657 and a standard deviation of 0.0652. The mean of the ratios is around 5.6 times of the standard deviation, which is consistent with the stability of the ratio between the electricity and natural gas prices despite the price evolution over time (see Figure 4C.1). The value of 0.3657 also aligns with the rule of thumb for the relationship between the electricity and natural gas prices in CenterPoint Energy (n.d.), i.e., the natural gas price is consistently two to three times lower than the electricity price.

Table 4C.1 Average commercial electricity and natural gas prices in Illinois (U.S. EIA, 2021c; U.S. EIA, 2022b)

Year	**Electricity price ($/kWh)**	**Natural gas price ($/kWh)**	**Ratio (natural gas price / electricity price)**
2001	0.0740	0.0292	0.3943
2002	0.0752	0.0255	0.3390
2003	0.0730	0.0282	0.3866
2004	0.0754	0.0311	0.4119
2005	0.0775	0.0382	0.4932
2006	0.0795	0.0372	0.4684
2007	0.0857	0.0355	0.4142
2008	0.0925	0.0399	0.4317

2009	0.0905	0.0296	0.3266
2010	0.0888	0.0299	0.3367
2011	0.0864	0.0282	0.3267
2012	0.0799	0.0266	0.3323
2013	0.0814	0.0258	0.3174
2014	0.0926	0.0302	0.3266
2015	0.0902	0.0249	0.2758
2016	0.0902	0.0244	0.2702

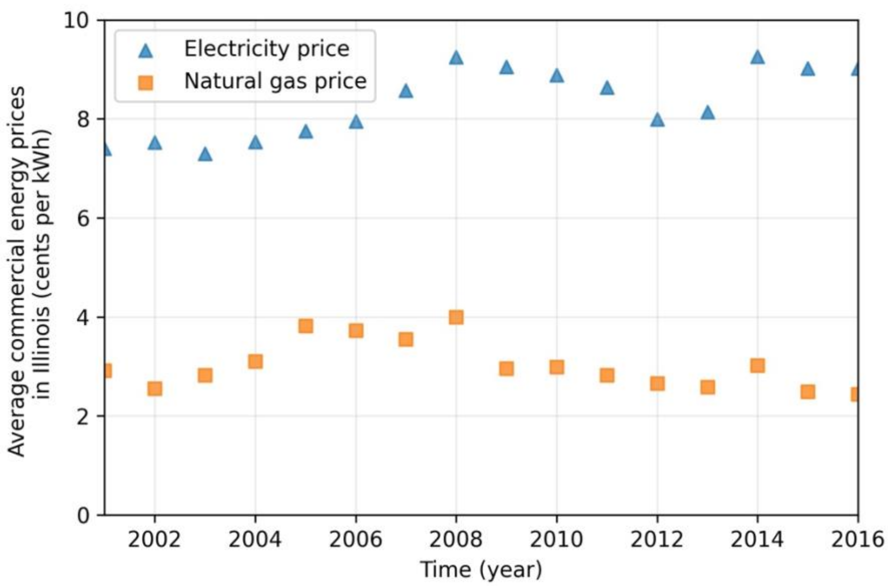

Figure 4C.1 Average commercial electricity and natural gas prices in Illinois

The retail stores are assumed to be single-story buildings with a size of 35,000 square-foot, referring to the size of Kohl's store (Kohl's, 2019).

The electricity and natural gas consumption are estimated from the energy intensity of the mercantile building for retail in U.S. EIA (2016a) and U.S. EIA (2016b) respectively (see Table 4C.2).

Table 4C.2 Energy intensity of mercantile building for retail (U.S. EIA, 2016a; U.S. EIA, 2016b)

Energy intensity	**Northeast**	**South**	**Source**
Electricity (kWh/square foot)	12.8	16.3	U.S. EIA (2016a)
Natural gas (cubic feet/square foot)	25.1	15.1	U.S. EIA (2016b)

Taking the electricity energy intensity in the Northeast as an example, the electricity consumption is given by 12.8 (kWh/square foot) * 35,000 (square foot) = 448,000 (kWh). Similarly for the natural gas consumption in the Northeast, which is estimated to be 25.1 (cubic feet/square foot) * 35,000 (square foot) * 0.01037 (therm/cubic foot) * 29.3 (kWh/therm) = 266,924 kWh, given the unit conversion where 1 cubic foot = 0.01037 therm (U.S. EIA, 2021b), and 1 therm = 29.3 kWh (Metric Conversions, 2018).

The percentage reduction (increase) in the electricity (natural gas) consumption after roof conversion is estimated from the percentage change in the annual electricity (natural gas) demand from high-albedo roofing (cool roof) for retail stores built after 1980 (see Akbari et al., 1999 for details). New York, NY is the benchmark of the Northeast of the United States, and Dallas/Fort Worth, TX, is the benchmark for the South of the United States.

To ensure the net energy saving is positive after the roof conversion, we would like the electricity cost saving exceeds the natural gas cost penalty at any time t, i.e., $\theta_C D_C C_t > \theta_H D_H H_t$. However, it is challenging to ensure this condition holds for any t in each simulation path. Instead, we require the expected values of the energy prices to satisfy the condition of $\theta_C D_C E[C_t] > \theta_H D_H E[H_t]$. With $E[C_t] = C_0 e^{\alpha_C t}$ and $E[H_t] = H_0 e^{\alpha_H t}$, the condition is equivalent to $e^{(\alpha_C - \alpha_H)t} > \frac{\theta_H D_H H_0}{\theta_C D_C C_0}$. As shown in Figure 4C.2, the value of $e^{(\alpha_C - \alpha_H)t}$ always exceeds the value of $\frac{\theta_H D_H H_0}{\theta_C D_C C_0}$ when t varies from 1 to 55, which indicates that the expected annual electricity cost saving exceeds the expected annual natural gas cost penalty during the modeling horizon of 55 years.

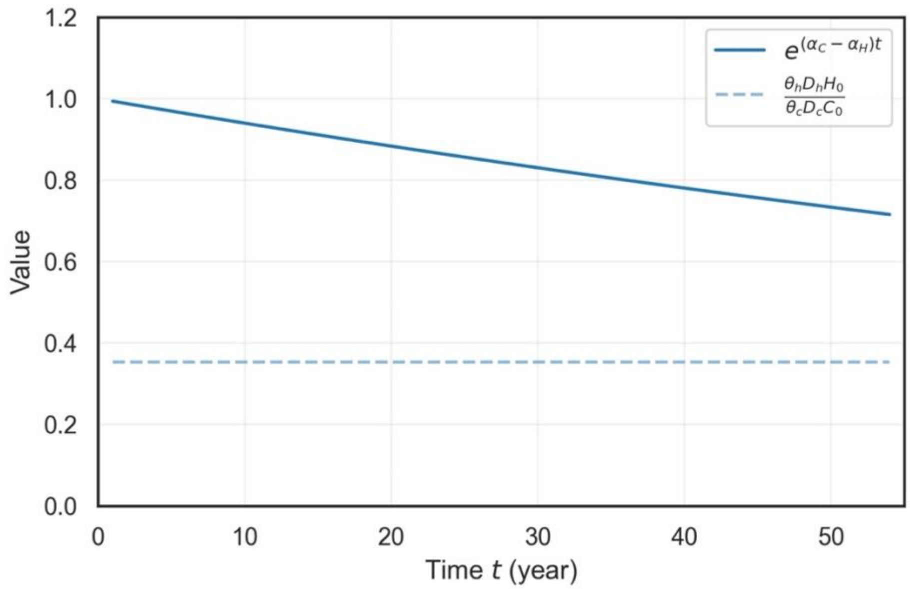

Figure 4C.2 Variation of $e^{(\alpha_C-\alpha_H)t}$ and $\frac{\theta_H D_H H_0}{\theta_C D_C C_0}$ with respect to time

Appendix 4D. Proof of Correlated GBM Processes

According to Sigman (2007),

"Let $W_1(t)$ and $W_2(t)$ denote standard Brownian motions (i.e., Wiener processes). Consider two Brownian motions $X_1(t) = \sigma_1 W_1(t) + \mu_1 t$ and $X_2(t) = \sigma_2 W_2(t) + \mu_2 t$. $\boldsymbol{X}(t) = \left(X_1(t), X_2(t)\right)^T$ is a two-dimensional Brownian motion (BM), where we shall assume the coordinates have a correlation coefficient r . For a given $-1 < r < 1$,

$$\frac{Cov\left(X_1(t), X_2(t)\right)}{\sigma_1\sqrt{t}\times\sigma_2\sqrt{t}} = r, t > 0 \tag{4D.1}$$

To construct this BM, we start with two independent standard BM's, $B_1(t)$ and $B_2(t)$, define $\boldsymbol{B}(t) = \left(B_1(t), B_2(t)\right)^T$, define the 2×2 matrix

$$\boldsymbol{A} = \begin{bmatrix} \sigma_1 & 0 \\ \sigma_2 r & \sigma_2\sqrt{1-r^2} \end{bmatrix} \tag{4D.2}$$

and construct

$$\boldsymbol{X}(t) = \boldsymbol{AB}(t) + \boldsymbol{\mu}t, t \geq 0 \tag{4D.3}$$

where $\boldsymbol{\mu} = (\mu_1, \mu_2)^T$.

We can then define correlated geometric BM's (GBM)."

$$S_1(t) = S_1(0)e^{X_1(t)} \tag{4D.4}$$

$$S_2(t) = S_2(0)e^{X_2(t)} \tag{4D.5}$$

From the above statements, we can derive the following:

For the correlated BM's, $X_1(t)$ and $X_2(t)$, we have

$$\begin{bmatrix} X_1(t) \\ X_2(t) \end{bmatrix} = \begin{bmatrix} \sigma_1 & 0 \\ \sigma_2 r & \sigma_2\sqrt{1-r^2} \end{bmatrix} \begin{bmatrix} B_1(t) \\ B_2(t) \end{bmatrix} + \begin{bmatrix} \mu_1 \\ \mu_2 \end{bmatrix} t \tag{4D.6}$$

That is,

$$X_1(t) = \mu_1 t + \sigma_1 B_1(t) \tag{4D.7}$$

$$X_2(t) = \mu_2 t + \sigma_2\left[rB_1(t) + \sqrt{1-r^2}B_2(t)\right] \tag{4D.8}$$

For the correlated GBM's, $S_1(t)$ and $S_2(t)$, we have

$$S_1(t) = S_1(0)e^{X_1(t)} = S_1(0)e^{\mu_1 t + \sigma_1 B_1(t)} \tag{4D.9}$$

$$S_2(t) = S_2(0)e^{X_2(t)} = S_2(0)e^{\mu_2 t + \sigma_2\left[rB_1(t) + \sqrt{1-r^2}B_2(t)\right]} \tag{4D.10}$$

In this paper, we assume that $dC_t = \alpha_C C_t dt + \sigma_C C_t dz_C$, where dz_C is the increment of a Wiener process, i.e., $dz_C = \varepsilon_C\sqrt{dt}$, $\varepsilon_C \sim N(0,1)$, and $dH_t = \alpha_H H_t dt + \sigma_H H_t dz_H$, where dz_H is the increment of a Wiener process, i.e., $dz_H = \varepsilon_H\sqrt{dt}$, $\varepsilon_H = r_{CH}\varepsilon_C + \sqrt{1-{r_{CH}}^2}\varepsilon_0$. r_{CH} is the constant correlation coefficient between the uncertainty incorporated in the change of C_t and H_t, $\varepsilon_0 \sim N(0,1)$, and ε_C and ε_0 are independent of each other (Liatard, 2022). It can be verified that

$$C_t = C_0 e^{\left(\alpha_C - \frac{1}{2}{\sigma_C}^2\right)t + \sigma_C z_C} \tag{4D.11}$$

With $\varepsilon_H = r_{CH}\varepsilon_C + \sqrt{1-{r_{CH}}^2}\varepsilon_0$, we have

$$\varepsilon_H dt = r_{CH}\varepsilon_C dt + \sqrt{1-r_{CH}{}^2}\varepsilon_0 dt \quad (4D.12)$$

$$dz_H = r_{CH} dz_C + \sqrt{1-r_{CH}{}^2} dz_0 \quad (4D.13)$$

where dz_0 is the increment of a Wiener process, i.e., $dz_0 = \varepsilon_0 dt$. Furthermore,

$$z_H = r_{CH} z_C + \sqrt{1-r_{CH}{}^2} z_0 \quad (4D.14)$$

Similarly, it can be verified that

$$H_t = H_0 e^{\left(\alpha_H - \frac{1}{2}\sigma_H{}^2\right)t + \sigma_H z_H} = H_0 e^{\left(\alpha_H - \frac{1}{2}\sigma_H{}^2\right)t + \sigma_H\left(r_{CH} z_C + \sqrt{1-r_{CH}{}^2} z_0\right)} \quad (4D.15)$$

Since Equations (4D.11) and (4D.15) have the same structure as Equations (4D.9) and (4D.10), the way that we define that C_t and H_t follow correlated GBM processes, essentially is the same as Sigman (2007).

Next, we first show that $\varepsilon_H \sim N(0,1)$, and $Corr(\varepsilon_C, \varepsilon_H) = r_{CH}$.

$$E[\varepsilon_H] = r_{CH} E[\varepsilon_C] + \sqrt{1-r_{CH}{}^2} E[\varepsilon_0] = r_{CH}(0) + \sqrt{1-r_{CH}{}^2}(0) = 0 \quad (4D.16)$$

$$Var[\varepsilon_H] = r_{CH}{}^2 Var[\varepsilon_C] + (1-r_{CH}{}^2) Var[\varepsilon_0] = r_{CH}{}^2(1) + (1-r_{CH}{}^2)(1) = 1$$

(D.17)

By definition,

$$Cov(\varepsilon_C, \varepsilon_H) = E[(\varepsilon_C - E[\varepsilon_C])(\varepsilon_H - E[\varepsilon_H])] = E\left[\varepsilon_C\varepsilon_H - \varepsilon_C E[\varepsilon_H] - \varepsilon_H E[\varepsilon_C] + E[\varepsilon_C]E[\varepsilon_H]\right]$$

$$= E[\varepsilon_C\varepsilon_H] - E[\varepsilon_C]E[\varepsilon_H] - E[\varepsilon_H]E[\varepsilon_C] + E[\varepsilon_C]E[\varepsilon_H] = E[\varepsilon_C\varepsilon_H] \quad (4D.18)$$

In terms of the correlation between ε_C and ε_H, by definition, we have

$$Corr(\varepsilon_C, \varepsilon_H) = \frac{Cov(\varepsilon_C, \varepsilon_H)}{\sqrt{Var[\varepsilon_C]}\sqrt{Var[\varepsilon_H]}} = \frac{E[\varepsilon_C\varepsilon_H]}{\sqrt{Var[\varepsilon_C]}\sqrt{Var[\varepsilon_H]}} = \frac{E[\varepsilon_C\varepsilon_H]}{\sqrt{1}\sqrt{1}} = E[\varepsilon_C\varepsilon_H] \quad (4D.19)$$

To obtain $E[\varepsilon_C\varepsilon_H]$, we first note that

$$Var[\varepsilon_C] = E[(\varepsilon_C - E[\varepsilon_C])^2] = E[\varepsilon_C{}^2 - 2\varepsilon_C E[\varepsilon_C] + E[\varepsilon_C]^2]$$

$$= E[\varepsilon_C{}^2] - 2E[\varepsilon_C]E[\varepsilon_C] + E[\varepsilon_C]^2 = E[\varepsilon_C{}^2] - 2(0)(0) + 0^2 = E[\varepsilon_C{}^2] = 1 \quad (4D.20)$$

Also, since ε_C and ε_0 are independent, the covariance between ε_C and ε_0 is 0. That is,

$$Cov(\varepsilon_C, \varepsilon_0) = E[\varepsilon_C \varepsilon_0] - E[\varepsilon_C]E[\varepsilon_0] = E[\varepsilon_C \varepsilon_0] - 0(0) = E[\varepsilon_C \varepsilon_0] = 0 \qquad \text{(4D.21)}$$

Hence, we have

$$E[\varepsilon_C \varepsilon_H] = E\left[r_{CH}{\varepsilon_C}^2 + \sqrt{1 - {r_{CH}}^2}\varepsilon_C \varepsilon_0\right] = r_{CH}E[{\varepsilon_C}^2] + \sqrt{1 - {r_{CH}}^2}E[\varepsilon_C \varepsilon_0]$$

$$= r_{CH}(1) + \sqrt{1 - {r_{CH}}^2}(0) = r_{CH} \qquad \text{(4D.22)}$$

Therefore, $Corr(\varepsilon_C, \varepsilon_H) = E[\varepsilon_C \varepsilon_H] = r_{CH}$. Furthermore,

$$E[dz_C dz_H] = E\left[\varepsilon_C \sqrt{dt}\varepsilon_H \sqrt{dt}\right] = E[\varepsilon_C \varepsilon_H]dt = r_{CH}dt \qquad \text{(4D.23)}$$

CHAPTER 5. GENERAL CONCLUSIONS

In this dissertation, we studied various economic transition endeavors, which are costly, irreversible, and made under uncertainties. For each case, under the assumption that the underlying uncertainty (i.e., the demand for a perishable agricultural product, the maintenance cost of an asphalt road, and the electricity and natural gas prices of a commercial building) follows a GBM process, we viewed the transition endeavor as a stochastic optimal control (real options) problem, investigated the optimal decisions and analyzed the economic consequences. That is, for the cases of conversion from conventional to blockchain-based SCIMS, asphalt roads resurfacing, and conversion from conventional to cool roofs, we derived the optimal thresholds of demand for a perishable agricultural product, the maintenance cost of an asphalt road, and the electricity price of a commercial building as well as the expected time of these transitions. Subsequently, managerial insights and economic implications were derived through analytical and numerical analyses and numerical examples.

In Chapter 2, for the retailer in a supply chain of a perishable agricultural product, we mathematically formulated the transition from a conventional SCIMS to a blockchain-based SCIMS without/with the presentence of a fixed subsidy and a variable subsidy from the government using a real options approach when the demand follows a GBM process. For both scenarios, we obtained the closed-form solutions of the optimal demand thresholds for transition and the corresponding expected time. By analytically and numerically examining the impact of parameter values on the transition decision, we derived the following critical managerial insights and policy implications. First, the retailer should defer the transition from a conventional SCIMS to a blockchain-based SCIMS when the customers' demand is volatile. Moreover, from the government's perspective, a small amount of variable subsidy is a more effective incentive if the government anticipates the retailers to rapidly transit to a blockchain-based SCIMS in a short time, while a fixed subsidy should be advocated if an even pace of switch among retailers is preferred. Meanwhile, in terms of motivating the retailer to transit to a blockchain-based SCIMS, the fixed subsidy is more efficient at its higher level, while the variable subsidy is more efficient at its lower level.

In Chapter 3, under the assumption that the maintenance cost of an asphalt road follows a GBM process, we constructed and analyzed a real options model for a profit-maximizing decision-maker where the threshold in the maintenance cost to resurface the road is the decision variable. After numerically solving the optimal threshold of the maintenance cost and deriving the expected resurfacing interval, we conducted sensitivity analyses on the optimal threshold and the expected resurfacing interval with respect to the parameter values. The resulting managerial insights and economic implications include: (1) when the road maintenance cost becomes more volatile, the resurfacing of the road should be deferred, and the expected resurfacing interval will be extended; (2) a higher initial road maintenance cost results in a deferral of the road resurfacing and a shorter expected resurfacing interval. From the numerical example, we observe that (1) when the maintenance cost grows faster, the road resurfacing should be deferred, and the expected resurfacing interval will be shortened; (2) when money becomes heavily discounted as time progresses, the decision-maker should postpone the road resurfacing and prolong the expected resurfacing interval; (3) the average total discounted profits under the interval-based policy are maximized at an interval close to the expected resurfacing interval under the threshold-based policy. However, the average total discounted profits under the threshold-based policy slightly surpass that under the interval-based policy.

In Chapter 4, for a commercial building that consumes electricity for cooling and natural gas for heating, where its electricity consumption sufficiently exceeds its natural gas consumption, we provided decision support for the conversion from a conventional roof to a cool roof using a real options approach. In the basic model, we constructed and analyzed the decision models to transit from a conventional roof to a cool roof when the electricity price follows a GBM process, and the natural gas price is equal to a constant multiplied by the electricity price. We analytically derived the closed-form solutions to the optimal electricity price threshold and the expected time. From analytical sensitivity analysis, we found that (1) when the electricity price becomes more uncertain, the decision-maker prefers to postpone the roof conversion; and (2) with a higher ratio of the natural gas price over the electricity price, the decision-maker should delay the roof conversion. In a numerical example for retail stores in the Northeast and the South of the United States, the numerical results indicated that the roof conversion should be implemented in the South earlier than in the Northeast. Numerical sensitivity analysis indicated that the roof conversion should be expedited when the electricity price grows faster and postponed when money becomes heavily discounted as time progresses.

In the extended model of Chapter 4, where the electricity and natural gas prices were assumed to follow correlated GBM processes, we valuated the roof conversion option using the Least Squares Monte Carlo simulation. The numerical results indicated that the roof conversion option is more valuable in the South than in the Northeast. We also observed that (1) the roof conversion option becomes less valuable when the discount rate for money is higher, (2) the roof conversion option is more valuable when the electricity price becomes more volatile, and is less valuable when the natural gas price becomes more volatile, and (3) the value of the roof conversion option first decreases and then increases as the correlation coefficient increases given that the electricity and natural gas prices are positively correlated.

In summary, in this dissertation, we proposed real options-based models and analyses for economic transitions toward sustainability in the cases of conversion from conventional to blockchain-based SCIMS, asphalt roads resurfacing, and conversion from conventional to cool roofs. The decision support provided in this dissertation is critical for such economic decisions as they are costly, irreversible, and made under uncertainties.

This dissertation serves as the basis for the research in relevant areas and can lead to several extensions. As an extension to Chapter 2 regarding the conversion from conventional to blockchain-based SCIMS under the demand uncertainty, first of all, research can be expanded by modeling the demand as a jump-diffusion process considering that there can be a substantial reduction in the demand when recalls happen. Secondly, besides the demand uncertainty, other uncertainties such as the uncertainties in the unit selling price and the technology innovations (e.g., blockchain may require updates or be replaced by a more advanced SCIMS in the future) can be incorporated into future research. Thirdly, one can formulate the decision model from the perspective of other stakeholders in the supply chain, such as the wholesaler or the farm cooperative. Discussions can also be expanded to the valuation of the blockchain-based system regarding other properties such as transparency, immutability, and irrefutability in various industries (e.g., financial, insurance, and manufacturing).

For Chapter 3, the resurfacing problem for asphalt roads, one can extend the decision support to a cost-minimization decision-maker to a non-profit decision maker with objectives such as minimizing the cost. Moreover, other uncertainties in the resurfacing decision can be taken into consideration, such as traffic demand, which has been modeled as a GBM process in the literature, such as Zhao et al. (2004), and Galera and Soliño (2010). Furthermore, one can relax our assumption that only one type of vehicle accesses the road by incorporating the impact of heavy vehicles on the maintenance cost. There has been discussion on heavy trucks causing more road deterioration than passenger cars (Gibby et al., 1990), which may further raise the maintenance cost. On a larger scale, one can model multiple decisions under uncertainties, e.g., resurfacing, reconstructing the road, and applying preventive surface treatment to the road (e.g., Zhao & Min, 2021).

As for Chapter 4, the conversion from a conventional roof to a cool roof, it is worthwhile to investigate the value of the roof conversion option when the energy prices are modeled as MR processes (e.g., Mayer et al., 2015; Borovkova & Schmeck, 2017; Elias et al., 2018) and the difference between the option value under the GBM formulation. In addition, one can relax the assumption of fixed energy consumption and incorporate the energy consumption uncertainties into the roof conversion problem, as addressed in the literature (e.g., Marathe & Ryan, 2005; Djauhari et al., 2020). In terms of the method used to estimate the expected payoff from continuation with the current electricity and natural gas prices, one can also incorporate the variance into the regression using the Weighted Least Squares method. Moreover, our models can be extended to other economic conversion decisions toward sustainability under energy price uncertainties, such as heating pump selection and conversion.

Concisely, for the economic decisions toward sustainability, the decision support can be enriched by modeling the uncertainties with stochastic processes other than GBM (e.g., MR). This can lead to further discussion on the tradeoff between the more accurate modeling of the random variables and more intuitive and traceable results. In addition, besides modeling the uncertainties as diffusion processes, one can consider the potentially substantial changes in the uncertain variables when economic decisions occur and model the uncertainties as jump-diffusion processes. Finally, more uncertainties can be considered for the decision support to better formulate the problems in various industries. For cases involving more than one uncertainty, simulation is more applicable than the analytical and lattice methods.

References

Borovkova, S., & Schmeck, M. D. (2017). Electricity price modeling with stochastic time change. *Energy Economics*, *63*, 51-65.

Djauhari, M. A., Asrah, N. M., Li, L. S., Djakaria, I., Badruzzaman, S. T. A. I. K., & KM10, J. R. S. (2020). Forecasting model of electricity consumption in Malaysia: A geometric Brownian motion approach. *Solid State Technology*, *63*(3), 40-46.

Elias, R. S., Wahab, M. I. M., & Fang, L. (2018). Retrofitting carbon capture and storage to natural gas-fired power plants: A real-options approach. *Journal of Cleaner Production*, *192*, 722-734.

Galera, A. L. L., & Soliño, A. S. (2010). A Real Options Approach for the Valuation of Highway Concessions. *Transportation Science*, *44*(3), 416–427. https://doi.org/10.1287/trsc.1090.0299

Gibby, R., Kitamura, R., & Zhao, H. (1990). Evaluation of truck impacts on pavement maintenance cost. *Transportation Research Record*, *1262*, 48-56.

Marathe, R. R., & Ryan, S. M. (2005). On the validity of the geometric Brownian motion assumption. *The Engineering Economist*, *50*(2), 159-192.

Mayer, K., Schmid, T., & Weber, F. (2015). Modeling electricity spot prices: combining mean reversion, spikes, and stochastic volatility. *The European Journal of Finance*, *21*(4), 292-315.

Zhao, T., Sundararajan, S. K., & Tseng, C. L. (2004). Highway Development Decision-Making under Uncertainty: A Real Options Approach. *Journal of Infrastructure Systems*, *10*(1), 23–32. https://doi.org/10.1061/(asce)1076-0342(2004)10:1(23)

Zhao, Z., & Min, K. J. (2021). Preventive Surface Treatment Decision on Asphalt Road under Maintenance Cost Uncertainty. In *IISE Annual Conference. Proceedings* (pp. 1183-1188). Institute of Industrial and Systems Engineers (IISE).

Appendix

Validation of GBM Process

Let us denote the data to be tested as C_t, in this case, the average commercial natural gas price in the state of Illinois.

According to Ross (2014, p. 612), we say that $\{X_t, t \geq 0\}$ is a Brownian motion process with drift μ and variance σ^2 if

(1) $X_0 = 0$;

(2) $\{X_t, t \geq 0\}$ has stationary and independent increments;

(3) X_t is normally distributed with mean μt and variance $\sigma^2 t$.

Furthermore, the process $\{C_t, t \geq 0\}$ that is defined by $C_t = C_0 e^{X_t}$ is called a geometric Brownian motion (GBM) process (Ross, 2011, p. 39).

Let us re-write X_t as $X_t = \ln\left(\frac{C_t}{C_0}\right)$ and define the increment of X_t as W_t where $W_t = X_{t+1} - X_t$ (Marathe & Ryan, 2005). The above statements imply that C_t is a GBM process if the following assumptions are satisfied:

(1) $X_0 = 0$;

(2) The increment of X_t is stationary (i.e., W_t is stationary);

(3) The increment of X_t is independent from past values (i.e., W_t is independent from past values);

(4) X_t is normally distributed;

(5) Given that X_t is normally distributed, the mean and variance are μt and $\sigma^2 t$, respectively.

We first calculate the value of X_t and W_t in the following table. The explanation on the column of W_t state will be provided later.

t	C_t	X_t	W_t	W_t state	t	C_t	X_t	W_t	W_t state
0	4.56	0.0000	0.0195	2	15	10.91	0.8724	-0.0479	1
1	4.65	0.0195	0.0924	2	16	10.40	0.8245	0.1178	2
2	5.10	0.1119	0.0039	2	17	11.70	0.9423	-0.3009	1
3	5.12	0.1158	-0.1470	1	18	8.66	0.6414	0.0115	2
4	4.42	-0.0312	0.1072	2	19	8.76	0.6529	-0.0576	1
5	4.92	0.0760	0.0986	2	20	8.27	0.5953	-0.0611	1
6	5.43	0.1746	-0.0686	1	21	7.78	0.5342	-0.0274	1
7	5.07	0.1060	0.0253	2	22	7.57	0.5069	0.1574	2
8	5.20	0.1313	0.2829	2	23	8.86	0.6642	-0.1950	1
9	6.90	0.4142	0.2144	2	24	7.29	0.4692	-0.0208	1
10	8.55	0.6286	-0.1350	1	25	7.14	0.4484	0.0858	2
11	7.47	0.4936	0.1017	2	26	7.78	0.5342	-0.0719	1
12	8.27	0.5953	0.0956	2	27	7.24	0.4623	-0.0309	1
13	9.10	0.6910	0.2076	2	28	7.02	0.4314	-0.0260	1
14	11.20	0.8986	-0.0262	1	29	6.84	0.4055	/	/

(1) $X_0 = 0$;

The first assumption can be verified through $X_0 = \ln\left(\frac{C_0}{C_0}\right) = \ln(1) = 0$ and from value of X_0 in the table above.

(2) The increment of X_t is stationary (i.e., W_t is stationary);

The stationary of w_t can be tested using Dickey-Fuller test, an autoregressive (AR) unit root test for a time series (Zivot & Wang, 2007). In an AR (1) model that is defined as $w_t =$

$\phi w_{t-1} + \varepsilon_t$, where $\varepsilon_t \sim WN(0, \sigma_\varepsilon{}^2)$, essentially, the existence of a unit root implies the process is non-stationary.

H_0: $\phi = 1$ (A unit root is present in the time series of W_t).

H_A: $|\phi| < 1$ (A unit root is not present in the time series of W_t).

The test statistic DF_γ is -5.6077, and the p-value is 0.0000. The p-value is lower than a critical value of $\alpha = 0.05$, meaning that we have evidence to reject the null hypothesis. Therefore, it is reasonable to assume that the increment of X_t, W_t, is stationary.

(3) The increment of X_t is independent from past values (i.e., W_t is independent from past values);

The independence of W_t from past values can be tested with a contingency table (Ross, 2011). First, we calculate the median of W_t, which can be verified to be 0.0039. Next, we assign state 1 to year t if $W_t < 0.0039$ and state 2 to year t if $W_t > 0.0039$. After that, for $i, j = 1, 2$, we count how many times that a state i year was followed by a state j year and summarize the number of occurrences in a contingency table.

Contingency table

i	j		Row Total
	1	2	
1	6	7	13
2	8	7	15
Column total	14	14	28

Then we use Fisher exact test to check for the independence of the contingency table since it is the appropriate test when the sample size is small (McDonald, 2014, p. 77-85).

H_0: The probability of getting state j is the same whether the year before is state 1 or 2;

H_A: The state of a year is not independent of the state of the year before.

The Fisher exact test gives a statistic 0.7500, and the p-value is 1.0000. The p-value is higher than a significance level $\alpha = 0.05$, which means that we fail to reject the null hypothesis. Stated otherwise, it is reasonable to assume that the state of a year is independent of the state of the year before.

Besides, in the scatter plot of W_t, points are randomly distributed around the line $y = 0$, and no apparent pattern can be observed. So, we can tentatively say W_t is independent (Marathe & Ryan, 2005).

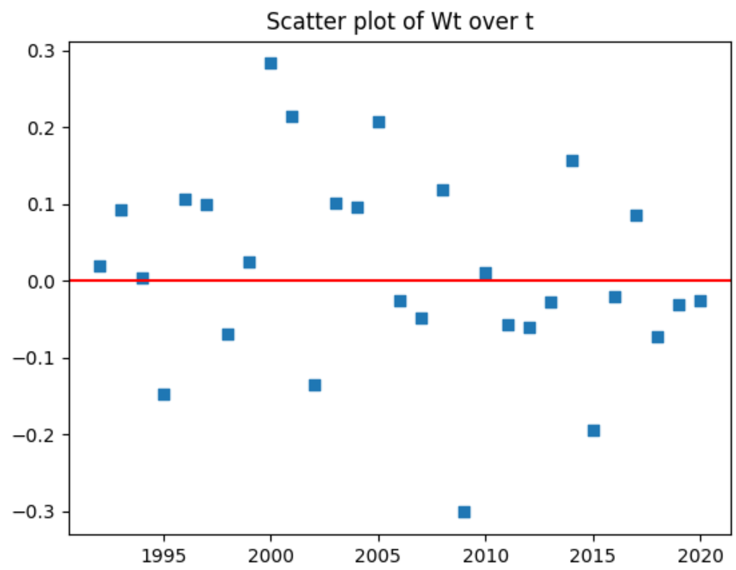

(4) X_t is normally distributed;

The normality of X_t can be tested through Shapiro-Wilk test as it tests whether data is from a normal distribution especially when the sample size is less than 2000 (Cool & Ockendon, 2015).

H_0: X_t is from a normal distribution.

H_A: X_t is not from a normal distribution.

Since the Shapiro-Wilk test W statistic is 0.9414, and the p-value is 0.0990 (higher than a significance level $\alpha = 0.05$), we fail to reject the null hypothesis that X_t is from a normal distribution (DAWG, 2014).

Moreover, in the Q-Q plot, points fall along the straight line, which is an indicator of X_t coming from a normal distribution.

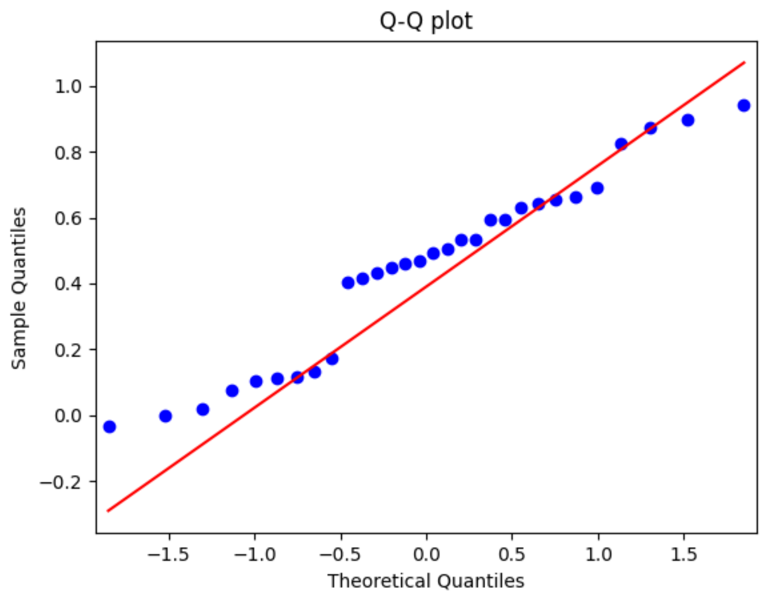

(5) Given that X_t is normally distributed, the mean and variance are μt and $\sigma^2 t$, respectively.

According to Ross (2011, p. 34), for all positive k and t, $X_{k+t} - X_k$ has a normal distribution with mean μt and variance $\sigma^2 t$. Suppose $k = 0$, X_t is normally distributed with μt and variance $\sigma^2 t$ since $X_0 = 0$. As t varies, the mean and variance of X_t vary and can approach to enormous values. However, for a specific value of t, the mean and variance both approach to constants. In the case of $t = 1$, the mean and variance become μ and σ^2 respectively.

Graphical evidence, the histogram of X_t and the Q-Q plot above, shows that X_t have fitted mean and variance (Marathe & Ryan, 2005).

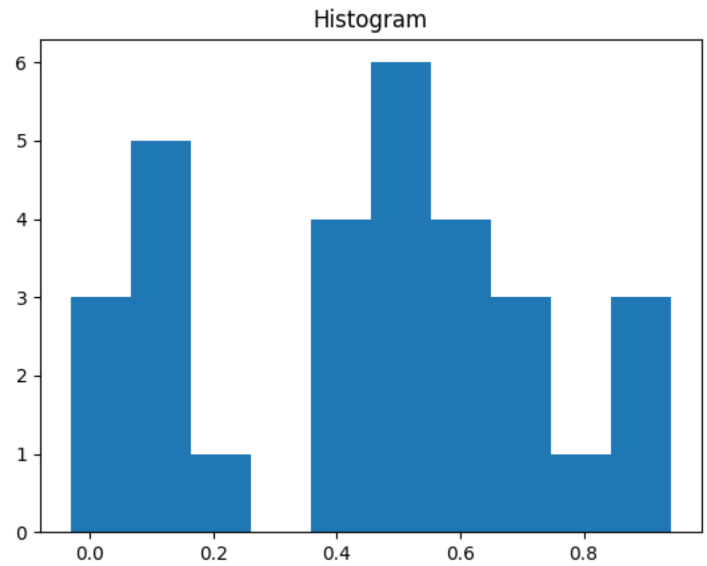

With the satisfaction of the above assumptions, we can conclude that it is reasonable to assume that C_t follows a GBM process.

References

Burn, C. R. (2018). Evidence on climate change effects and their management and investigation in the western Arctic. *Special Senate Committee on the Arctic*. Retrieved from https://sencanada.ca/content/sen/committee/421/ARCT/Briefs/2018-03-19_Brief_CBurn_e.pdf

Marathe, R. R., & Ryan, S. M. (2005). On the validity of the geometric Brownian motion assumption. *The Engineering Economist*, *50*(2), 159-192.

McDonald, J. H. (2009). *Handbook of biological statistics* (Vol. 2, pp. 6-59). Baltimore, MD: sparky house publishing.

Ross, S. M. (2011). *An elementary introduction to mathematical finance*. Cambridge University Press.

Ross, S. M. (2014). *Introduction to probability models (11th edition)*. Academic press.

Zivot, E., & Wang, J. (2007). *Modeling financial time series with S-Plus®* (Vol. 191). Springer Science & Business Media.